Quality documentation of MFASIS coeffcients production for RTTOV v14.1

Pascal Raisig[1], Leonhard Scheck[1,2], Christina Köpken-Watts[1], Olaf Stiller[1], and Christina Stumpf[1]

[1]DWD
[2]Hans-Ertel-Zentrum/LMU München

Friday 20th March, 2026

Contents

1 Introduction

This document gives an overview on the quality of reflectance simulations with MFASIS in its neural network (NN) version as utilized in RTTOV v14.1 using the available MFASIS coefficients.

The uncertainties of the reflectances simulated with MFASIS are quantified with respect to reflectances simulated with the RTTOV Discrete Ordinates Method (DOM) (see Hocking, 2016). As reference for the simulation input the NWP model profile dataset, provided by the NWP SAF, is used to cover a wide range of atmospheric cloud simulations. For each channel of an instrument a specific neuronal network definition is available as RTTOV coefficient. This neural network definition is optimized to achieve high accuracy and speed.
Section 2 summarizes the results as overview tables per instrument. Each table contains the neuronal network definition (NN def column) in terms of number of layers (L) and neurons per layer (N), as well as, the uncertainties from the reflectance simulations with MFASIS for three explicit albedos: 0, 0.5 and 1.0. Listed in the tables are the mean error (me), mean absolute error (mae), root mean square error (rmse) and the 99th percentile (p99).
Section 3 provides additionally more detailed figures for each instrument and channel. Depicted are the differences between the simulated MFASIS and DOM reflectances (MFASIS - DOM) as function of the cloud optical depth τ as one-dimensional probability density functions.

For more detailed information about MFASIS please see the RTTOV science and validation report for RTTOV v14.1.

2 Uncertainty tables

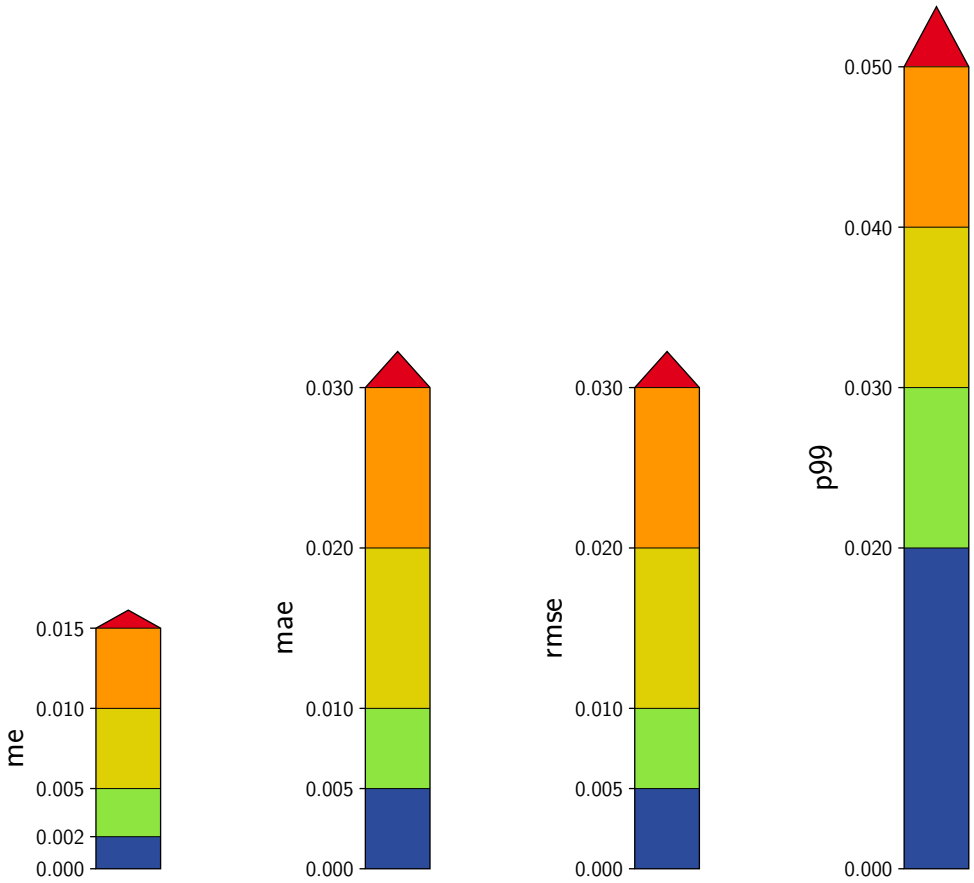

Figure 1: Color coding for the different uncertainty values in the tables for the instruments.

Dscovr 1 Epic

Channel	Wavelength [µm]	NN-Def	NN-Parameters	Albedo	mae	me	p99	rmse
1	0.442	L8-N25	5000	0.0	0.0016	0.0007	0.0103	0.0028
				0.5	0.0014	0.0003	0.0099	0.0027
				1.0	0.0016	0.0002	0.01	0.0028
2	0.551	L8-N15	1800	0.0	0.0042	-0.0002	0.0196	0.006
				0.5	0.0045	0.0001	0.0194	0.0063
				1.0	0.0054	0.0008	0.0245	0.0076
3	0.68	L8-N15	1800	0.0	0.0032	0.0007	0.0193	0.0054
				0.5	0.0035	-0.0003	0.0187	0.0055
				1.0	0.0039	-0.0001	0.0192	0.0058
4	0.688	L8-N25	5000	0.0	0.0031	-0.0008	0.0194	0.0053
				0.5	0.0038	-0.0006	0.0197	0.0056
				1.0	0.005	-0.0007	0.0215	0.0068
5	0.764	L8-N64	32768	0.0	0.003	-0.0016	0.02	0.0056
				0.5	0.0054	-0.0035	0.021	0.0069
				1.0	0.008	-0.0053	0.0224	0.0096
6	0.779	L8-N15	1800	0.0	0.0044	0.0005	0.023	0.0069
				0.5	0.005	0.0004	0.0246	0.0072
				1.0	0.0071	-0.0006	0.0325	0.0097

Figure 2: MFASIS uncertainties for the instrument: Dscovr 1 Epic

Eos 1 Modis

Channel	Wavelength [µm]	NN-Def	NN-Parameters	Albedo	mae	me	p99	rmse
1	0.645	L8-N15	1800	0.0	0.0049	0.0019	0.0262	0.0075
				0.5	0.0056	0.0019	0.0268	0.008
				1.0	0.0075	0.0027	0.0324	0.0103
2	0.856	L8-N25	5000	0.0	0.0039	-0.0026	0.0223	0.0067
				0.5	0.005	-0.0011	0.0225	0.0074
				1.0	0.007	-0.0022	0.0303	0.0095
3	0.466	L8-N15	1800	0.0	0.005	0.0017	0.022	0.0068
				0.5	0.0045	-0.0007	0.024	0.0067
				1.0	0.0051	-0.0012	0.0313	0.0078
4	0.554	L8-N15	1800	0.0	0.0048	-0.0003	0.0241	0.0072
				0.5	0.0048	0.0007	0.0215	0.0068
				1.0	0.0069	0.0003	0.03	0.0094
5	1.242	L8-N25	5000	0.0	0.0036	-0.0012	0.0194	0.006
				0.5	0.0053	-0.0027	0.0216	0.0072
				1.0	0.0081	-0.0048	0.0292	0.0103
6	1.629	L8-N64	32768	0.0	0.0045	-0.0019	0.0343	0.009
				0.5	0.0068	-0.0001	0.0343	0.0102
				1.0	0.0103	0.0029	0.0399	0.0137
7	2.114	L8-N64	32768	0.0	0.004	-0.0028	0.0371	0.0092
				0.5	0.0058	-0.0045	0.0433	0.011
				1.0	0.0079	-0.006	0.0685	0.0149
8	0.412	L8-N15	1800	0.0	0.0042	0.0029	0.021	0.0063
				0.5	0.0033	0.0018	0.018	0.0052
				1.0	0.003	0.0011	0.0164	0.0047
9	0.442	L8-N15	1800	0.0	0.0043	0.0015	0.0235	0.0066
				0.5	0.0041	0.0009	0.0225	0.0063
				1.0	0.0051	0.0023	0.0242	0.0072
10	0.487	L8-N15	1800	0.0	0.0042	0.0001	0.0204	0.0061
				0.5	0.0038	-0.0002	0.019	0.0055
				1.0	0.0046	-0.0007	0.0189	0.0062
11	0.53	L8-N15	1800	0.0	0.0054	-0.0022	0.0244	0.0074
				0.5	0.0039	-0.0001	0.0212	0.006
				1.0	0.0042	0.0008	0.0213	0.0061
12	0.547	L8-N15	1800	0.0	0.0053	0.0033	0.0283	0.0079
				0.5	0.0059	0.0044	0.0232	0.0077
				1.0	0.0072	0.0049	0.0262	0.0093
13	0.666	L8-N15	1800	0.0	0.004	0.0003	0.0234	0.0064
				0.5	0.0051	0.0022	0.0259	0.0072
				1.0	0.006	0.0038	0.0314	0.0086
14	0.677	L8-N15	1800	0.0	0.0035	-0.0008	0.02	0.0055
				0.5	0.0037	0.0004	0.0186	0.0054
				1.0	0.0042	0.0015	0.0188	0.0058
15	0.747	L8-N15	1800	0.0	0.0048	-0.0005	0.0241	0.0074
				0.5	0.0062	0.0018	0.0227	0.0081
				1.0	0.009	0.0051	0.0366	0.012
16	0.866	L8-N15	1800	0.0	0.004	0.0015	0.0245	0.0067
				0.5	0.0039	0.0011	0.024	0.0064
				1.0	0.0048	0.0016	0.024	0.0071
17	0.904	L8-N64	32768	0.0	0.0029	-0.0008	0.0224	0.0057
				0.5	0.0037	-0.0016	0.0227	0.0061
				1.0	0.0052	-0.0028	0.0238	0.0075
18	0.936	L8-N64	32768	0.0	0.0034	0.0	0.0276	0.0071
				0.5	0.0048	0.0013	0.0294	0.0081

Eos 2 Modis

Channel	Wavelength [µm]	NN-Def	NN-Parameters	Albedo	mae	me	p99	rmse
1	0.645	L8-N15	1800	0.0	0.0055	0.003	0.0327	0.0088
				0.5	0.0074	0.0049	0.0301	0.0098
				1.0	0.0082	0.0042	0.034	0.0111
2	0.856	L8-N15	1800	0.0	0.0056	0.0004	0.0297	0.0089
				0.5	0.0064	0.0007	0.0256	0.0088
				1.0	0.0089	-0.0013	0.0444	0.0126
3	0.466	L8-N15	1800	0.0	0.005	0.0038	0.0253	0.0075
				0.5	0.004	0.0023	0.0209	0.006
				1.0	0.0037	0.0003	0.0188	0.0055
4	0.554	L8-N15	1800	0.0	0.0038	0.0009	0.0205	0.0058
				0.5	0.0041	0.0007	0.02	0.006
				1.0	0.0047	-0.0	0.021	0.0066
5	1.241	L8-N25	5000	0.0	0.003	-0.0004	0.0183	0.0053
				0.5	0.0039	-0.0004	0.0191	0.0059
				1.0	0.0057	-0.0011	0.0272	0.0081
6	1.628	L8-N64	32768	0.0	0.0059	-0.0008	0.0376	0.0105
				0.5	0.0105	0.0043	0.0386	0.0136
				1.0	0.0163	0.0102	0.0515	0.0201
7	2.113	L8-N64	32768	0.0	0.0044	-0.003	0.0393	0.0098
				0.5	0.0056	-0.0045	0.0395	0.0102
				1.0	0.0074	-0.0058	0.0397	0.0114
8	0.412	L8-N15	1800	0.0	0.0052	0.0001	0.0304	0.0081
				0.5	0.0038	0.0002	0.0215	0.0061
				1.0	0.0038	0.0004	0.0199	0.0056
9	0.442	L8-N15	1800	0.0	0.0034	-0.0009	0.0175	0.0053
				0.5	0.0036	-0.001	0.017	0.0053
				1.0	0.004	0.0001	0.0178	0.0056
10	0.487	L8-N15	1800	0.0	0.0054	0.0026	0.0248	0.0078
				0.5	0.0046	0.0012	0.0235	0.0069
				1.0	0.0054	-0.0005	0.0239	0.0075
11	0.53	L8-N15	1800	0.0	0.0039	-0.0015	0.0246	0.0064
				0.5	0.0039	-0.0003	0.0235	0.0062
				1.0	0.0043	0.0007	0.0229	0.0064
12	0.547	L8-N15	1800	0.0	0.0059	0.0046	0.0275	0.0085
				0.5	0.0051	0.003	0.0227	0.0071
				1.0	0.0056	0.0031	0.0223	0.0075
13	0.666	L8-N15	1800	0.0	0.0034	0.0007	0.0239	0.0061
				0.5	0.0036	0.0008	0.0237	0.0061
				1.0	0.0046	0.0014	0.0244	0.0069
14	0.678	L8-N15	1800	0.0	0.0036	0.0009	0.0215	0.0058
				0.5	0.0037	0.0007	0.0201	0.0057
				1.0	0.0044	0.0013	0.0206	0.0062
15	0.747	L8-N15	1800	0.0	0.0046	-0.002	0.0268	0.0074
				0.5	0.0059	0.0005	0.0281	0.0083
				1.0	0.0085	0.0046	0.0325	0.0114
16	0.867	L8-N15	1800	0.0	0.0034	0.0011	0.0211	0.0059
				0.5	0.0038	0.0007	0.0208	0.0059
				1.0	0.0049	0.0012	0.0219	0.0071
17	0.904	L8-N64	32768	0.0	0.0033	-0.001	0.0286	0.0068
				0.5	0.0039	-0.0012	0.0287	0.0071
				1.0	0.0049	-0.0011	0.0294	0.0078
18	0.936	L8-N64	32768	0.0	0.0045	-0.0009	0.0364	0.0089
				0.5	0.0055	-0.0003	0.0372	0.0096

Fy3 3 Virr

Channel	Wavelength [µm]	NN-Def	NN-Parameters	Albedo	mae	me	p99	rmse
1	0.46	L8-N15	1800	0.0	0.0032	0.0006	0.0209	0.0054
				0.5	0.0031	0.0002	0.0206	0.0052
				1.0	0.0036	-0.0	0.0211	0.0055
2	0.501	L8-N15	1800	0.0	0.0045	0.0014	0.0218	0.0066
				0.5	0.0049	0.002	0.0221	0.0069
				1.0	0.0058	0.0031	0.0242	0.008
3	0.543	L8-N15	1800	0.0	0.0052	0.0034	0.0247	0.0078
				0.5	0.0045	0.0027	0.0196	0.0064
				1.0	0.0049	0.003	0.0204	0.0067
4	0.635	L8-N15	1800	0.0	0.0081	0.007	0.0326	0.0108
				0.5	0.0069	0.0053	0.0309	0.0096
				1.0	0.007	0.0037	0.0296	0.0094
5	0.841	L8-N64	32768	0.0	0.0024	-0.0004	0.0201	0.0049
				0.5	0.0025	-0.001	0.0202	0.0049
				1.0	0.0029	-0.0011	0.0207	0.0052
6	1.362	L8-N64	32768	0.0	0.0043	0.0007	0.0385	0.0091
				0.5	0.0069	0.0028	0.0408	0.0109
				1.0	0.0096	0.0048	0.0515	0.0146
7	1.593	L8-N25	5000	0.0	0.0048	-0.0019	0.0358	0.0093
				0.5	0.0077	0.0008	0.0365	0.0111
				1.0	0.0112	0.0042	0.0478	0.0152

Figure 5: MFASIS uncertainties for the instrument: Fy3 3 Virr

Fy3 4 Mersi2

Channel	Wavelength [µm]	NN-Def	NN-Parameters	Albedo	mae	me	p99	rmse
1	0.412	L8-N15	1800	0.0	0.0039	0.0008	0.0225	0.0063
				0.5	0.0034	0.0009	0.0212	0.0058
				1.0	0.0041	-0.0003	0.022	0.0064
2	0.444	L8-N15	1800	0.0	0.0044	0.0006	0.0224	0.0069
				0.5	0.0039	0.0003	0.0209	0.0062
				1.0	0.0046	-0.0016	0.0232	0.0069
3	0.469	L8-N15	1800	0.0	0.0046	-0.0005	0.0195	0.0063
				0.5	0.004	-0.0002	0.0204	0.0059
				1.0	0.0045	0.0001	0.0254	0.0066
4	0.491	L8-N15	1800	0.0	0.0039	-0.0005	0.0245	0.0067
				0.5	0.0039	0.0003	0.026	0.0068
				1.0	0.0046	0.0013	0.0268	0.0073
5	0.553	L8-N15	1800	0.0	0.0058	0.0034	0.0242	0.008
				0.5	0.0048	0.0028	0.0212	0.0067
				1.0	0.0051	0.0024	0.0202	0.0068
6	0.556	L8-N15	1800	0.0	0.0044	-0.0026	0.0203	0.0066
				0.5	0.0055	0.0002	0.0197	0.0072
				1.0	0.0066	0.0024	0.0273	0.0087
7	0.653	L8-N15	1800	0.0	0.006	0.0039	0.0266	0.0085
				0.5	0.0064	0.0034	0.0264	0.0086
				1.0	0.0088	0.0052	0.0317	0.0115
8	0.67	L8-N15	1800	0.0	0.0046	-0.0022	0.0252	0.0072
				0.5	0.0048	-0.0006	0.0245	0.0071
				1.0	0.0058	0.002	0.0243	0.0078
9	0.709	L8-N64	32768	0.0	0.0026	-0.0012	0.0227	0.0054
				0.5	0.0032	-0.0008	0.0227	0.0058
				1.0	0.0041	-0.0003	0.0245	0.0067
10	0.746	L8-N25	5000	0.0	0.0037	-0.0018	0.0199	0.0062
				0.5	0.0046	-0.0019	0.0202	0.0067
				1.0	0.006	-0.0021	0.0236	0.008
11	0.865	L8-N15	1800	0.0	0.0052	0.0005	0.0305	0.0085
				0.5	0.0058	0.0018	0.0291	0.0082
				1.0	0.0088	0.005	0.032	0.0113
12	0.868	L8-N25	5000	0.0	0.003	-0.0008	0.0179	0.0049
				0.5	0.0037	-0.0006	0.0176	0.0054
				1.0	0.0059	-0.0001	0.0245	0.008
13	0.906	L8-N64	32768	0.0	0.0035	-0.0017	0.0278	0.0071
				0.5	0.0065	0.0007	0.0342	0.0101
				1.0	0.0092	0.0023	0.0527	0.0145
14	0.937	L8-N64	32768	0.0	0.004	-0.0001	0.0323	0.008
				0.5	0.0049	0.0001	0.0333	0.0086
				1.0	0.0062	0.0001	0.038	0.0101
15	0.94	L8-N64	32768	0.0	0.0036	-0.0001	0.0305	0.0074
				0.5	0.0045	0.0001	0.0314	0.008
				1.0	0.0059	-0.0002	0.0356	0.0095
16	1.03	L8-N15	1800	0.0	0.0054	0.0041	0.0256	0.0083
				0.5	0.0064	0.004	0.0254	0.0087
				1.0	0.0083	0.0041	0.0331	0.0111
17	1.381	L8-N64	32768	0.0	0.0045	-0.0011	0.0335	0.0082
				0.5	0.005	-0.0009	0.0375	0.0092
				1.0	0.0057	-0.0007	0.0462	0.0118
18	1.644	L8-N25	5000	0.0	0.0047	-0.0009	0.0277	0.0078
				0.5	0.0073	0.002	0.0283	0.0099

Fy4 1 Agri

Channel	Wavelength [µm]	NN-Def	NN-Parameters	Albedo	mae	me	p99	rmse
1	0.469	L8-N15	1800	0.0	0.0055	0.0027	0.0238	0.0078
				0.5	0.0058	0.003	0.0255	0.0082
				1.0	0.0053	0.0028	0.0261	0.0078
2	0.631	L8-N25	5000	0.0	0.0037	-0.0022	0.0196	0.0059
				0.5	0.0044	-0.0014	0.0197	0.0062
				1.0	0.0062	-0.0002	0.0221	0.0081
3	0.819	L8-N64	32768	0.0	0.0027	-0.0009	0.0214	0.0054
				0.5	0.0029	-0.0015	0.0215	0.0055
				1.0	0.0035	-0.0021	0.0219	0.0058
5	1.607	L8-N25	5000	0.0	0.0047	-0.0025	0.035	0.0092
				0.5	0.0057	-0.003	0.0351	0.0097
				1.0	0.0074	-0.0042	0.0367	0.011
6	2.226	L8-N64	32768	0.0	0.0039	-0.0024	0.0298	0.0078
				0.5	0.0053	-0.0028	0.0307	0.0086
				1.0	0.0069	-0.0034	0.0335	0.0101

Figure 7: MFASIS uncertainties for the instrument: Fy4 1 Agri

Fy4 2 Agri

Channel	Wavelength [µm]	NN-Def	NN-Parameters	Albedo	mae	me	p99	rmse
1	0.47	L8-N15	1800	0.0	0.0043	-0.0004	0.0256	0.0066
				0.5	0.0043	-0.0002	0.0251	0.0065
				1.0	0.0048	0.0005	0.0239	0.0068
2	0.628	L8-N25	5000	0.0	0.0029	-0.0009	0.0186	0.0051
				0.5	0.0035	-0.0012	0.0188	0.0055
				1.0	0.0046	-0.002	0.0203	0.0065
3	0.816	L8-N64	32768	0.0	0.0022	-0.0009	0.0166	0.0044
				0.5	0.0025	-0.0012	0.0166	0.0045
				1.0	0.0032	-0.0016	0.0172	0.005
4	1.377	L8-N64	32768	0.0	0.0036	-0.0007	0.0372	0.0085
				0.5	0.0041	-0.0007	0.0412	0.0097
				1.0	0.0047	-0.0007	0.0501	0.0128
5	1.611	L8-N25	5000	0.0	0.0044	-0.0022	0.0324	0.0088
				0.5	0.0069	0.0001	0.0331	0.0102
				1.0	0.0098	0.0023	0.0406	0.0134
6	2.219	L8-N64	32768	0.0	0.0041	-0.0021	0.033	0.0083
				0.5	0.0056	-0.0043	0.0294	0.0087
				1.0	0.0081	-0.0068	0.0388	0.0118

Figure 8: MFASIS uncertainties for the instrument: Fy4 2 Agri

Gkompsat2 1 Ami

Channel	Wavelength [µm]	NN-Def	NN-Parameters	Albedo	mae	me	p99	rmse
1	0.47	L8-N15	1800	0.0	0.0038	0.0009	0.0207	0.0058
				0.5	0.0043	0.0009	0.0208	0.0061
				1.0	0.0046	0.0009	0.0216	0.0065
2	0.509	L8-N15	1800	0.0	0.004	0.0009	0.0205	0.006
				0.5	0.0042	0.0016	0.0201	0.0061
				1.0	0.0058	0.0039	0.0246	0.0079
3	0.639	L8-N15	1800	0.0	0.006	0.0036	0.0312	0.009
				0.5	0.0067	0.0052	0.0268	0.0089
				1.0	0.0101	0.0082	0.0335	0.0131
4	0.863	L8-N15	1800	0.0	0.005	-0.0004	0.0277	0.0078
				0.5	0.006	0.0024	0.0263	0.0083
				1.0	0.0092	0.0051	0.0367	0.0125
5	1.374	L8-N64	32768	0.0	0.0033	0.0003	0.0336	0.0078
				0.5	0.0037	0.0004	0.0365	0.0086
				1.0	0.0042	0.0006	0.0438	0.0106
6	1.609	L8-N25	5000	0.0	0.0047	-0.0026	0.0349	0.0093
				0.5	0.0059	-0.0027	0.0349	0.0097
				1.0	0.0074	-0.0024	0.0357	0.0108

Figure 9: MFASIS uncertainties for the instrument: Gkompsat2 1 Ami

Goes 13 Imager

Channel	Wavelength [µm]	NN-Def	NN-Parameters	Albedo	mae	me	p99	rmse
1	0.623	L8-N15	1800	0.0	0.0052	0.0025	0.0275	0.0078
				0.5	0.0058	0.0026	0.0273	0.0083
				1.0	0.0083	0.0041	0.0348	0.0112

Figure 10: MFASIS uncertainties for the instrument: Goes 13 Imager

Goes 14 Imager

Channel	Wavelength [µm]	NN-Def	NN-Parameters	Albedo	mae	me	p99	rmse
1	0.621	L8-N15	1800	0.0	0.0055	0.0027	0.0284	0.0081
				0.5	0.0058	0.0014	0.026	0.008
				1.0	0.0079	-0.0	0.0296	0.0104

Figure 11: MFASIS uncertainties for the instrument: Goes 14 Imager

Goes 15 Imager

Channel	Wavelength [µm]	NN-Def	NN-Parameters	Albedo	mae	me	p99	rmse
1	0.621	L8-N25	5000	0.0	0.003	-0.0005	0.0165	0.0049
				0.5	0.0034	-0.0003	0.0166	0.005
				1.0	0.0042	0.0001	0.0175	0.0058

Figure 12: MFASIS uncertainties for the instrument: Goes 15 Imager

Goes 16 Abi

Channel	Wavelength [µm]	NN-Def	NN-Parameters	Albedo	mae	me	p99	rmse
1	0.47	L8-N15	1800	0.0	0.0053	0.0025	0.0238	0.0076
				0.5	0.0051	0.0015	0.0234	0.0072
				1.0	0.0056	-0.0001	0.0241	0.0078
2	0.636	L8-N15	1800	0.0	0.0047	0.0006	0.0254	0.0071
				0.5	0.0052	0.0016	0.0252	0.0073
				1.0	0.0066	0.0029	0.0269	0.0088
3	0.864	L8-N25	5000	0.0	0.0031	-0.0008	0.0183	0.0053
				0.5	0.004	-0.0018	0.0184	0.0058
				1.0	0.0057	-0.0022	0.0217	0.0077
4	1.373	L8-N64	32768	0.0	0.0037	0.0007	0.0385	0.0089
				0.5	0.0045	0.0014	0.0455	0.0109
				1.0	0.0053	0.002	0.0591	0.0155
5	1.609	L8-N15	1800	0.0	0.0044	-0.0026	0.0311	0.0086
				0.5	0.0056	-0.0032	0.0313	0.0092
				1.0	0.0075	-0.0034	0.0352	0.0108
6	2.242	L8-N64	32768	0.0	0.0036	-0.0021	0.0275	0.0072
				0.5	0.005	-0.0036	0.0275	0.0079
				1.0	0.0069	-0.0053	0.0313	0.01

Figure 13: MFASIS uncertainties for the instrument: Goes 16 Abi

Goes 17 Abi

Channel	Wavelength [µm]	NN-Def	NN-Parameters	Albedo	mae	me	p99	rmse
1	0.47	L8-N15	1800	0.0	0.0056	0.0029	0.0264	0.0082
				0.5	0.0051	0.0027	0.0234	0.0071
				1.0	0.0044	0.0012	0.024	0.0067
2	0.636	L8-N15	1800	0.0	0.0042	0.0012	0.0212	0.0063
				0.5	0.0049	0.0018	0.0209	0.0067
				1.0	0.0068	0.0035	0.0251	0.009
3	0.864	L8-N15	1800	0.0	0.0048	-0.0022	0.0253	0.0075
				0.5	0.0059	0.0004	0.0261	0.0081
				1.0	0.0093	0.0039	0.0353	0.0123
4	1.372	L8-N64	32768	0.0	0.0039	0.0014	0.0395	0.0091
				0.5	0.0045	0.0017	0.0447	0.0104
				1.0	0.0052	0.002	0.0551	0.0136
5	1.608	L8-N25	5000	0.0	0.0047	-0.0024	0.0343	0.0091
				0.5	0.0069	-0.0004	0.0343	0.0101
				1.0	0.0101	0.0023	0.0354	0.0129
6	2.242	L8-N64	32768	0.0	0.0038	-0.0025	0.0272	0.0074
				0.5	0.0054	-0.0043	0.0281	0.0085
				1.0	0.0076	-0.0061	0.0371	0.0113

Figure 14: MFASIS uncertainties for the instrument: Goes 17 Abi

Goes 18 Abi

Channel	Wavelength [µm]	NN-Def	NN-Parameters	Albedo	mae	me	p99	rmse
1	0.47	L8-N15	1800	0.0	0.0049	0.0025	0.0239	0.0069
				0.5	0.0045	0.0024	0.0235	0.0067
				1.0	0.0049	0.0025	0.0246	0.0073
2	0.636	L8-N15	1800	0.0	0.0045	0.0005	0.0224	0.0067
				0.5	0.0051	0.0015	0.0234	0.0072
				1.0	0.0067	0.0022	0.0329	0.0094
3	0.863	L8-N15	1800	0.0	0.0054	0.0015	0.0305	0.0088
				0.5	0.0072	0.0041	0.0294	0.0097
				1.0	0.0115	0.0083	0.0415	0.015
4	1.372	L8-N64	32768	0.0	0.0041	0.0024	0.0385	0.0092
				0.5	0.0049	0.0031	0.0468	0.0112
				1.0	0.0057	0.0037	0.0613	0.0154
5	1.608	L8-N64	32768	0.0	0.0057	-0.0013	0.0373	0.0103
				0.5	0.0091	0.0023	0.0394	0.0126
				1.0	0.0133	0.0064	0.0486	0.0171
6	2.241	L8-N64	32768	0.0	0.0034	-0.002	0.0267	0.0069
				0.5	0.005	-0.0016	0.0271	0.0076
				1.0	0.0066	-0.0021	0.0306	0.0094

Figure 15: MFASIS uncertainties for the instrument: Goes 18 Abi

Goes 19 Abi

Channel	Wavelength [µm]	NN-Def	NN-Parameters	Albedo	mae	me	p99	rmse
1	0.47	L8-N15	1800	0.0	0.0039	0.0015	0.0195	0.0057
				0.5	0.0036	0.0005	0.0189	0.0054
				1.0	0.0041	-0.0004	0.0187	0.0058
2	0.636	L8-N15	1800	0.0	0.005	0.0009	0.0245	0.0075
				0.5	0.0059	0.001	0.0291	0.0084
				1.0	0.0085	0.0021	0.042	0.012
3	0.863	L8-N25	5000	0.0	0.0037	-0.0001	0.0219	0.0062
				0.5	0.0057	-0.001	0.0281	0.0083
				1.0	0.0086	-0.0021	0.0455	0.0127
4	1.372	L8-N64	32768	0.0	0.0035	0.0009	0.0364	0.0082
				0.5	0.004	0.0009	0.0394	0.0091
				1.0	0.0045	0.0009	0.0431	0.0117
5	1.608	L8-N15	1800	0.0	0.0066	-0.0003	0.0378	0.0115
				0.5	0.0126	0.0057	0.0395	0.0155
				1.0	0.0164	0.0094	0.0545	0.0203
6	2.241	L8-N64	32768	0.0	0.0038	-0.0022	0.0294	0.0075
				0.5	0.0049	-0.0019	0.0294	0.0079
				1.0	0.0063	-0.0016	0.0295	0.0089

Figure 16: MFASIS uncertainties for the instrument: Goes 19 Abi

Himawari 8 Ahi

Channel	Wavelength [µm]	NN-Def	NN-Parameters	Albedo	mae	me	p99	rmse
1	0.47	L8-N15	1800	0.0	0.0036	0.0005	0.0215	0.0058
				0.5	0.0036	0.0007	0.0218	0.0058
				1.0	0.004	0.0011	0.0223	0.0061
2	0.509	L8-N15	1800	0.0	0.005	0.0013	0.0236	0.0074
				0.5	0.0049	0.0018	0.022	0.0069
				1.0	0.0062	0.0032	0.0231	0.0082
3	0.636	L8-N15	1800	0.0	0.0055	0.0028	0.0278	0.0082
				0.5	0.0061	0.0029	0.0298	0.0087
				1.0	0.0071	0.0029	0.0321	0.0099
4	0.856	L8-N25	5000	0.0	0.0033	-0.0006	0.0213	0.0058
				0.5	0.0041	-0.0025	0.021	0.0062
				1.0	0.0076	-0.0065	0.0311	0.0102
5	1.61	L8-N25	5000	0.0	0.0048	-0.0022	0.0324	0.0089
				0.5	0.0058	-0.0018	0.0328	0.0095
				1.0	0.0071	-0.0018	0.0353	0.0107
6	2.256	L8-N64	32768	0.0	0.0037	-0.0022	0.028	0.0073
				0.5	0.0047	-0.0032	0.0279	0.0079
				1.0	0.0064	-0.0045	0.0327	0.0097

Figure 17: MFASIS uncertainties for the instrument: Himawari 8 Ahi

Himawari 9 Ahi

Channel	Wavelength [µm]	NN-Def	NN-Parameters	Albedo	mae	me	p99	rmse
1	0.47	L8-N15	1800	0.0	0.005	-0.0001	0.0255	0.0075
				0.5	0.0039	0.0004	0.0232	0.0064
				1.0	0.0039	0.0007	0.0228	0.0062
2	0.509	L8-N15	1800	0.0	0.004	-0.001	0.0229	0.0063
				0.5	0.004	0.0002	0.0205	0.006
				1.0	0.0056	0.0024	0.0215	0.0075
3	0.637	L8-N15	1800	0.0	0.0061	0.0042	0.0256	0.0082
				0.5	0.0057	0.003	0.0256	0.0079
				1.0	0.0069	0.0031	0.0269	0.0092
4	0.856	L8-N25	5000	0.0	0.0033	-0.0014	0.0211	0.0059
				0.5	0.0044	-0.0008	0.0216	0.0065
				1.0	0.0061	-0.0017	0.0262	0.0083
5	1.606	L8-N15	1800	0.0	0.005	-0.0018	0.0354	0.0095
				0.5	0.0092	0.0024	0.0359	0.0121
				1.0	0.0139	0.007	0.0456	0.0173
6	2.257	L8-N64	32768	0.0	0.0037	-0.002	0.0271	0.0071
				0.5	0.0054	-0.0018	0.0276	0.0081
				1.0	0.0075	-0.0018	0.0376	0.0107

Figure 18: MFASIS uncertainties for the instrument: Himawari 9 Ahi

Insat3 6 Imager

Channel	Wavelength [µm]	NN-Def	NN-Parameters	Albedo	mae	me	p99	rmse
1	0.639	L8-N25	5000	0.0	0.0036	0.0003	0.0195	0.0056
				0.5	0.0045	0.0008	0.0209	0.0065
				1.0	0.0059	0.0024	0.0289	0.0084
2	1.61	L8-N25	5000	0.0	0.0048	-0.0016	0.0325	0.0089
				0.5	0.0071	-0.0001	0.0341	0.0106
				1.0	0.0104	0.0018	0.0487	0.0147

Figure 19: MFASIS uncertainties for the instrument: Insat3 6 Imager

Jpss 0 Viirs

Channel	Wavelength [µm]	NN-Def	NN-Parameters	Albedo	mae	me	p99	rmse
1	0.635	L8-N15	1800	0.0	0.0045	0.0018	0.0259	0.0071
				0.5	0.0053	0.0014	0.0258	0.0076
				1.0	0.0072	0.0028	0.0278	0.0096
2	0.861	L8-N15	1800	0.0	0.0052	0.0004	0.0285	0.0086
				0.5	0.0072	0.0026	0.0279	0.0097
				1.0	0.0113	0.0058	0.0395	0.0149
3	0.41	L8-N15	1800	0.0	0.0047	0.0005	0.0273	0.0073
				0.5	0.0046	0.0006	0.028	0.0072
				1.0	0.005	0.0002	0.0287	0.0077
4	0.443	L8-N15	1800	0.0	0.0065	0.0042	0.0264	0.0087
				0.5	0.0055	0.0022	0.0252	0.0075
				1.0	0.0051	0.0004	0.0281	0.0075
5	0.486	L8-N15	1800	0.0	0.005	0.0031	0.0254	0.0078
				0.5	0.0042	0.0032	0.0222	0.0063
				1.0	0.0038	0.0019	0.0207	0.0057
6	0.55	L8-N15	1800	0.0	0.0048	0.0029	0.0256	0.0074
				0.5	0.0044	0.0023	0.0214	0.0064
				1.0	0.0052	0.0032	0.0193	0.0068
7	0.671	L8-N15	1800	0.0	0.0039	-0.0013	0.0243	0.0066
				0.5	0.0041	-0.0007	0.0241	0.0066
				1.0	0.0049	0.0014	0.0239	0.0072
8	0.745	L8-N15	1800	0.0	0.005	-0.0006	0.0301	0.0081
				0.5	0.0064	0.0008	0.0298	0.009
				1.0	0.0095	0.0028	0.0366	0.0124
9	0.861	L8-N25	5000	0.0	0.0029	-0.0008	0.0197	0.0052
				0.5	0.0037	0.0002	0.0194	0.0055
				1.0	0.0043	-0.0005	0.0208	0.0064
10	0.657	L8-N25	5000	0.0	0.0039	-0.0011	0.0204	0.0062
				0.5	0.0042	-0.0015	0.0203	0.0062
				1.0	0.0054	-0.0005	0.0218	0.0074
11	1.238	L8-N25	5000	0.0	0.0041	-0.0018	0.0325	0.0077
				0.5	0.0072	0.0018	0.0238	0.0089
				1.0	0.0111	0.0046	0.0351	0.014
13	1.601	L8-N25	5000	0.0	0.005	-0.0032	0.0369	0.0097
				0.5	0.0075	-0.0007	0.0371	0.011
				1.0	0.01	0.0016	0.0421	0.0136
14	1.601	L8-N15	1800	0.0	0.006	-0.0012	0.0363	0.0105
				0.5	0.0119	0.0053	0.0453	0.0153
				1.0	0.0191	0.0125	0.0734	0.0247
15	2.257	L8-N64	32768	0.0	0.0036	-0.0021	0.0277	0.0072
				0.5	0.0046	-0.0028	0.0277	0.0077
				1.0	0.0061	-0.0034	0.0329	0.0093

Figure 20: MFASIS uncertainties for the instrument: Jpss 0 Viirs

Metop 1 Avhrr

Channel	Wavelength [µm]	NN-Def	NN-Parameters	Albedo	mae	me	p99	rmse
1	0.633	L8-N15	1800	0.0	0.005	0.0019	0.0266	0.0076
				0.5	0.0058	0.0026	0.0241	0.0079
				1.0	0.0081	0.0042	0.029	0.0107
2	0.848	L8-N64	32768	0.0	0.0028	-0.0016	0.0232	0.0056
				0.5	0.0033	-0.0019	0.0232	0.0058
				1.0	0.004	-0.0018	0.0242	0.0064
3	1.608	L8-N25	5000	0.0	0.0043	-0.002	0.0337	0.0088
				0.5	0.0057	-0.001	0.034	0.0095
				1.0	0.0075	-0.0002	0.0371	0.0111

Figure 21: MFASIS uncertainties for the instrument: Metop 1 Avhrr

Metop 2 Avhrr

Channel	Wavelength [µm]	NN-Def	NN-Parameters	Albedo	mae	me	p99	rmse
1	0.631	L8-N25	5000	0.0	0.003	0.0005	0.017	0.0048
				0.5	0.0029	0.0003	0.0171	0.0049
				1.0	0.0035	-0.0005	0.0191	0.0055
2	0.835	L8-N64	32768	0.0	0.0028	-0.001	0.0243	0.0058
				0.5	0.003	-0.0016	0.0244	0.0059
				1.0	0.0037	-0.0025	0.0251	0.0063
3	1.606	L8-N64	32768	0.0	0.0047	-0.0026	0.0349	0.0091
				0.5	0.007	-0.0003	0.0349	0.0103
				1.0	0.0098	0.0021	0.0396	0.0131

Figure 22: MFASIS uncertainties for the instrument: Metop 2 Avhrr

Metop 3 Avhrr

Channel	Wavelength [µm]	NN-Def	NN-Parameters	Albedo	mae	me	p99	rmse
1	0.627	L8-N15	1800	0.0	0.0056	0.0006	0.0296	0.0086
				0.5	0.0061	0.0024	0.0263	0.0083
				1.0	0.0097	0.0051	0.0324	0.0125
2	0.832	L8-N64	32768	0.0	0.0028	-0.0006	0.0197	0.0051
				0.5	0.003	-0.0019	0.0199	0.0052
				1.0	0.0041	-0.003	0.0211	0.006
3	1.607	L8-N25	5000	0.0	0.0048	-0.0021	0.0345	0.0092
				0.5	0.0064	-0.0007	0.0348	0.0102
				1.0	0.0083	0.0003	0.0387	0.012

Figure 23: MFASIS uncertainties for the instrument: Metop 3 Avhrr

Metopsg 1 Metimage

Channel	Wavelength [µm]	NN-Def	NN-Parameters	Albedo	mae	me	p99	rmse
1	0.443	L8-N15	1800	0.0	0.0048	0.0031	0.0242	0.0075
				0.5	0.0043	0.0025	0.0236	0.0067
				1.0	0.0041	0.0019	0.0232	0.0063
2	0.556	L8-N15	1800	0.0	0.0035	0.0003	0.021	0.0056
				0.5	0.0042	-0.0012	0.0209	0.006
				1.0	0.0054	-0.002	0.0213	0.0074
3	0.669	L8-N15	1800	0.0	0.0036	-0.0015	0.0192	0.0057
				0.5	0.0045	0.0012	0.0174	0.0059
				1.0	0.0057	0.0033	0.0185	0.0072
4	0.753	L8-N15	1800	0.0	0.0051	-0.0019	0.0261	0.0074
				0.5	0.0039	-0.0006	0.0227	0.0062
				1.0	0.004	-0.0008	0.0218	0.0062
5	0.762	L8-N25	5000	0.0	0.0032	-0.0019	0.0237	0.006
				0.5	0.0034	-0.0024	0.0238	0.0061
				1.0	0.0041	-0.0034	0.0248	0.0066
6	0.863	L8-N15	1800	0.0	0.0042	0.0004	0.026	0.0071
				0.5	0.0052	0.0019	0.0239	0.0073
				1.0	0.0081	0.0043	0.029	0.0107
7	0.914	L8-N64	32768	0.0	0.0031	-0.0014	0.0274	0.0066
				0.5	0.0043	-0.0006	0.0277	0.0072
				1.0	0.0057	-0.0001	0.0297	0.0086
8	1.241	L8-N25	5000	0.0	0.0031	-0.0004	0.0201	0.0056
				0.5	0.0054	0.0003	0.021	0.0071
				1.0	0.0094	0.0017	0.0319	0.0121
9	1.377	L8-N64	32768	0.0	0.0035	0.0006	0.0377	0.0084
				0.5	0.0041	0.0009	0.0396	0.0092
				1.0	0.0046	0.0013	0.0488	0.0111
11	2.25	L8-N64	32768	0.0	0.0039	-0.002	0.0294	0.0077
				0.5	0.0057	-0.0007	0.0294	0.0086
				1.0	0.0076	0.0002	0.0305	0.0104

Figure 24: MFASIS uncertainties for the instrument: Metopsg 1 Metimage

Msg 1 Seviri

Channel	Wavelength [µm]	NN-Def	NN-Parameters	Albedo	mae	me	p99	rmse
1	0.639	L8-N15	1800	0.0	0.005	-0.0017	0.0263	0.0074
				0.5	0.0049	-0.0016	0.026	0.0073
				1.0	0.0057	-0.0015	0.0264	0.0078
2	0.809	L8-N25	5000	0.0	0.0046	-0.0017	0.0296	0.0079
				0.5	0.0061	-0.0037	0.03	0.0088
				1.0	0.0103	-0.0082	0.0405	0.014
3	1.634	L8-N64	32768	0.0	0.0051	-0.0015	0.0337	0.0094
				0.5	0.0071	-0.0002	0.0347	0.0106
				1.0	0.0099	0.0014	0.0428	0.0137
12	0.677	L8-N25	5000	0.0	0.004	-0.0016	0.0231	0.0065
				0.5	0.0046	-0.0017	0.0235	0.0069
				1.0	0.0055	-0.002	0.0249	0.0077

Figure 25: MFASIS uncertainties for the instrument: Msg 1 Seviri

Msg 2 Seviri

Channel	Wavelength [µm]	NN-Def	NN-Parameters	Albedo	mae	me	p99	rmse
1	0.639	L8-N15	1800	0.0	0.0048	0.001	0.0228	0.0071
				0.5	0.0045	-0.0002	0.0218	0.0066
				1.0	0.0053	0.0001	0.0215	0.0071
2	0.808	L8-N64	32768	0.0	0.0021	-0.0004	0.016	0.0042
				0.5	0.0026	-0.0006	0.0163	0.0045
				1.0	0.0034	-0.0008	0.0172	0.0053
3	1.637	L8-N64	32768	0.0	0.0053	-0.0031	0.0372	0.0101
				0.5	0.008	-0.0009	0.0391	0.012
				1.0	0.0111	0.0008	0.0519	0.0156
12	0.675	L8-N64	32768	0.0	0.0024	-0.0008	0.018	0.0047
				0.5	0.0026	-0.0012	0.0181	0.0048
				1.0	0.0034	-0.0023	0.0184	0.0053

Figure 26: MFASIS uncertainties for the instrument: Msg 2 Seviri

Msg 3 Seviri

Channel	Wavelength [µm]	NN-Def	NN-Parameters	Albedo	mae	me	p99	rmse
1	0.637	L8-N25	5000	0.0	0.0026	-0.0005	0.0154	0.0044
				0.5	0.0027	-0.0004	0.0156	0.0044
				1.0	0.0034	-0.0011	0.017	0.005
2	0.808	L8-N64	32768	0.0	0.0046	-0.0019	0.0351	0.0087
				0.5	0.0058	-0.0013	0.0354	0.0092
				1.0	0.0072	-0.0005	0.0368	0.0104
3	1.637	L8-N64	32768	0.0	0.0047	-0.0015	0.0339	0.0089
				0.5	0.0079	0.0016	0.035	0.0111
				1.0	0.0113	0.0048	0.0468	0.0154
12	0.676	L8-N25	5000	0.0	0.003	-0.0006	0.0198	0.0052
				0.5	0.0036	-0.0004	0.02	0.0056
				1.0	0.0049	0.0002	0.0214	0.0069

Figure 27: MFASIS uncertainties for the instrument: Msg 3 Seviri

Msg 4 Seviri

Channel	Wavelength [µm]	NN-Def	NN-Parameters	Albedo	mae	me	p99	rmse
1	0.637	L8-N25	5000	0.0	0.0034	-0.0004	0.0172	0.0052
				0.5	0.0035	0.0003	0.0167	0.0053
				1.0	0.0044	0.0007	0.0186	0.0061
2	0.807	L8-N64	32768	0.0	0.0043	-0.0009	0.0322	0.008
				0.5	0.0057	-0.0017	0.0329	0.0089
				1.0	0.008	-0.0039	0.0376	0.0115
3	1.636	L8-N64	32768	0.0	0.0052	-0.0023	0.0342	0.0094
				0.5	0.0071	-0.0008	0.0348	0.0106
				1.0	0.0096	-0.0008	0.0391	0.0129
12	0.612	L8-N64	32768	0.0	0.004	-0.0021	0.0307	0.0077
				0.5	0.0058	-0.0018	0.0308	0.0086
				1.0	0.0072	-0.0038	0.0318	0.0101

Figure 28: MFASIS uncertainties for the instrument: Msg 4 Seviri

Mtg 1 Fci

Channel	Wavelength [µm]	NN-Def	NN-Parameters	Albedo	mae	me	p99	rmse
1	0.444	L8-N15	1800	0.0	0.0051	0.0023	0.0274	0.008
				0.5	0.0043	0.0012	0.0251	0.0068
				1.0	0.0044	0.0008	0.0245	0.0066
2	0.51	L8-N15	1800	0.0	0.004	0.0011	0.0228	0.0063
				0.5	0.004	0.0013	0.0218	0.0061
				1.0	0.0047	0.0022	0.0224	0.0068
3	0.64	L8-N15	1800	0.0	0.0042	-0.0001	0.0217	0.0066
				0.5	0.0059	0.002	0.0226	0.0079
				1.0	0.0084	0.0047	0.0318	0.0112
4	0.865	L8-N25	5000	0.0	0.0029	-0.0007	0.0165	0.0049
				0.5	0.0039	-0.0016	0.0175	0.0056
				1.0	0.0059	-0.0033	0.0268	0.0083
5	0.914	L8-N64	32768	0.0	0.0028	0.0004	0.0226	0.0058
				0.5	0.0043	-0.0007	0.0235	0.0067
				1.0	0.0059	-0.0016	0.027	0.0085
6	1.38	L8-N64	32768	0.0	0.0038	0.0013	0.0383	0.0095
				0.5	0.0043	0.0017	0.0413	0.0101
				1.0	0.0049	0.0021	0.0496	0.0118
7	1.61	L8-N25	5000	0.0	0.0046	-0.0026	0.0348	0.009
				0.5	0.0059	-0.0017	0.0354	0.0096
				1.0	0.0073	-0.001	0.0367	0.0109
8	2.25	L8-N64	32768	0.0	0.0034	-0.0019	0.0257	0.0068
				0.5	0.0054	-0.0044	0.0259	0.0082
				1.0	0.0082	-0.0073	0.0375	0.0121

Figure 29: MFASIS uncertainties for the instrument: Mtg 1 Fci

Noaa 14 Avhrr

Channel	Wavelength [µm]	NN-Def	NN-Parameters	Albedo	mae	me	p99	rmse
1	0.636	L8-N25	5000	0.0	0.0033	0.0001	0.0172	0.0053
				0.5	0.0037	0.0007	0.017	0.0054
				1.0	0.0048	0.0013	0.0181	0.0065
2	0.831	L8-N64	32768	0.0	0.0031	-0.0015	0.0271	0.0063
				0.5	0.0034	-0.0017	0.0271	0.0064
				1.0	0.0041	-0.002	0.0276	0.0068

Figure 30: MFASIS uncertainties for the instrument: Noaa 14 Avhrr

Noaa 20 Viirs

Channel	Wavelength [µm]	NN-Def	NN-Parameters	Albedo	mae	me	p99	rmse
1	0.641	L8-N15	1800	0.0	0.0052	0.0006	0.0226	0.0073
				0.5	0.005	0.0001	0.0216	0.007
				1.0	0.0058	0.0004	0.0237	0.0078
2	0.867	L8-N15	1800	0.0	0.0053	0.0003	0.0259	0.0081
				0.5	0.0059	0.0016	0.0236	0.008
				1.0	0.0093	0.0047	0.0317	0.0119
3	0.411	L8-N15	1800	0.0	0.0062	0.0048	0.024	0.008
				0.5	0.0049	0.0027	0.0227	0.0068
				1.0	0.0047	0.0012	0.0235	0.0067
4	0.444	L8-N15	1800	0.0	0.0038	0.0011	0.0219	0.0061
				0.5	0.0037	0.0017	0.0208	0.0059
				1.0	0.0045	0.0021	0.0211	0.0066
5	0.489	L8-N15	1800	0.0	0.0041	0.0017	0.0233	0.0065
				0.5	0.0035	0.0013	0.0221	0.0058
				1.0	0.004	0.0002	0.0226	0.006
6	0.556	L8-N15	1800	0.0	0.004	0.0013	0.0203	0.006
				0.5	0.0042	-0.0001	0.0201	0.006
				1.0	0.0053	-0.0008	0.0255	0.0075
7	0.667	L8-N15	1800	0.0	0.0049	-0.0009	0.0263	0.0075
				0.5	0.0054	-0.0004	0.0313	0.0083
				1.0	0.0069	0.0001	0.0355	0.0101
8	0.746	L8-N25	5000	0.0	0.0035	-0.0013	0.0193	0.0058
				0.5	0.0043	-0.0014	0.0201	0.0064
				1.0	0.0055	-0.0022	0.0232	0.0076
9	0.867	L8-N15	1800	0.0	0.0053	0.0001	0.0236	0.0077
				0.5	0.0057	0.0012	0.0235	0.0078
				1.0	0.0084	0.0043	0.0301	0.0111
10	0.652	L8-N64	32768	0.0	0.0063	0.0006	0.0335	0.0097
				0.5	0.007	-0.0007	0.033	0.01
				1.0	0.0103	-0.001	0.0367	0.0132
11	1.238	L8-N25	5000	0.0	0.0034	0.0003	0.0207	0.0059
				0.5	0.0046	-0.0001	0.0211	0.0067
				1.0	0.0073	-0.0006	0.0322	0.0101
12	1.375	L8-N64	32768	0.0	0.0035	0.0012	0.0345	0.0081
				0.5	0.0041	0.0015	0.039	0.0091
				1.0	0.0047	0.0018	0.0489	0.0115
13	1.603	L8-N25	5000	0.0	0.0051	-0.0019	0.0352	0.0095
				0.5	0.0084	0.0013	0.0366	0.0117
				1.0	0.0119	0.0046	0.0478	0.0159
14	1.604	L8-N25	5000	0.0	0.0046	-0.0023	0.0347	0.0091
				0.5	0.0074	0.0004	0.0351	0.0108
				1.0	0.0097	0.0023	0.0406	0.0134
15	2.258	L8-N64	32768	0.0	0.0037	-0.0024	0.027	0.0073
				0.5	0.0053	-0.0038	0.0273	0.0083
				1.0	0.0074	-0.0052	0.0355	0.011

Figure 31: MFASIS uncertainties for the instrument: Noaa 20 Viirs

Noaa 21 Viirs

Channel	Wavelength [µm]	NN-Def	NN-Parameters	Albedo	mae	me	p99	rmse
1	0.64	L8-N15	1800	0.0	0.0046	-0.0002	0.0236	0.007
				0.5	0.0045	-0.0019	0.0216	0.0068
				1.0	0.0059	-0.0031	0.0257	0.0082
2	0.867	L8-N15	1800	0.0	0.0048	0.0009	0.0299	0.0081
				0.5	0.006	0.0032	0.0293	0.0087
				1.0	0.0102	0.0073	0.0364	0.0134
3	0.411	L8-N15	1800	0.0	0.0048	0.0008	0.0274	0.0075
				0.5	0.0059	-0.0022	0.0327	0.0088
				1.0	0.0075	-0.0035	0.0353	0.0108
4	0.445	L8-N15	1800	0.0	0.0041	0.0006	0.0246	0.0068
				0.5	0.0041	0.0003	0.0237	0.0066
				1.0	0.0046	0.0013	0.025	0.0072
5	0.488	L8-N15	1800	0.0	0.004	0.0002	0.0255	0.0066
				0.5	0.0039	0.0012	0.0211	0.006
				1.0	0.0041	0.002	0.0218	0.0062
6	0.555	L8-N15	1800	0.0	0.0039	0.0017	0.021	0.0061
				0.5	0.0033	0.0008	0.0174	0.0051
				1.0	0.0035	-0.0002	0.0173	0.0051
7	0.671	L8-N15	1800	0.0	0.004	-0.0004	0.021	0.0062
				0.5	0.0046	0.0006	0.0224	0.0067
				1.0	0.0055	0.0006	0.0302	0.0081
8	0.747	L8-N15	1800	0.0	0.0049	0.0012	0.0252	0.0075
				0.5	0.0084	0.0046	0.0352	0.0111
				1.0	0.0122	0.0087	0.0508	0.0165
9	0.868	L8-N15	1800	0.0	0.0051	0.0002	0.0269	0.0078
				0.5	0.0062	0.0013	0.0259	0.0085
				1.0	0.0098	0.0044	0.0365	0.013
10	0.653	L8-N15	1800	0.0	0.0058	0.0018	0.0319	0.0088
				0.5	0.0062	0.0007	0.0288	0.0087
				1.0	0.0085	0.001	0.0326	0.0111
11	1.241	L8-N25	5000	0.0	0.0031	0.0002	0.0197	0.0055
				0.5	0.0039	-0.0012	0.0201	0.0059
				1.0	0.0056	-0.0025	0.0231	0.0075
12	1.382	L8-N64	32768	0.0	0.0035	0.0017	0.0353	0.0081
				0.5	0.004	0.0021	0.0373	0.0088
				1.0	0.0046	0.0025	0.0453	0.0104
13	1.613	L8-N25	5000	0.0	0.0047	-0.0018	0.0338	0.009
				0.5	0.0072	0.0006	0.0344	0.0103
				1.0	0.0106	0.0037	0.0388	0.0136
14	1.613	L8-N64	32768	0.0	0.0034	-0.002	0.0293	0.0076
				0.5	0.0039	-0.0018	0.0294	0.0078
				1.0	0.0048	-0.0019	0.0296	0.0084
15	2.251	L8-N64	32768	0.0	0.0036	-0.0024	0.0278	0.0073
				0.5	0.0071	0.0001	0.0477	0.0121
				1.0	0.0099	0.0013	0.073	0.0172

Figure 32: MFASIS uncertainties for the instrument: Noaa 21 Viirs

Sentinel3 1 Olci2Chn

Channel	Wavelength [µm]	NN-Def	NN-Parameters	Albedo	mae	me	p99	rmse
1	0.665	L8-N15	1800	0.0	0.0034	-0.0005	0.0236	0.0061
				0.5	0.0044	0.001	0.023	0.0064
				1.0	0.0061	0.0032	0.0237	0.008
2	0.865	L8-N15	1800	0.0	0.0041	0.0009	0.0212	0.0064
				0.5	0.004	0.0018	0.0194	0.006
				1.0	0.0053	0.0026	0.0211	0.0074

Figure 33: MFASIS uncertainties for the instrument: Sentinel3 1 Olci2Chn

Sentinel3 2 Olci2Chn

Channel	Wavelength [µm]	NN-Def	NN-Parameters	Albedo	mae	me	p99	rmse
1	0.665	L8-N15	1800	0.0	0.0042	-0.0003	0.0247	0.0068
				0.5	0.0046	0.0014	0.0221	0.0066
				1.0	0.0066	0.0041	0.0305	0.009
2	0.865	L8-N15	1800	0.0	0.0045	0.0001	0.0225	0.007
				0.5	0.0049	0.0009	0.0219	0.0069
				1.0	0.0067	0.0026	0.0234	0.0087

Figure 34: MFASIS uncertainties for the instrument: Sentinel3 2 Olci2Chn

3 Uncertainty figures

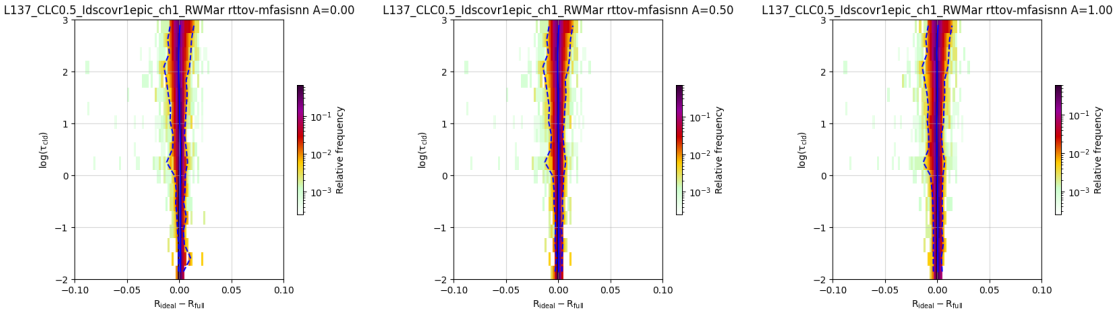

(a) (b) (c)

Figure 35: MFASIS $\Delta r_{\mathrm{MFASIS}-ref}$ as function of the cloud optical depth τ at albedo(s) of 0.0, 0.5, 1.0 (from left to right) for the instrument: DSCOVR 1 EPIC CH1

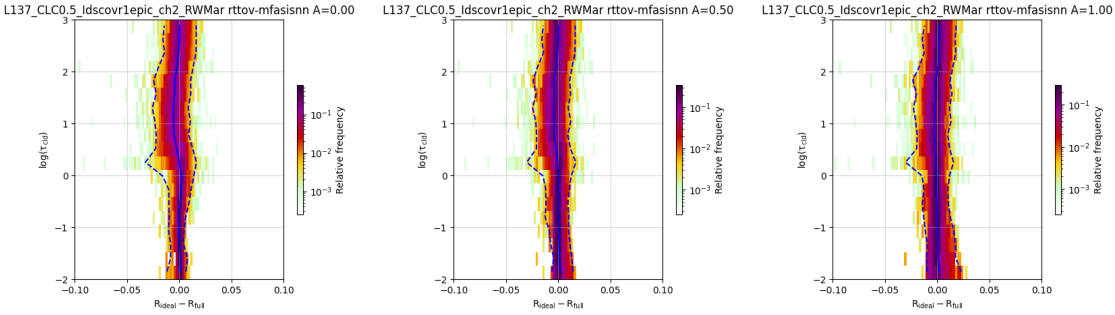

(a) (b) (c)

Figure 36: MFASIS $\Delta r_{\mathrm{MFASIS}-ref}$ as function of the cloud optical depth τ at albedo(s) of 0.0, 0.5, 1.0 (from left to right) for the instrument: DSCOVR 1 EPIC CH2

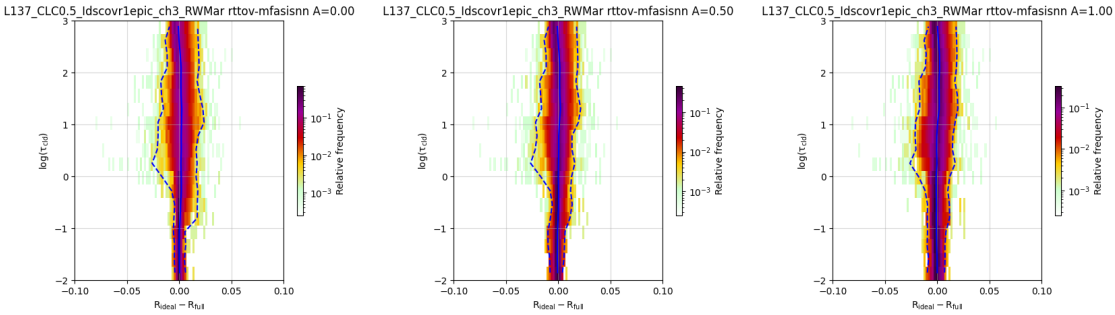

(a) (b) (c)

Figure 37: MFASIS $\Delta r_{\mathrm{MFASIS}-ref}$ as function of the cloud optical depth τ at albedo(s) of 0.0, 0.5, 1.0 (from left to right) for the instrument: DSCOVR 1 EPIC CH3

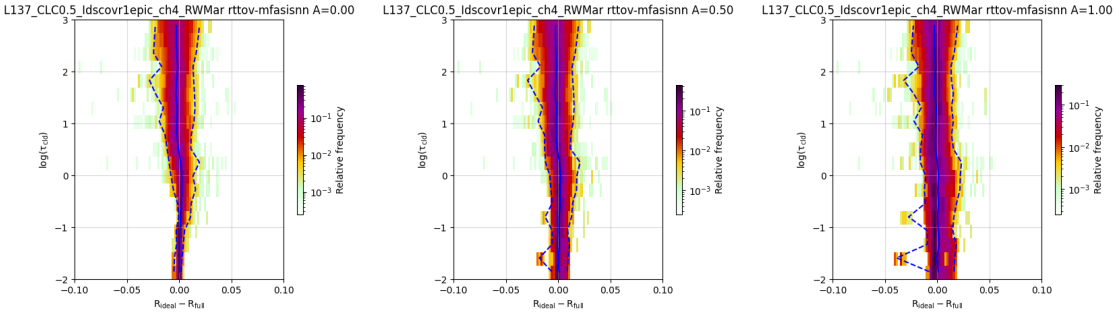

(a) (b) (c)

Figure 38: MFASIS $\Delta r_{\mathrm{MFASIS}-ref}$ as function of the cloud optical depth τ at albedo(s) of 0.0, 0.5, 1.0 (from left to right) for the instrument: DSCOVR 1 EPIC CH4

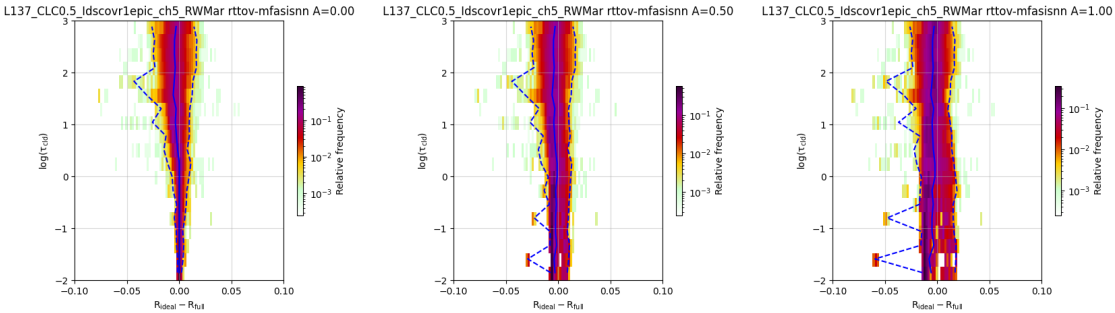

(a) (b) (c)

Figure 39: MFASIS $\Delta r_{\mathrm{MFASIS}-ref}$ as function of the cloud optical depth τ at albedo(s) of 0.0, 0.5, 1.0 (from left to right) for the instrument: DSCOVR 1 EPIC CH5

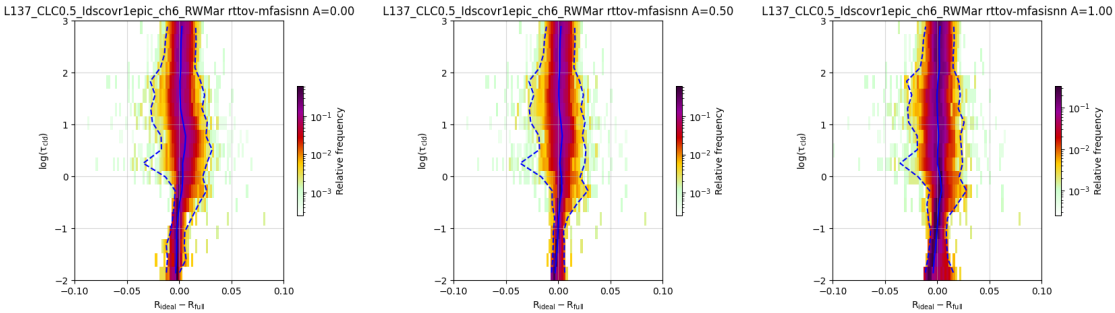

(a) (b) (c)

Figure 40: MFASIS $\Delta r_{\mathrm{MFASIS}-ref}$ as function of the cloud optical depth τ at albedo(s) of 0.0, 0.5, 1.0 (from left to right) for the instrument: DSCOVR 1 EPIC CH6

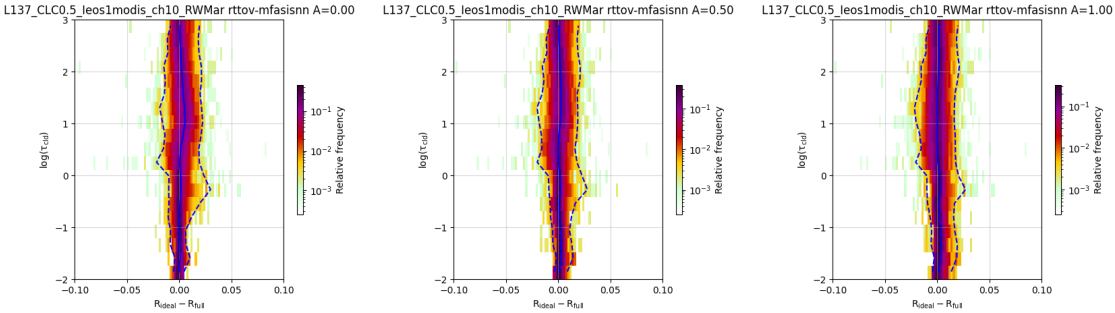

(a) (b) (c)

Figure 41: MFASIS $\Delta r_{\mathrm{MFASIS}-ref}$ as function of the cloud optical depth τ at albedo(s) of 0.0, 0.5, 1.0 (from left to right) for the instrument: EOS 1 MODIS CH10

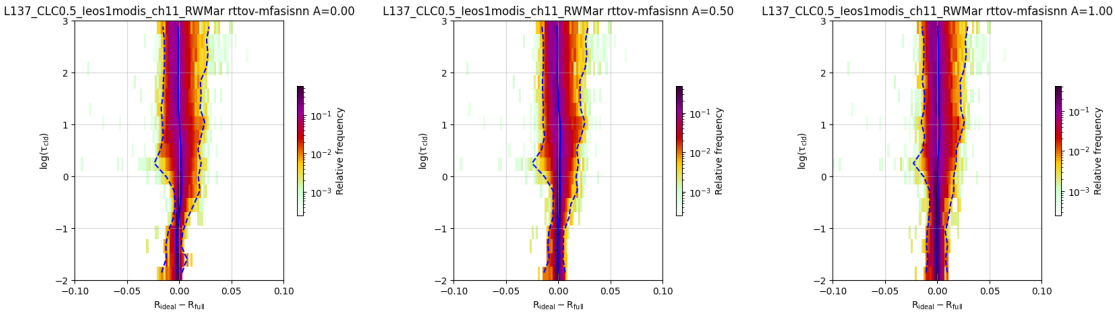

(a) (b) (c)

Figure 42: MFASIS $\Delta r_{\mathrm{MFASIS}-ref}$ as function of the cloud optical depth τ at albedo(s) of 0.0, 0.5, 1.0 (from left to right) for the instrument: EOS 1 MODIS CH11

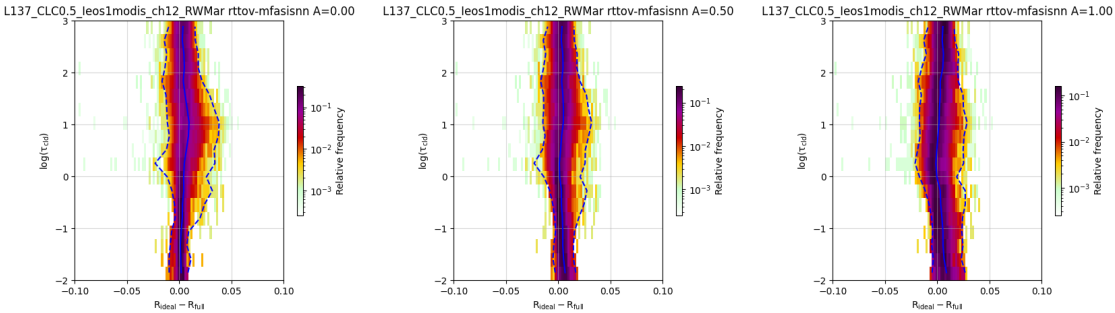

(a) (b) (c)

Figure 43: MFASIS $\Delta r_{\mathrm{MFASIS}-ref}$ as function of the cloud optical depth τ at albedo(s) of 0.0, 0.5, 1.0 (from left to right) for the instrument: EOS 1 MODIS CH12

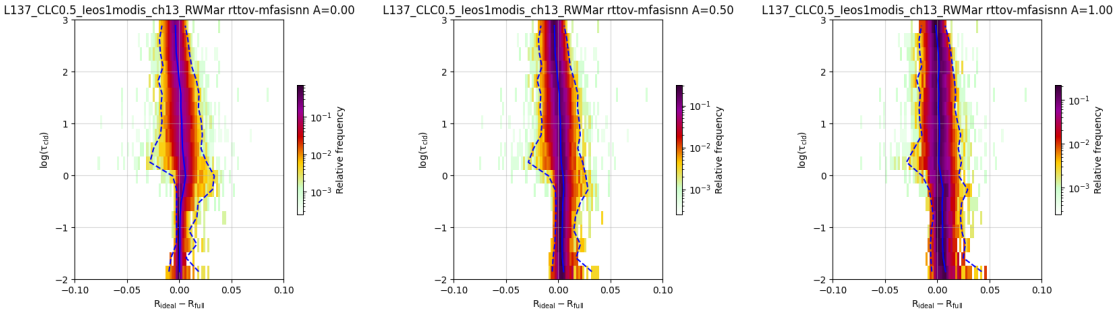

(a) (b) (c)

Figure 44: MFASIS $\Delta r_{\mathrm{MFASIS}-ref}$ as function of the cloud optical depth τ at albedo(s) of 0.0, 0.5, 1.0 (from left to right) for the instrument: EOS 1 MODIS CH13

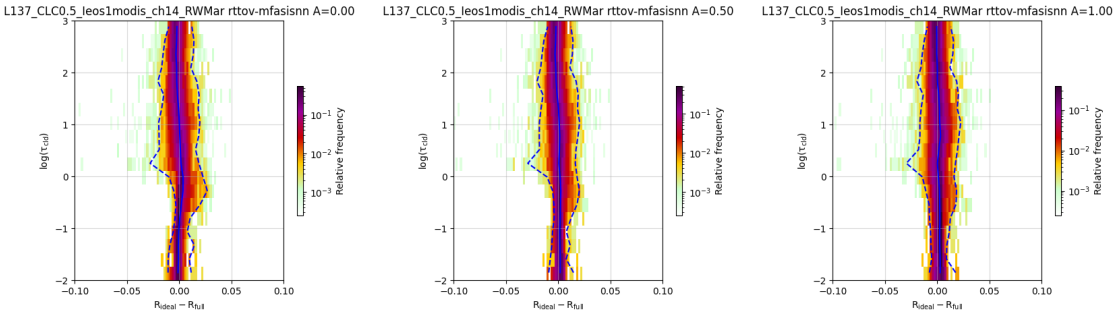

(a) (b) (c)

Figure 45: MFASIS $\Delta r_{\mathrm{MFASIS}-ref}$ as function of the cloud optical depth τ at albedo(s) of 0.0, 0.5, 1.0 (from left to right) for the instrument: EOS 1 MODIS CH14

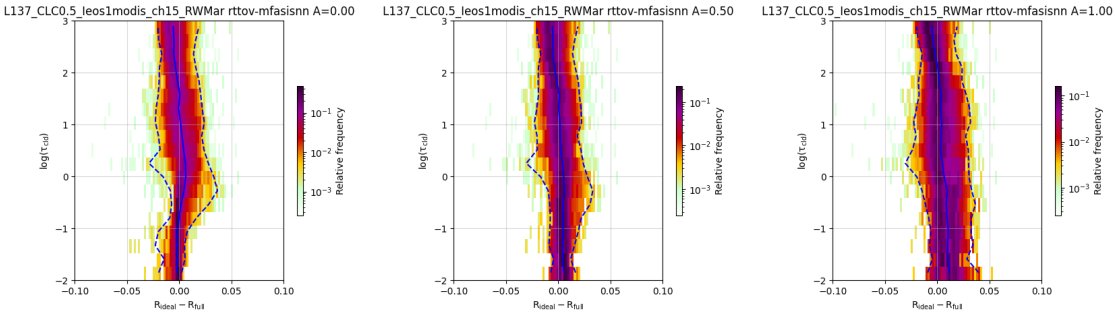

(a) (b) (c)

Figure 46: MFASIS $\Delta r_{\mathrm{MFASIS}-ref}$ as function of the cloud optical depth τ at albedo(s) of 0.0, 0.5, 1.0 (from left to right) for the instrument: EOS 1 MODIS CH15

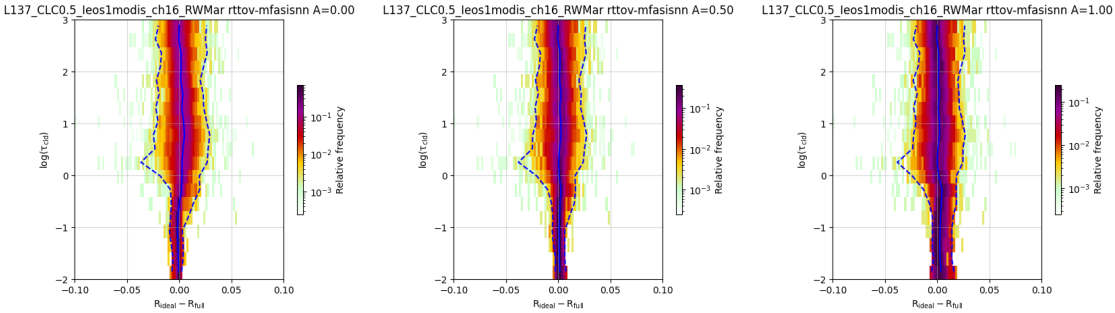

(a) (b) (c)

Figure 47: MFASIS $\Delta r_{\mathrm{MFASIS}-ref}$ as function of the cloud optical depth τ at albedo(s) of 0.0, 0.5, 1.0 (from left to right) for the instrument: EOS 1 MODIS CH16

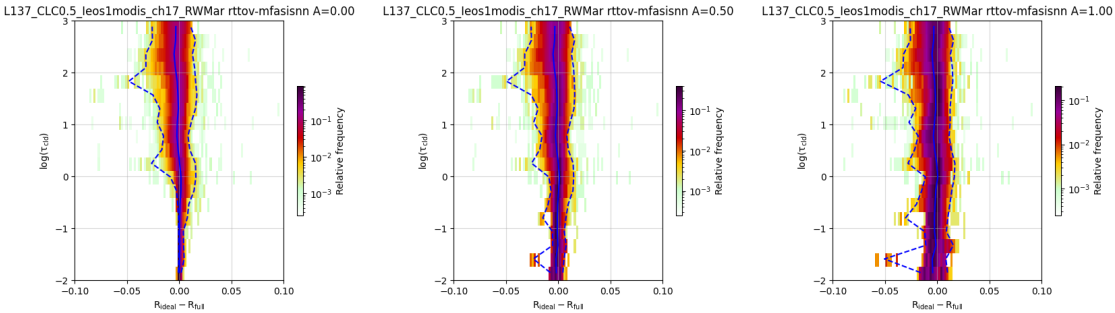

(a) (b) (c)

Figure 48: MFASIS $\Delta r_{\mathrm{MFASIS}-ref}$ as function of the cloud optical depth τ at albedo(s) of 0.0, 0.5, 1.0 (from left to right) for the instrument: EOS 1 MODIS CH17

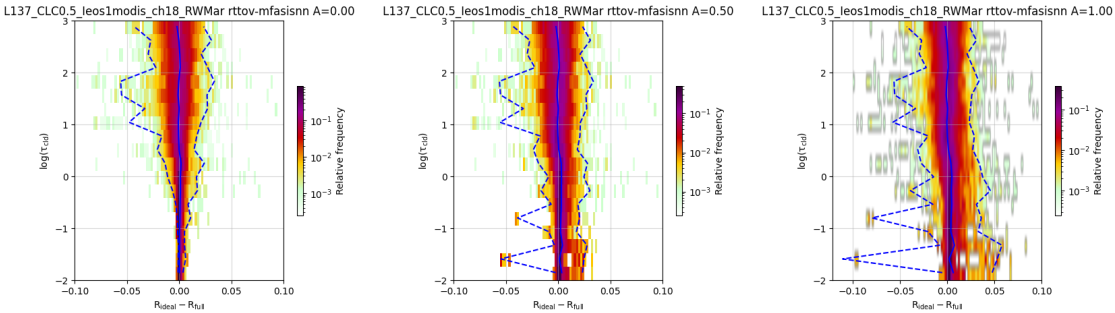

(a) (b) (c)

Figure 49: MFASIS $\Delta r_{\mathrm{MFASIS}-ref}$ as function of the cloud optical depth τ at albedo(s) of 0.0, 0.5, 1.0 (from left to right) for the instrument: EOS 1 MODIS CH18

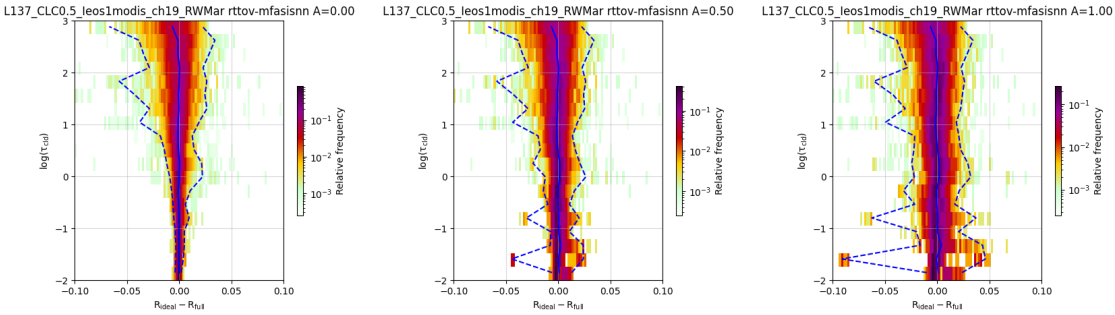

(a) (b) (c)

Figure 50: MFASIS $\Delta r_{\mathrm{MFASIS}-ref}$ as function of the cloud optical depth τ at albedo(s) of 0.0, 0.5, 1.0 (from left to right) for the instrument: EOS 1 MODIS CH19

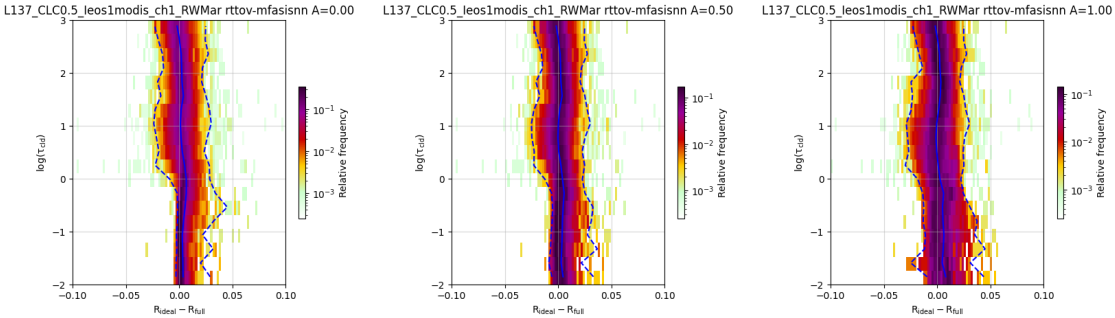

(a) (b) (c)

Figure 51: MFASIS $\Delta r_{\mathrm{MFASIS}-ref}$ as function of the cloud optical depth τ at albedo(s) of 0.0, 0.5, 1.0 (from left to right) for the instrument: EOS 1 MODIS CH1

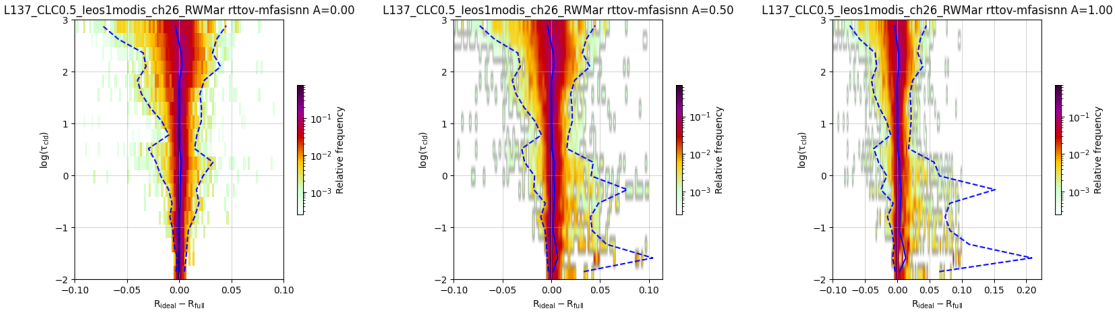

(a) (b) (c)

Figure 52: MFASIS $\Delta r_{\mathrm{MFASIS}-ref}$ as function of the cloud optical depth τ at albedo(s) of 0.0, 0.5, 1.0 (from left to right) for the instrument: EOS 1 MODIS CH26

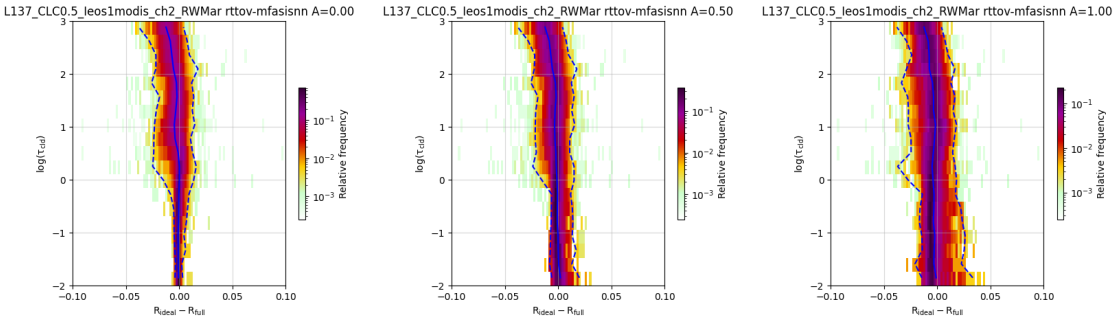

(a) (b) (c)

Figure 53: MFASIS $\Delta r_{\mathrm{MFASIS}-ref}$ as function of the cloud optical depth τ at albedo(s) of 0.0, 0.5, 1.0 (from left to right) for the instrument: EOS 1 MODIS CH2

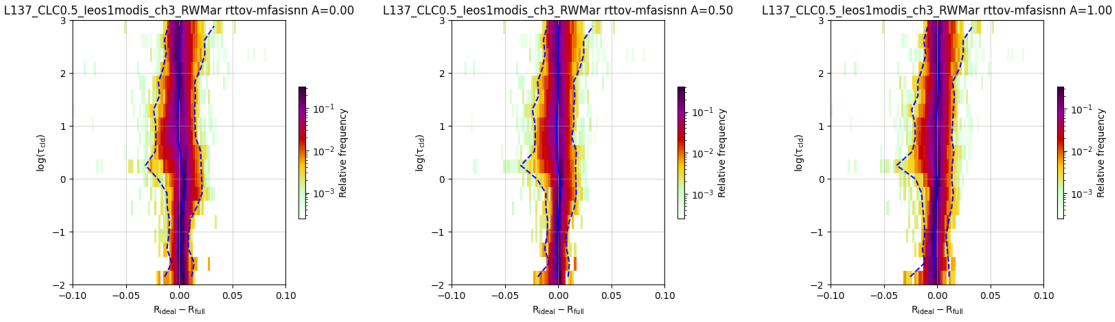

(a) (b) (c)

Figure 54: MFASIS $\Delta r_{\mathrm{MFASIS}-ref}$ as function of the cloud optical depth τ at albedo(s) of 0.0, 0.5, 1.0 (from left to right) for the instrument: EOS 1 MODIS CH3

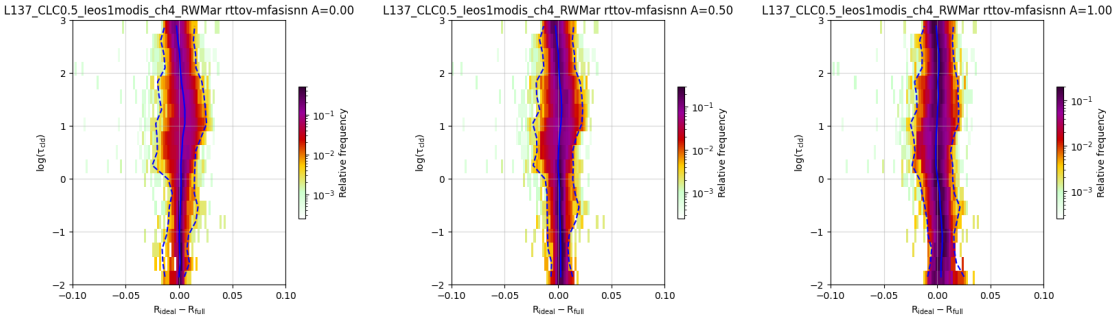

(a) (b) (c)

Figure 55: MFASIS $\Delta r_{\mathrm{MFASIS}-ref}$ as function of the cloud optical depth τ at albedo(s) of 0.0, 0.5, 1.0 (from left to right) for the instrument: EOS 1 MODIS CH4

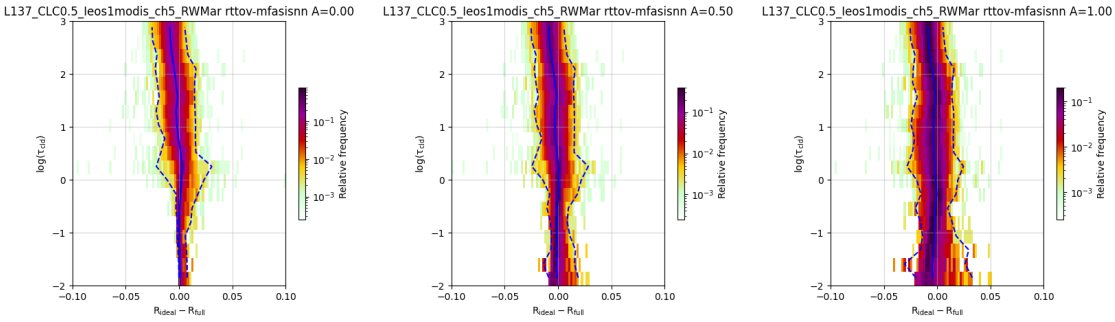

(a) (b) (c)

Figure 56: MFASIS $\Delta r_{\mathrm{MFASIS}-ref}$ as function of the cloud optical depth τ at albedo(s) of 0.0, 0.5, 1.0 (from left to right) for the instrument: EOS 1 MODIS CH5

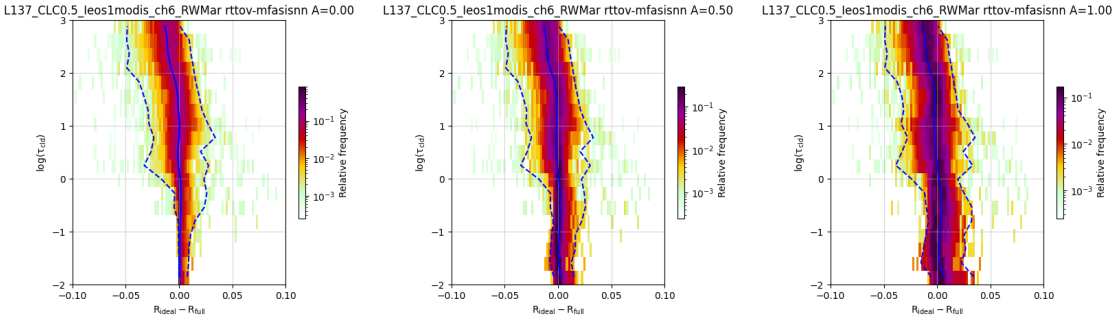

(a) (b) (c)

Figure 57: MFASIS $\Delta r_{\mathrm{MFASIS}-ref}$ as function of the cloud optical depth τ at albedo(s) of 0.0, 0.5, 1.0 (from left to right) for the instrument: EOS 1 MODIS CH6

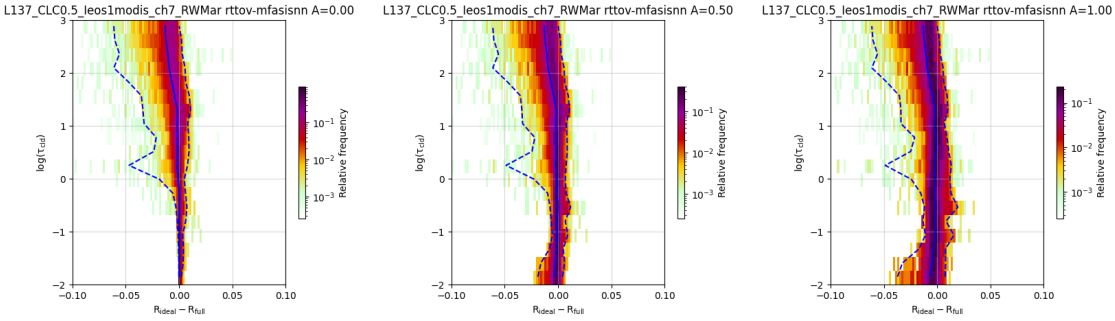

(a) (b) (c)

Figure 58: MFASIS $\Delta r_{\mathrm{MFASIS}-ref}$ as function of the cloud optical depth τ at albedo(s) of 0.0, 0.5, 1.0 (from left to right) for the instrument: EOS 1 MODIS CH7

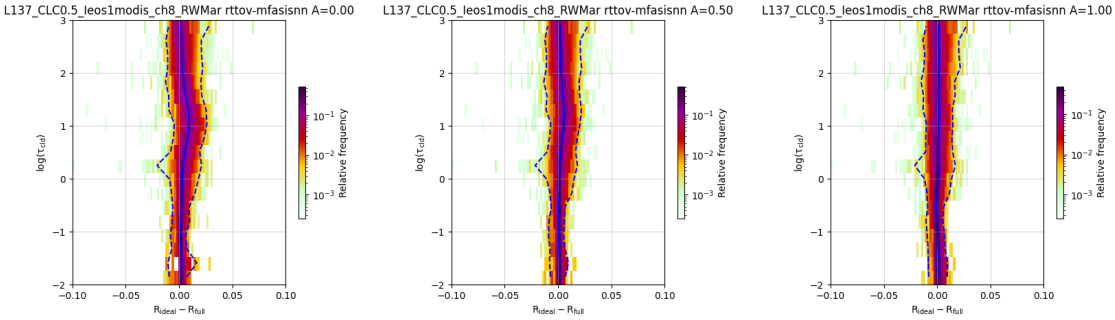

(a) (b) (c)

Figure 59: MFASIS $\Delta r_{\mathrm{MFASIS}-ref}$ as function of the cloud optical depth τ at albedo(s) of 0.0, 0.5, 1.0 (from left to right) for the instrument: EOS 1 MODIS CH8

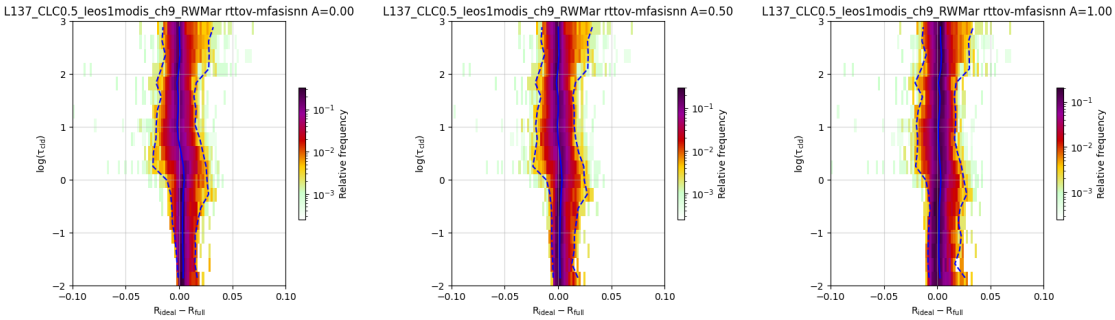

(a) (b) (c)

Figure 60: MFASIS $\Delta r_{\mathrm{MFASIS}-ref}$ as function of the cloud optical depth τ at albedo(s) of 0.0, 0.5, 1.0 (from left to right) for the instrument: EOS 1 MODIS CH9

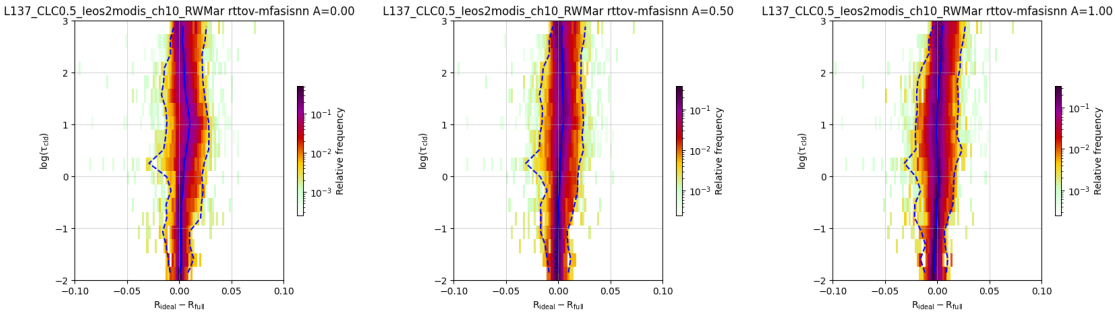

(a) (b) (c)

Figure 61: MFASIS $\Delta r_{\mathrm{MFASIS}-ref}$ as function of the cloud optical depth τ at albedo(s) of 0.0, 0.5, 1.0 (from left to right) for the instrument: EOS 2 MODIS CH10

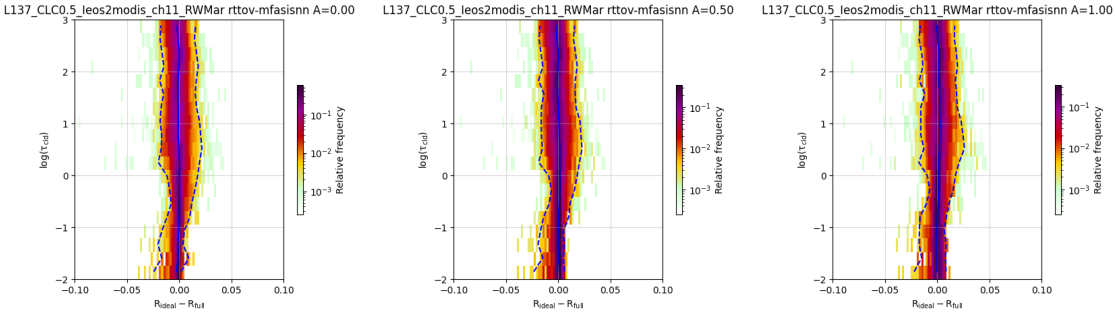

(a) (b) (c)

Figure 62: MFASIS $\Delta r_{\mathrm{MFASIS}-ref}$ as function of the cloud optical depth τ at albedo(s) of 0.0, 0.5, 1.0 (from left to right) for the instrument: EOS 2 MODIS CH11

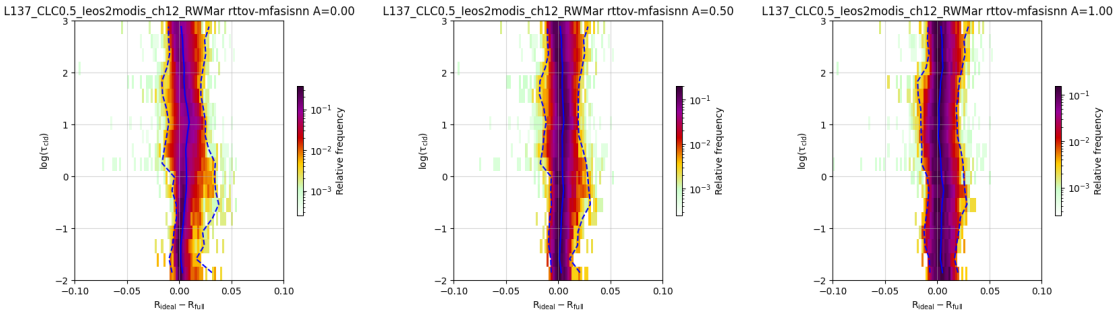

(a) (b) (c)

Figure 63: MFASIS $\Delta r_{\mathrm{MFASIS}-ref}$ as function of the cloud optical depth τ at albedo(s) of 0.0, 0.5, 1.0 (from left to right) for the instrument: EOS 2 MODIS CH12

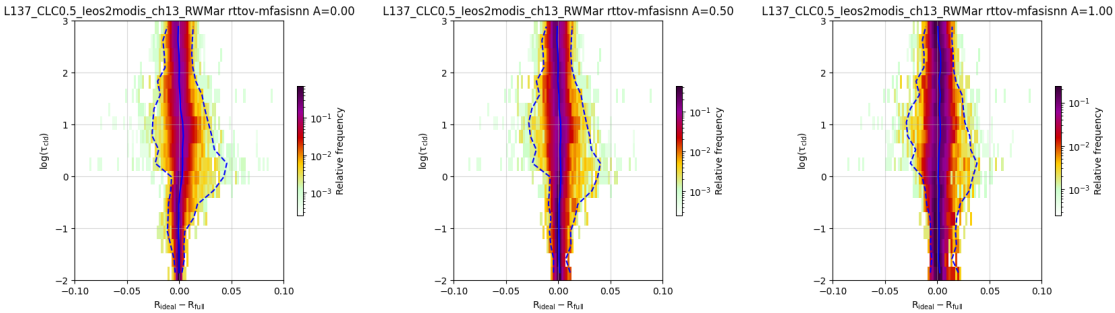

(a) (b) (c)

Figure 64: MFASIS $\Delta r_{\mathrm{MFASIS}-ref}$ as function of the cloud optical depth τ at albedo(s) of 0.0, 0.5, 1.0 (from left to right) for the instrument: EOS 2 MODIS CH13

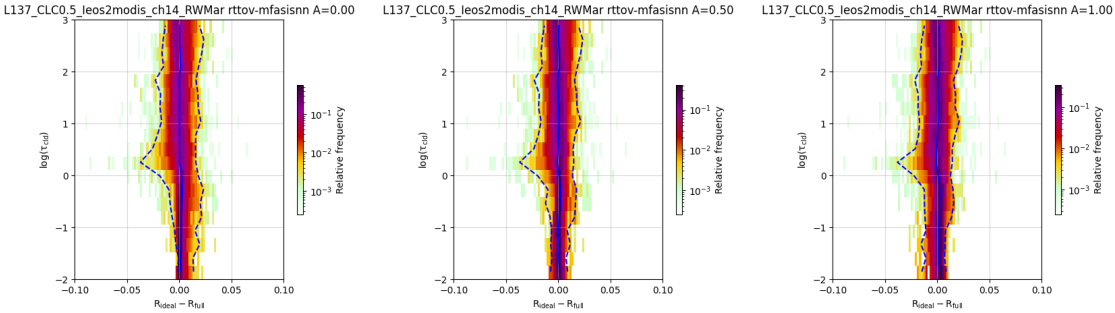

(a) (b) (c)

Figure 65: MFASIS $\Delta r_{\mathrm{MFASIS}-ref}$ as function of the cloud optical depth τ at albedo(s) of 0.0, 0.5, 1.0 (from left to right) for the instrument: EOS 2 MODIS CH14

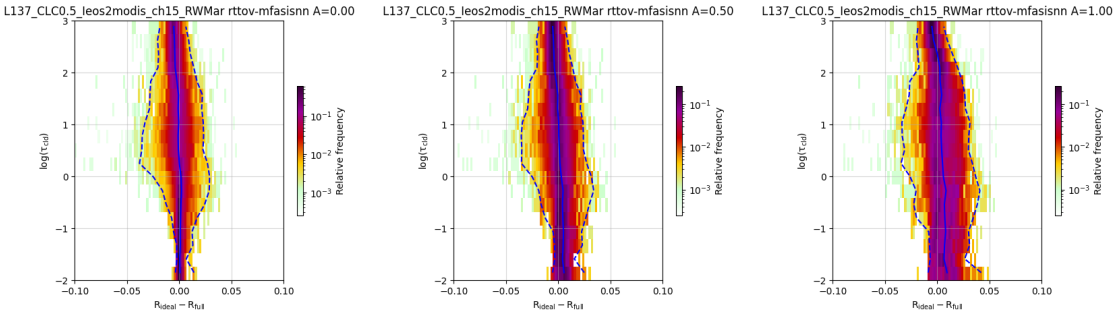

(a) (b) (c)

Figure 66: MFASIS $\Delta r_{\mathrm{MFASIS}-ref}$ as function of the cloud optical depth τ at albedo(s) of 0.0, 0.5, 1.0 (from left to right) for the instrument: EOS 2 MODIS CH15

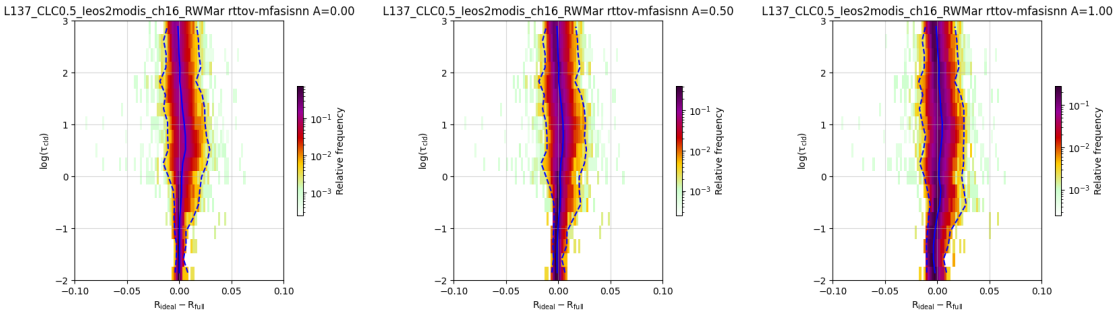

(a) (b) (c)

Figure 67: MFASIS $\Delta r_{\mathrm{MFASIS}-ref}$ as function of the cloud optical depth τ at albedo(s) of 0.0, 0.5, 1.0 (from left to right) for the instrument: EOS 2 MODIS CH16

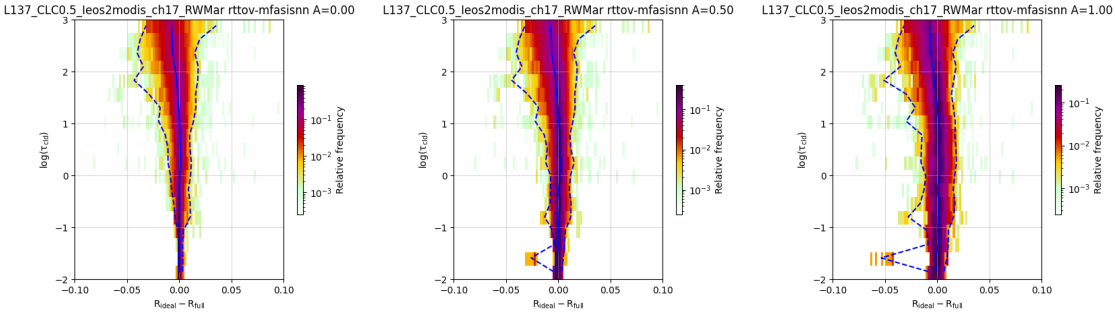

(a) (b) (c)

Figure 68: MFASIS $\Delta r_{\mathrm{MFASIS}-ref}$ as function of the cloud optical depth τ at albedo(s) of 0.0, 0.5, 1.0 (from left to right) for the instrument: EOS 2 MODIS CH17

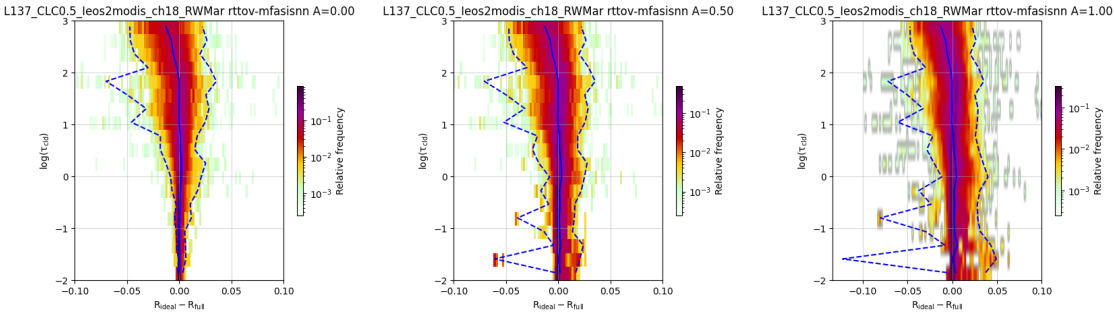

(a) (b) (c)

Figure 69: MFASIS $\Delta r_{\mathrm{MFASIS}-ref}$ as function of the cloud optical depth τ at albedo(s) of 0.0, 0.5, 1.0 (from left to right) for the instrument: EOS 2 MODIS CH18

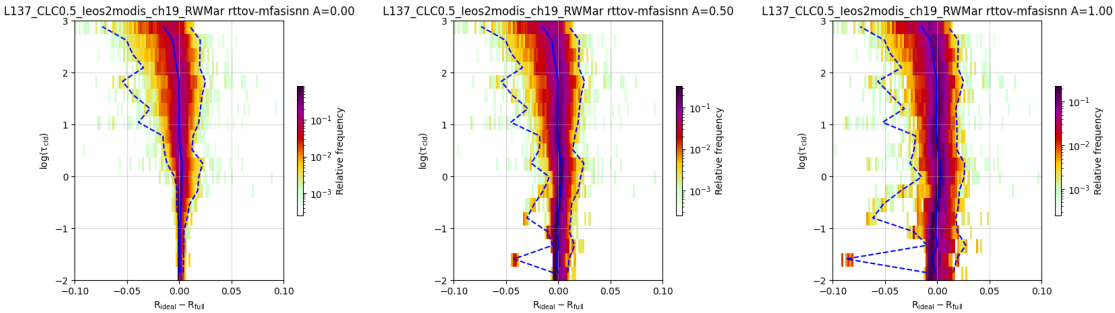

(a) (b) (c)

Figure 70: MFASIS $\Delta r_{\mathrm{MFASIS}-ref}$ as function of the cloud optical depth τ at albedo(s) of 0.0, 0.5, 1.0 (from left to right) for the instrument: EOS 2 MODIS CH19

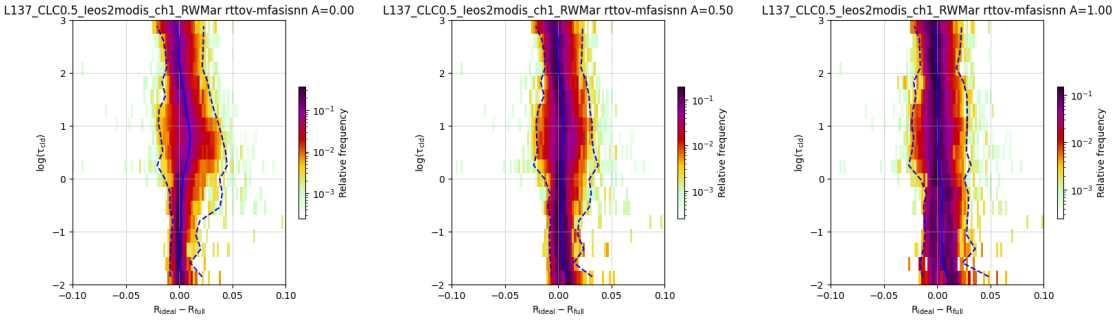

(a) (b) (c)

Figure 71: MFASIS $\Delta r_{\mathrm{MFASIS}-ref}$ as function of the cloud optical depth τ at albedo(s) of 0.0, 0.5, 1.0 (from left to right) for the instrument: EOS 2 MODIS CH1

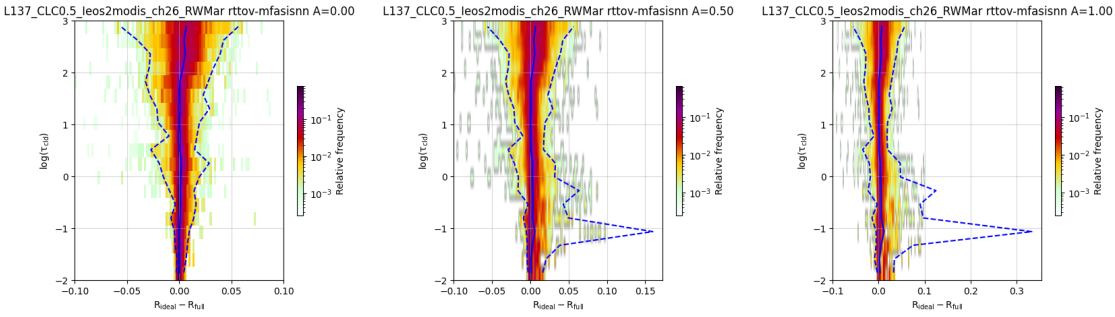

(a) (b) (c)

Figure 72: MFASIS $\Delta r_{\mathrm{MFASIS}-ref}$ as function of the cloud optical depth τ at albedo(s) of 0.0, 0.5, 1.0 (from left to right) for the instrument: EOS 2 MODIS CH26

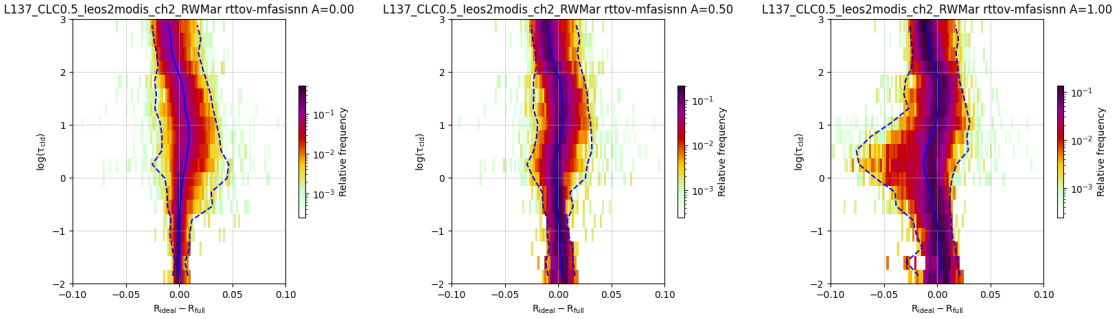

(a) (b) (c)

Figure 73: MFASIS $\Delta r_{\mathrm{MFASIS}-ref}$ as function of the cloud optical depth τ at albedo(s) of 0.0, 0.5, 1.0 (from left to right) for the instrument: EOS 2 MODIS CH2

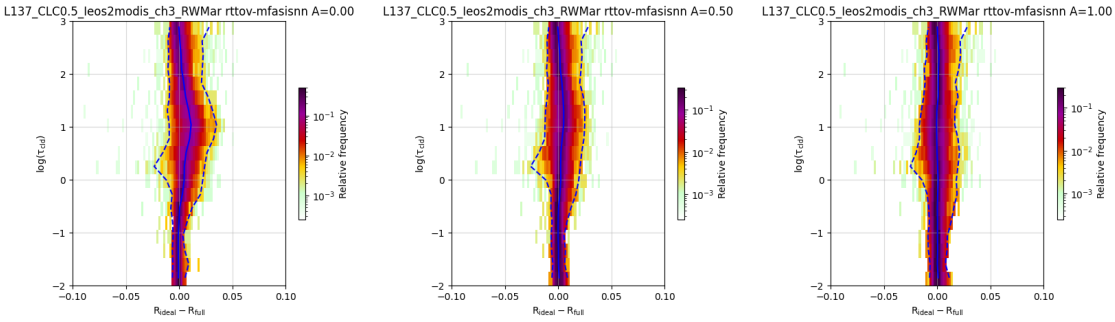

(a) (b) (c)

Figure 74: MFASIS $\Delta r_{\mathrm{MFASIS}-ref}$ as function of the cloud optical depth τ at albedo(s) of 0.0, 0.5, 1.0 (from left to right) for the instrument: EOS 2 MODIS CH3

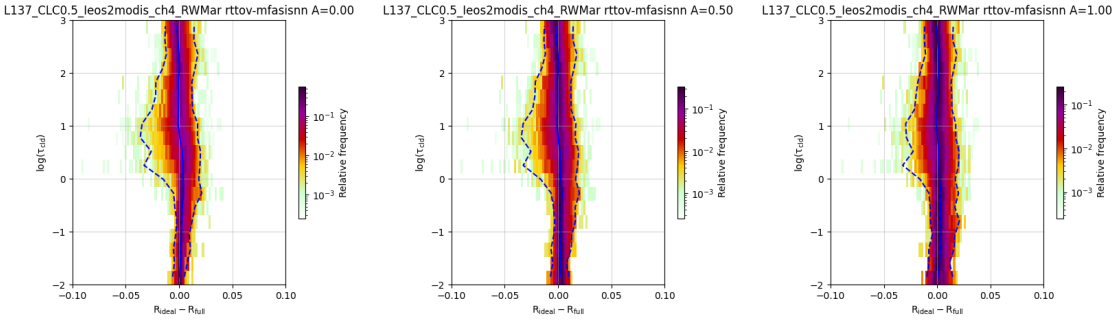

(a) (b) (c)

Figure 75: MFASIS $\Delta r_{\mathrm{MFASIS}-ref}$ as function of the cloud optical depth τ at albedo(s) of 0.0, 0.5, 1.0 (from left to right) for the instrument: EOS 2 MODIS CH4

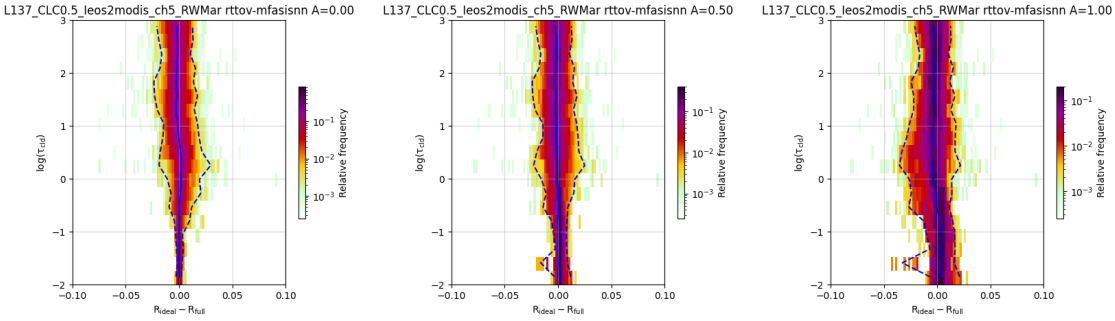

(a) (b) (c)

Figure 76: MFASIS $\Delta r_{\mathrm{MFASIS}-ref}$ as function of the cloud optical depth τ at albedo(s) of 0.0, 0.5, 1.0 (from left to right) for the instrument: EOS 2 MODIS CH5

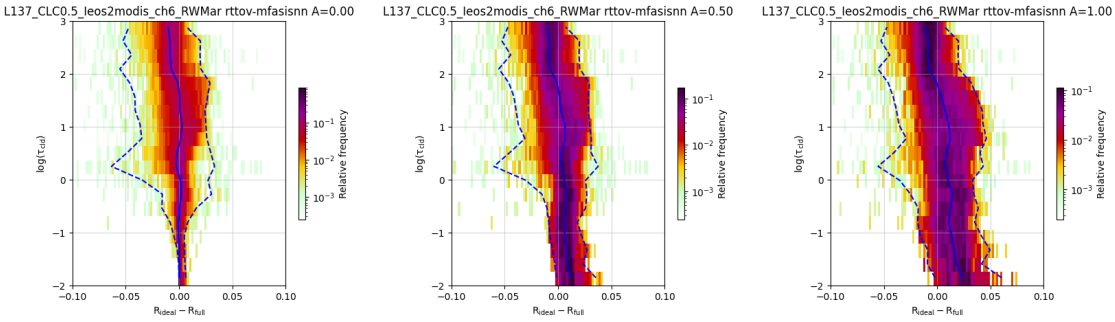

(a) (b) (c)

Figure 77: MFASIS $\Delta r_{\mathrm{MFASIS}-ref}$ as function of the cloud optical depth τ at albedo(s) of 0.0, 0.5, 1.0 (from left to right) for the instrument: EOS 2 MODIS CH6

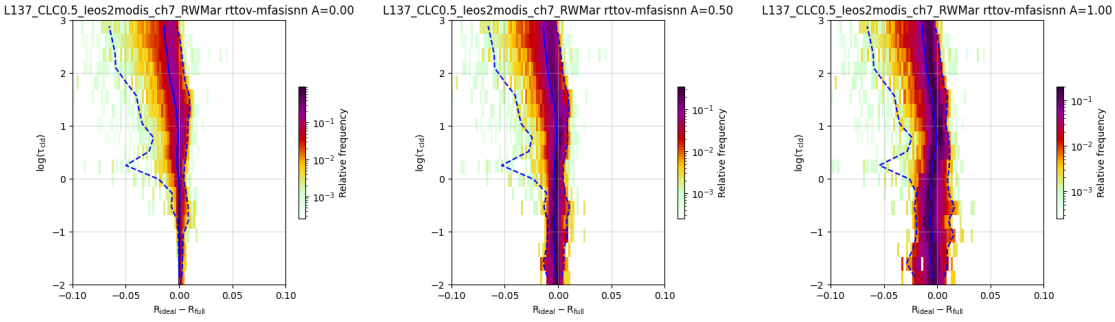

(a) (b) (c)

Figure 78: MFASIS $\Delta r_{\mathrm{MFASIS}-ref}$ as function of the cloud optical depth τ at albedo(s) of 0.0, 0.5, 1.0 (from left to right) for the instrument: EOS 2 MODIS CH7

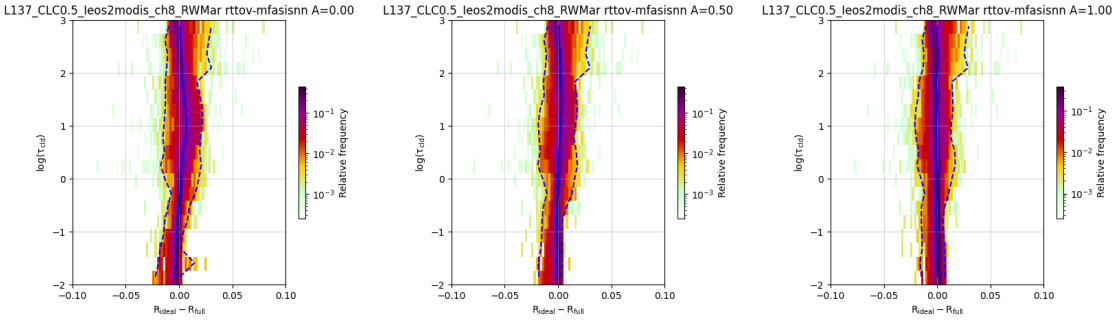

(a) (b) (c)

Figure 79: MFASIS $\Delta r_{\mathrm{MFASIS}-ref}$ as function of the cloud optical depth τ at albedo(s) of 0.0, 0.5, 1.0 (from left to right) for the instrument: EOS 2 MODIS CH8

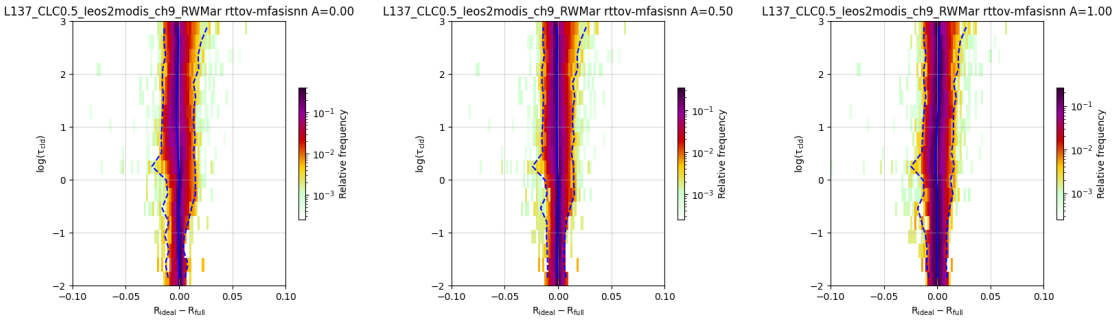

(a) (b) (c)

Figure 80: MFASIS $\Delta r_{\mathrm{MFASIS}-ref}$ as function of the cloud optical depth τ at albedo(s) of 0.0, 0.5, 1.0 (from left to right) for the instrument: EOS 2 MODIS CH9

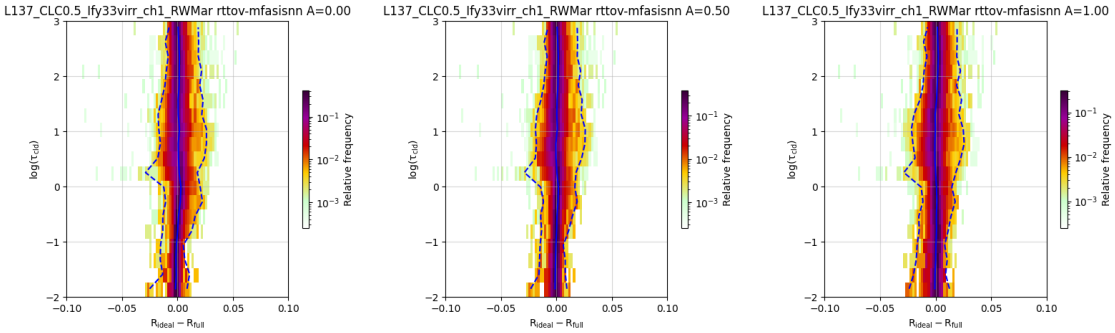

(a) (b) (c)

Figure 81: MFASIS $\Delta r_{\mathrm{MFASIS}-ref}$ as function of the cloud optical depth τ at albedo(s) of 0.0, 0.5, 1.0 (from left to right) for the instrument: FY3 3 VIRR CH1

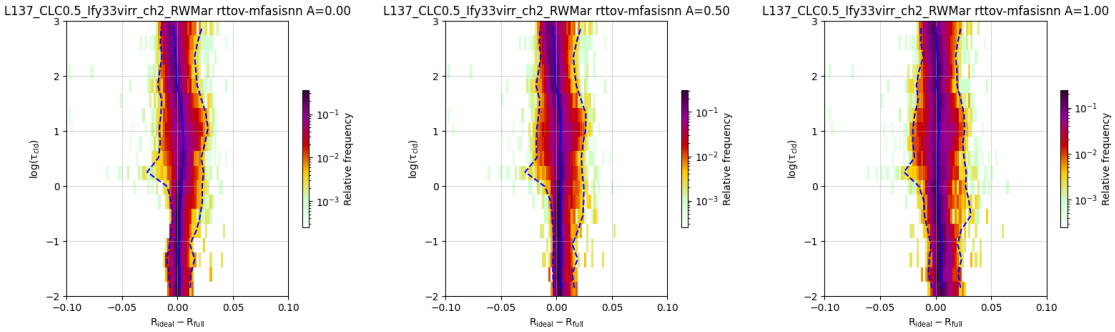

(a) (b) (c)

Figure 82: MFASIS $\Delta r_{\mathrm{MFASIS}-ref}$ as function of the cloud optical depth τ at albedo(s) of 0.0, 0.5, 1.0 (from left to right) for the instrument: FY3 3 VIRR CH2

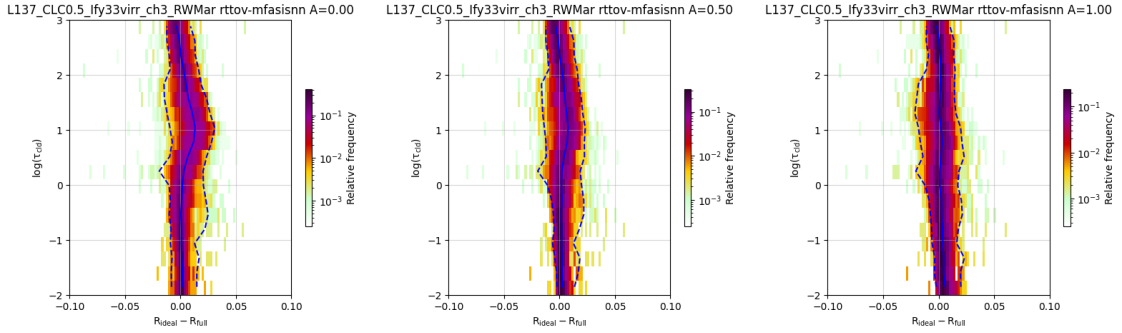

(a) (b) (c)

Figure 83: MFASIS $\Delta r_{\mathrm{MFASIS}-ref}$ as function of the cloud optical depth τ at albedo(s) of 0.0, 0.5, 1.0 (from left to right) for the instrument: FY3 3 VIRR CH3

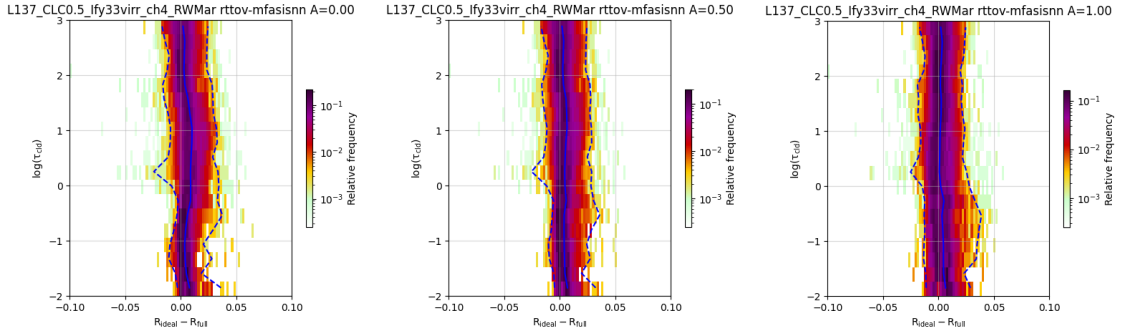

(a) (b) (c)

Figure 84: MFASIS $\Delta r_{\mathrm{MFASIS}-ref}$ as function of the cloud optical depth τ at albedo(s) of 0.0, 0.5, 1.0 (from left to right) for the instrument: FY3 3 VIRR CH4

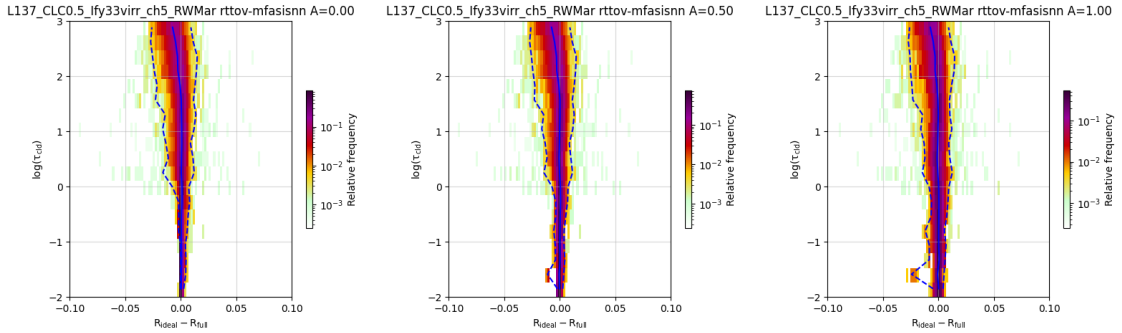

(a) (b) (c)

Figure 85: MFASIS $\Delta r_{\mathrm{MFASIS}-ref}$ as function of the cloud optical depth τ at albedo(s) of 0.0, 0.5, 1.0 (from left to right) for the instrument: FY3 3 VIRR CH5

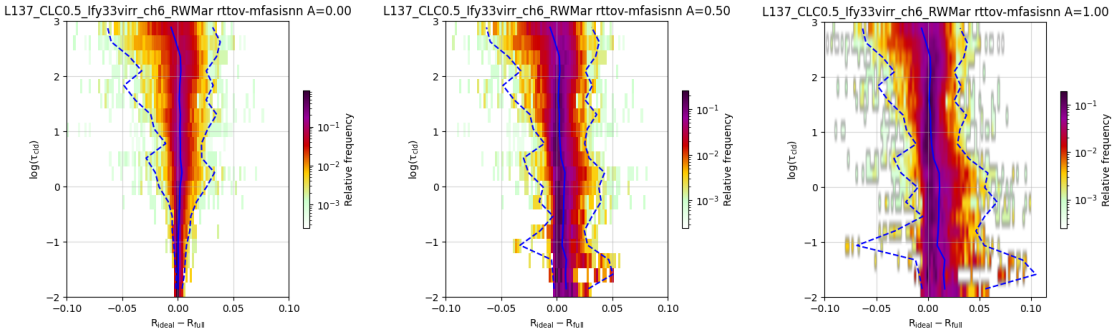

(a) (b) (c)

Figure 86: MFASIS $\Delta r_{\mathrm{MFASIS}-ref}$ as function of the cloud optical depth τ at albedo(s) of 0.0, 0.5, 1.0 (from left to right) for the instrument: FY3 3 VIRR CH6

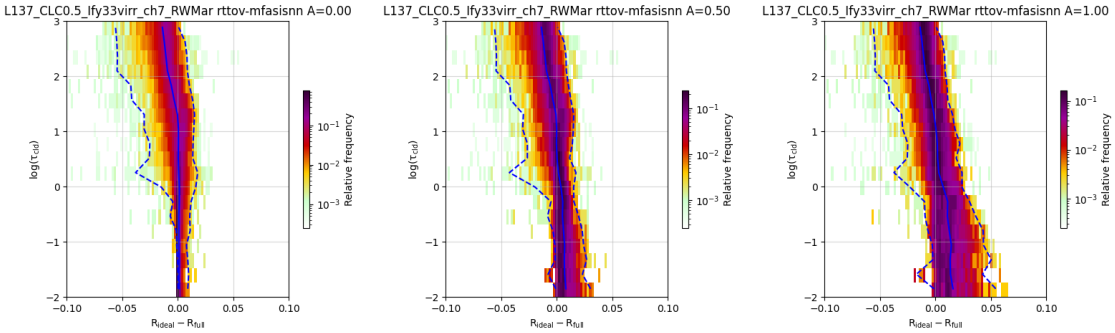

(a) (b) (c)

Figure 87: MFASIS $\Delta r_{\mathrm{MFASIS}-ref}$ as function of the cloud optical depth τ at albedo(s) of 0.0, 0.5, 1.0 (from left to right) for the instrument: FY3 3 VIRR CH7

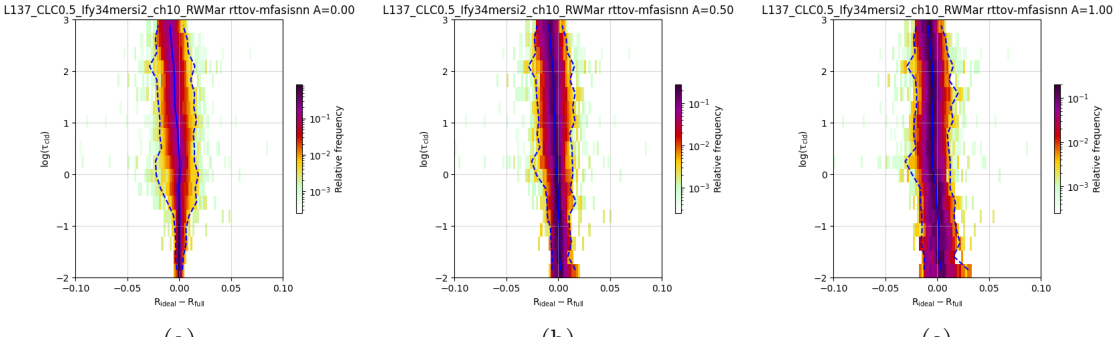

(a) (b) (c)

Figure 88: MFASIS $\Delta r_{\mathrm{MFASIS}-ref}$ as function of the cloud optical depth τ at albedo(s) of 0.0, 0.5, 1.0 (from left to right) for the instrument: FY3 4 MERSI2 CH10

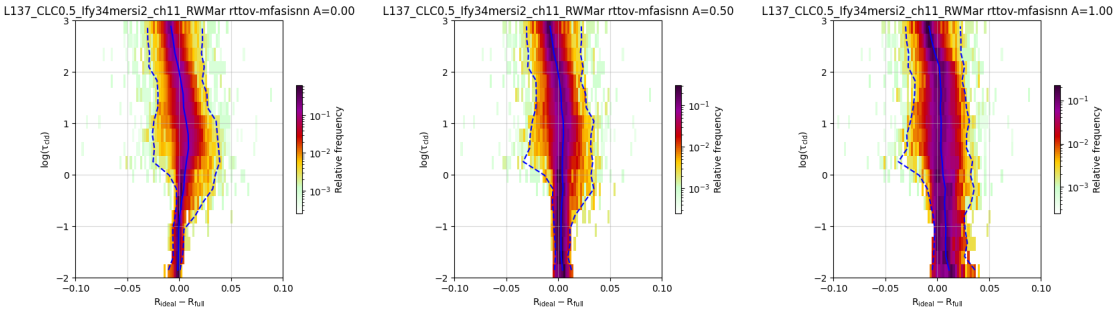

(a) (b) (c)

Figure 89: MFASIS $\Delta r_{\mathrm{MFASIS}-ref}$ as function of the cloud optical depth τ at albedo(s) of 0.0, 0.5, 1.0 (from left to right) for the instrument: FY3 4 MERSI2 CH11

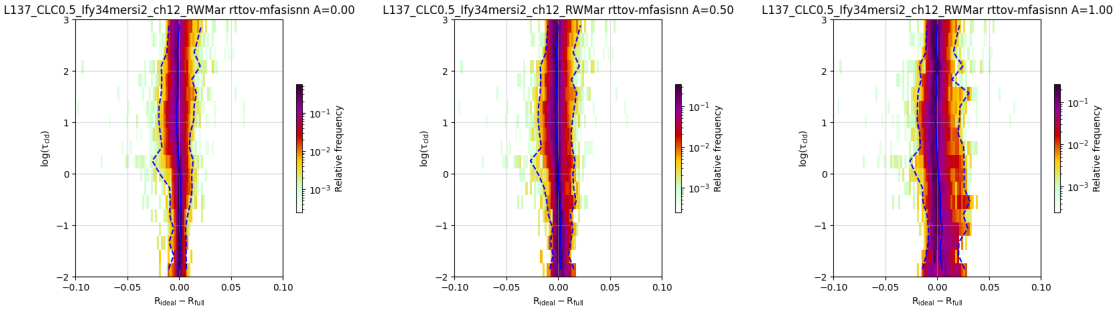

(a) (b) (c)

Figure 90: MFASIS $\Delta r_{\mathrm{MFASIS}-ref}$ as function of the cloud optical depth τ at albedo(s) of 0.0, 0.5, 1.0 (from left to right) for the instrument: FY3 4 MERSI2 CH12

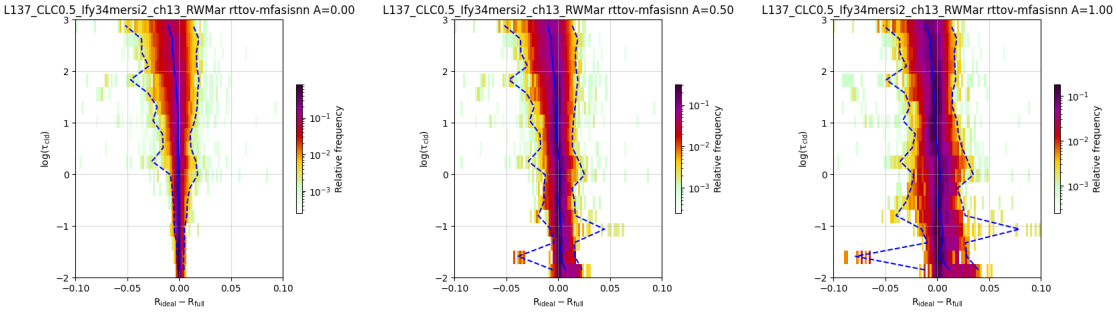

(a) (b) (c)

Figure 91: MFASIS $\Delta r_{\mathrm{MFASIS}-ref}$ as function of the cloud optical depth τ at albedo(s) of 0.0, 0.5, 1.0 (from left to right) for the instrument: FY3 4 MERSI2 CH13

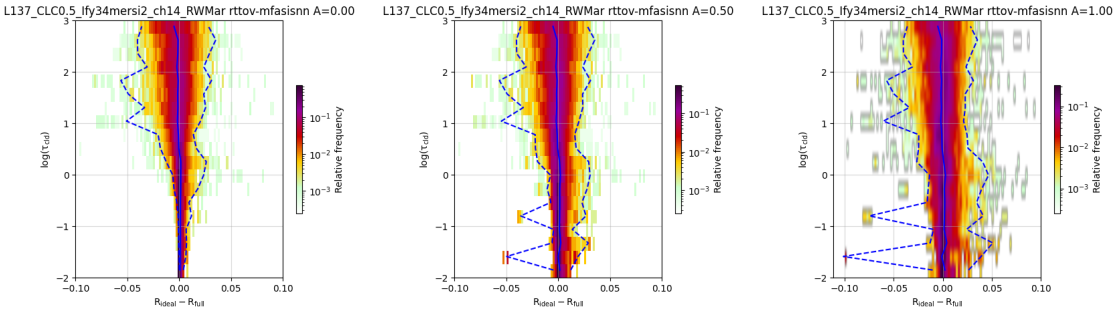

(a) (b) (c)

Figure 92: MFASIS $\Delta r_{\mathrm{MFASIS}-ref}$ as function of the cloud optical depth τ at albedo(s) of 0.0, 0.5, 1.0 (from left to right) for the instrument: FY3 4 MERSI2 CH14

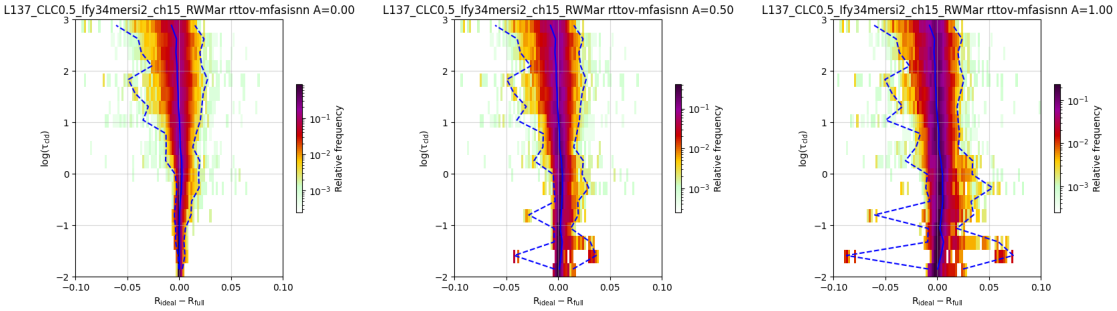

(a) (b) (c)

Figure 93: MFASIS $\Delta r_{\mathrm{MFASIS}-ref}$ as function of the cloud optical depth τ at albedo(s) of 0.0, 0.5, 1.0 (from left to right) for the instrument: FY3 4 MERSI2 CH15

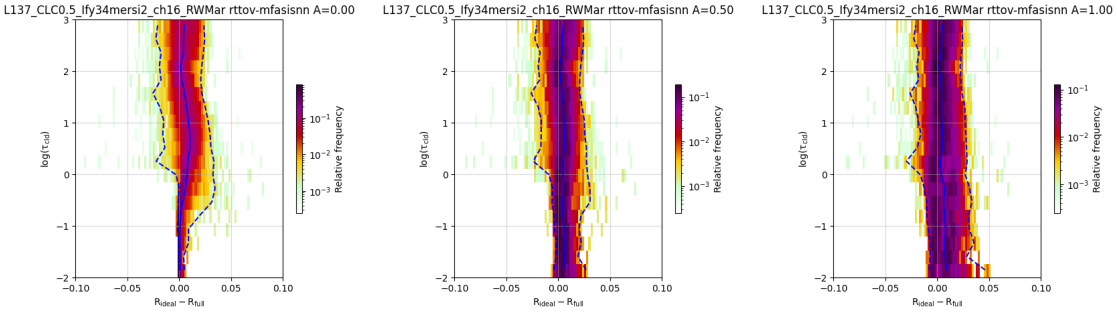

(a) (b) (c)

Figure 94: MFASIS $\Delta r_{\mathrm{MFASIS}-ref}$ as function of the cloud optical depth τ at albedo(s) of 0.0, 0.5, 1.0 (from left to right) for the instrument: FY3 4 MERSI2 CH16

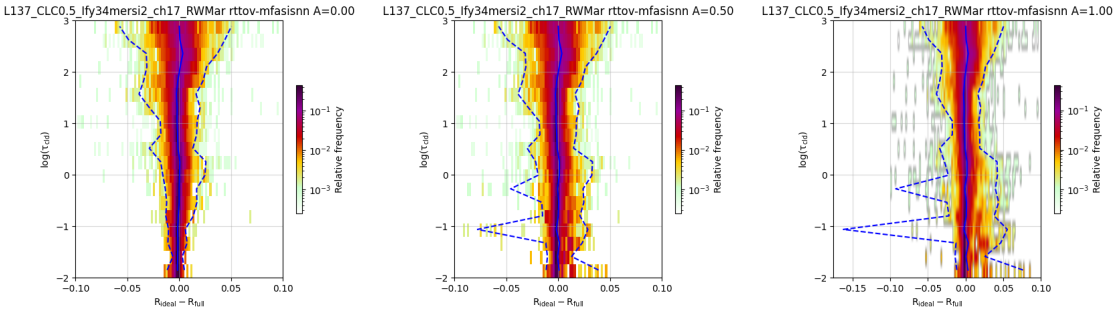

(a) (b) (c)

Figure 95: MFASIS $\Delta r_{\mathrm{MFASIS}-ref}$ as function of the cloud optical depth τ at albedo(s) of 0.0, 0.5, 1.0 (from left to right) for the instrument: FY3 4 MERSI2 CH17

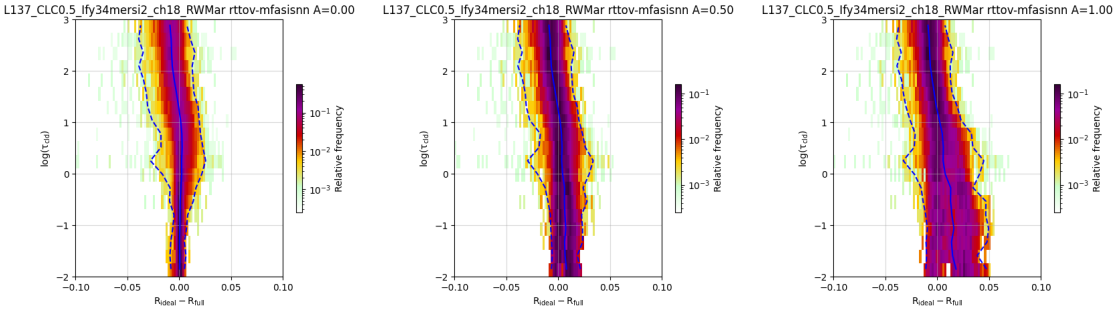

(a) (b) (c)

Figure 96: MFASIS $\Delta r_{\mathrm{MFASIS}-ref}$ as function of the cloud optical depth τ at albedo(s) of 0.0, 0.5, 1.0 (from left to right) for the instrument: FY3 4 MERSI2 CH18

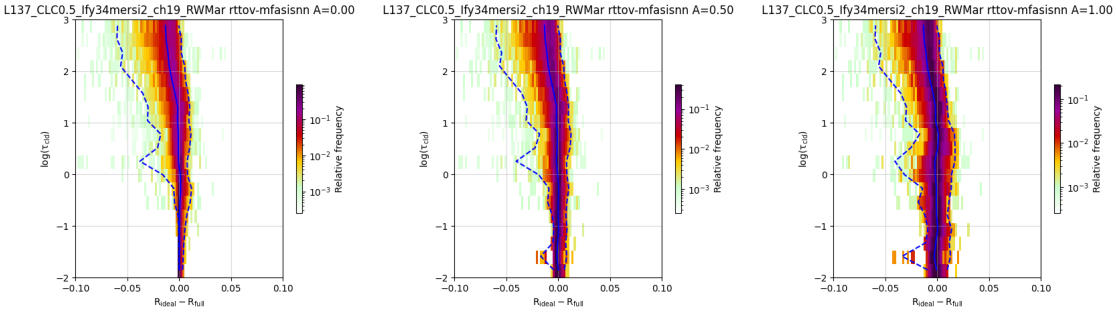

(a) (b) (c)

Figure 97: MFASIS $\Delta r_{\mathrm{MFASIS}-ref}$ as function of the cloud optical depth τ at albedo(s) of 0.0, 0.5, 1.0 (from left to right) for the instrument: FY3 4 MERSI2 CH19

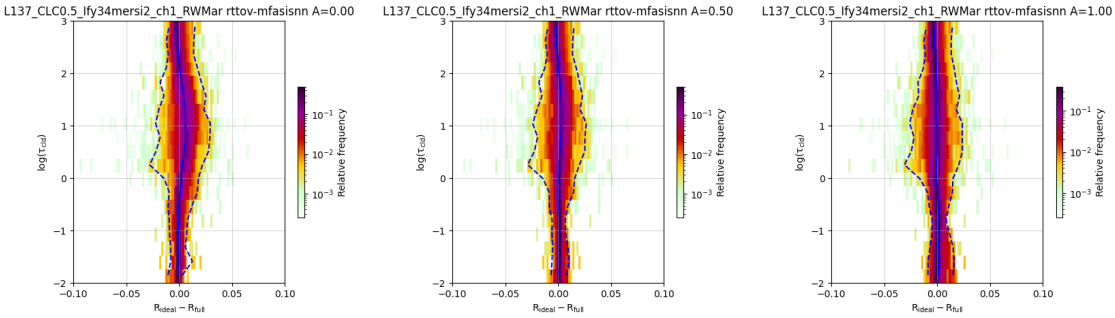

(a) (b) (c)

Figure 98: MFASIS $\Delta r_{\mathrm{MFASIS}-ref}$ as function of the cloud optical depth τ at albedo(s) of 0.0, 0.5, 1.0 (from left to right) for the instrument: FY3 4 MERSI2 CH1

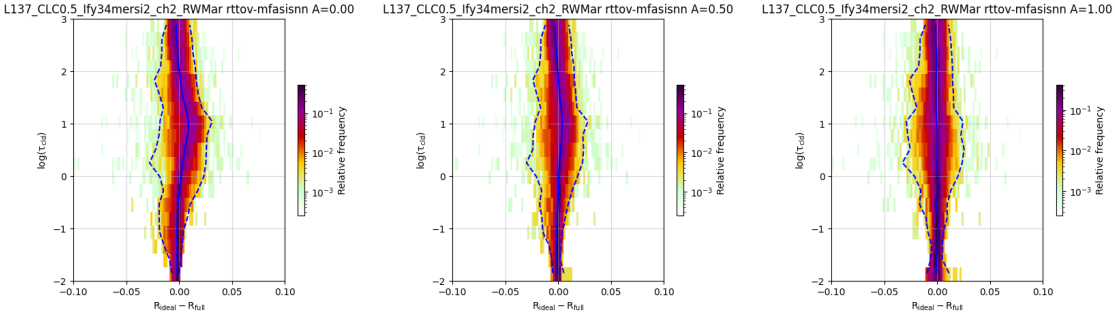

(a) (b) (c)

Figure 99: MFASIS $\Delta r_{\mathrm{MFASIS}-ref}$ as function of the cloud optical depth τ at albedo(s) of 0.0, 0.5, 1.0 (from left to right) for the instrument: FY3 4 MERSI2 CH2

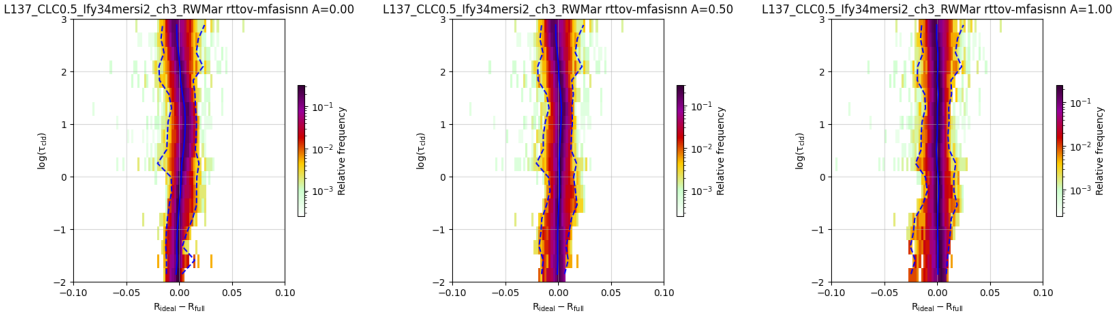

(a) (b) (c)

Figure 100: MFASIS $\Delta r_{\mathrm{MFASIS}-ref}$ as function of the cloud optical depth τ at albedo(s) of 0.0, 0.5, 1.0 (from left to right) for the instrument: FY3 4 MERSI2 CH3

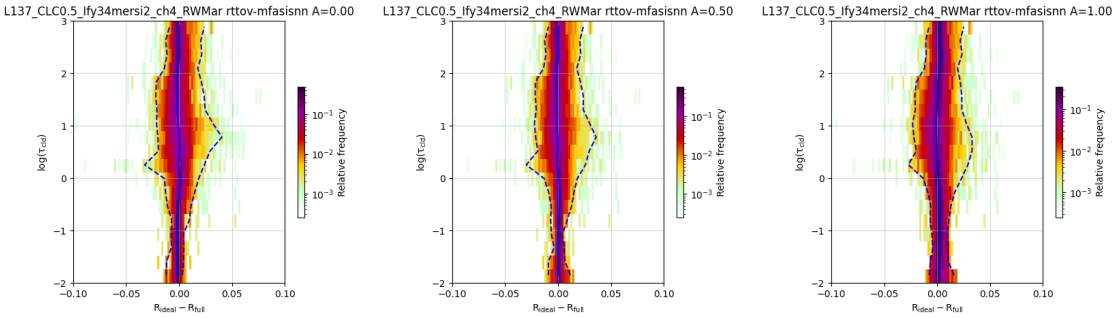

(a) (b) (c)

Figure 101: MFASIS $\Delta r_{\mathrm{MFASIS}-ref}$ as function of the cloud optical depth τ at albedo(s) of 0.0, 0.5, 1.0 (from left to right) for the instrument: FY3 4 MERSI2 CH4

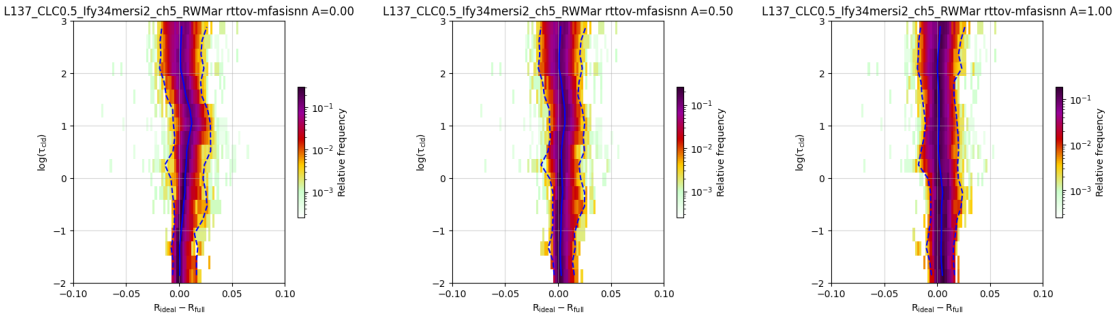

(a) (b) (c)

Figure 102: MFASIS $\Delta r_{\mathrm{MFASIS}-ref}$ as function of the cloud optical depth τ at albedo(s) of 0.0, 0.5, 1.0 (from left to right) for the instrument: FY3 4 MERSI2 CH5

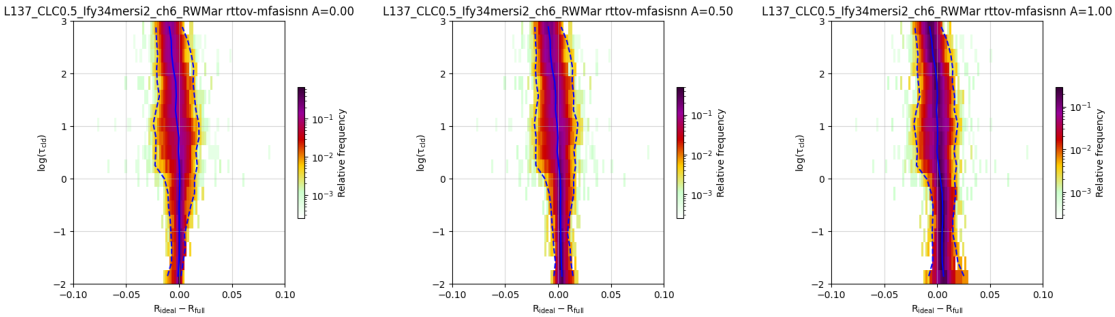

(a) (b) (c)

Figure 103: MFASIS $\Delta r_{\mathrm{MFASIS}-ref}$ as function of the cloud optical depth τ at albedo(s) of 0.0, 0.5, 1.0 (from left to right) for the instrument: FY3 4 MERSI2 CH6

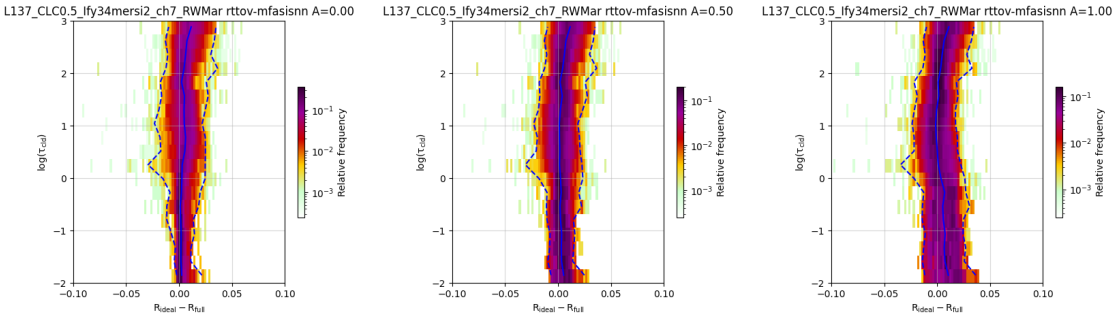

(a) (b) (c)

Figure 104: MFASIS $\Delta r_{\mathrm{MFASIS}-ref}$ as function of the cloud optical depth τ at albedo(s) of 0.0, 0.5, 1.0 (from left to right) for the instrument: FY3 4 MERSI2 CH7

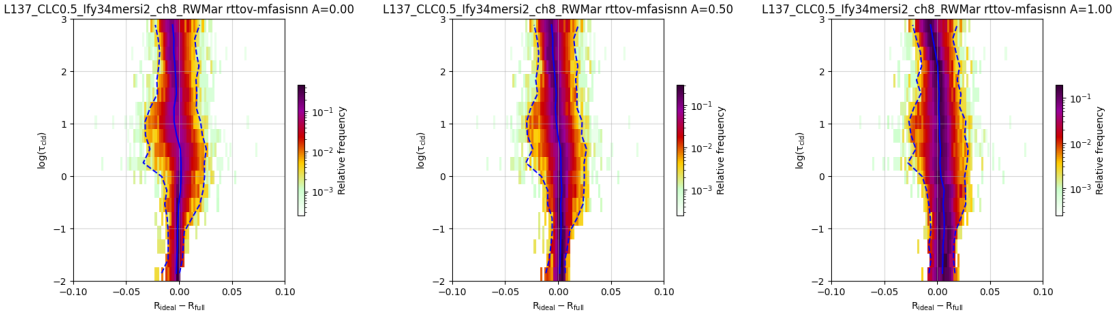

(a) (b) (c)

Figure 105: MFASIS $\Delta r_{\mathrm{MFASIS}-ref}$ as function of the cloud optical depth τ at albedo(s) of 0.0, 0.5, 1.0 (from left to right) for the instrument: FY3 4 MERSI2 CH8

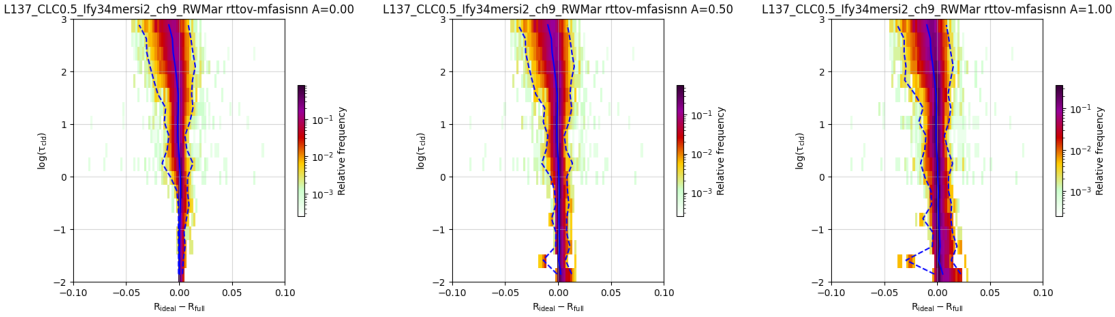

(a) (b) (c)

Figure 106: MFASIS $\Delta r_{\mathrm{MFASIS}-ref}$ as function of the cloud optical depth τ at albedo(s) of 0.0, 0.5, 1.0 (from left to right) for the instrument: FY3 4 MERSI2 CH9

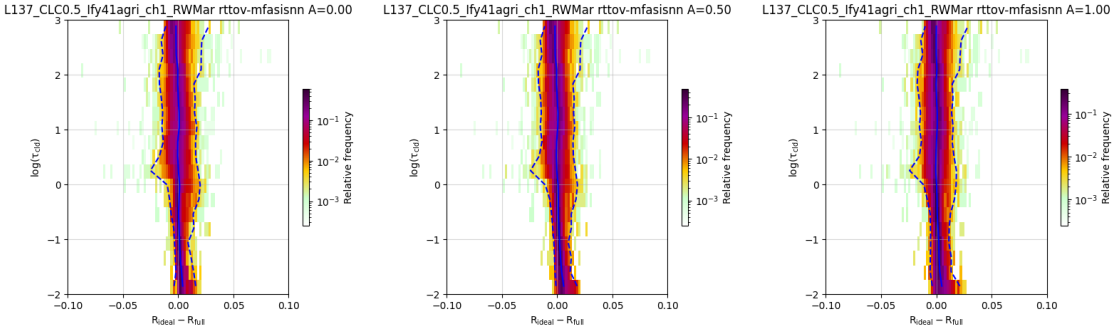

(a) (b) (c)

Figure 107: MFASIS $\Delta r_{\mathrm{MFASIS}-ref}$ as function of the cloud optical depth τ at albedo(s) of 0.0, 0.5, 1.0 (from left to right) for the instrument: FY4 1 AGRI CH1

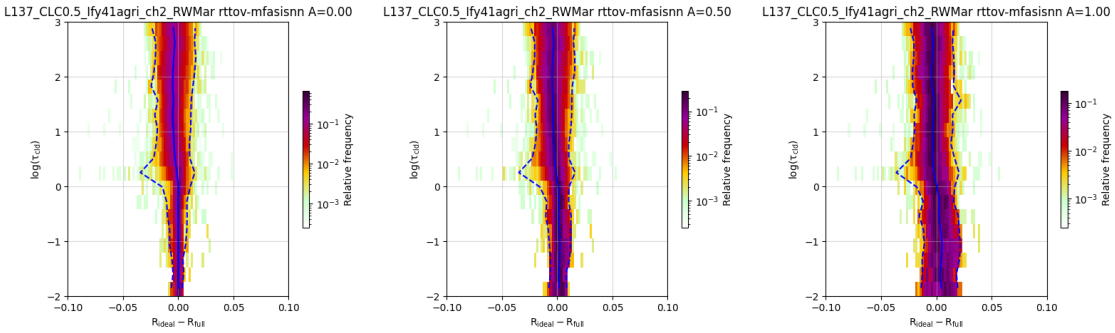

(a) (b) (c)

Figure 108: MFASIS $\Delta r_{\mathrm{MFASIS}-ref}$ as function of the cloud optical depth τ at albedo(s) of 0.0, 0.5, 1.0 (from left to right) for the instrument: FY4 1 AGRI CH2

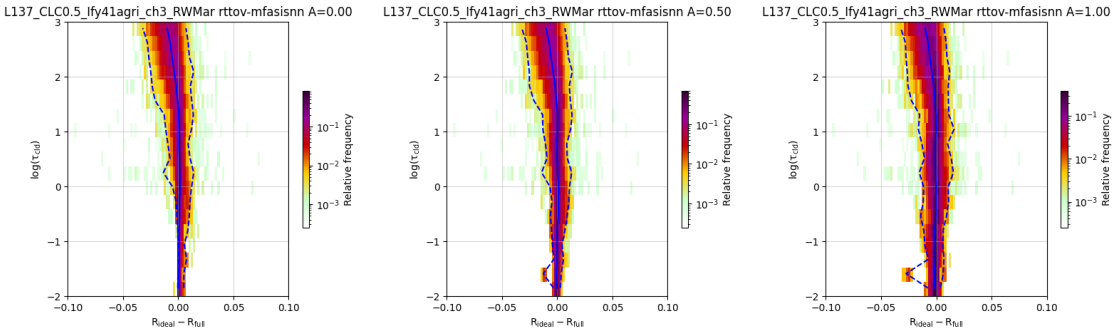

(a) (b) (c)

Figure 109: MFASIS $\Delta r_{\mathrm{MFASIS}-ref}$ as function of the cloud optical depth τ at albedo(s) of 0.0, 0.5, 1.0 (from left to right) for the instrument: FY4 1 AGRI CH3

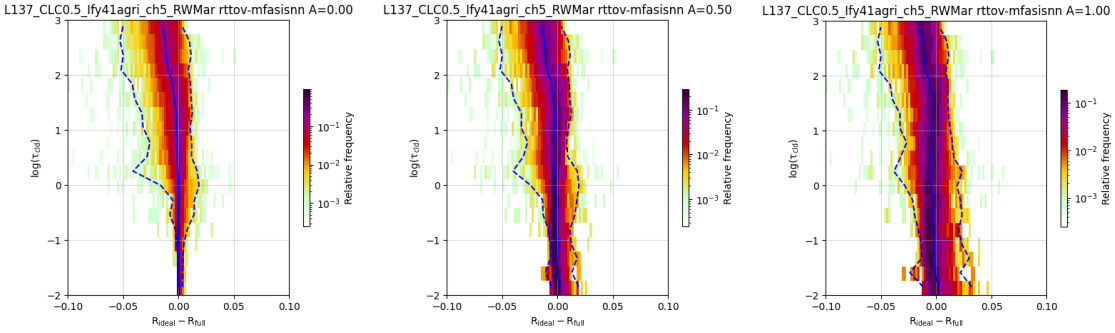

(a) (b) (c)

Figure 110: MFASIS $\Delta r_{\mathrm{MFASIS}-ref}$ as function of the cloud optical depth τ at albedo(s) of 0.0, 0.5, 1.0 (from left to right) for the instrument: FY4 1 AGRI CH5

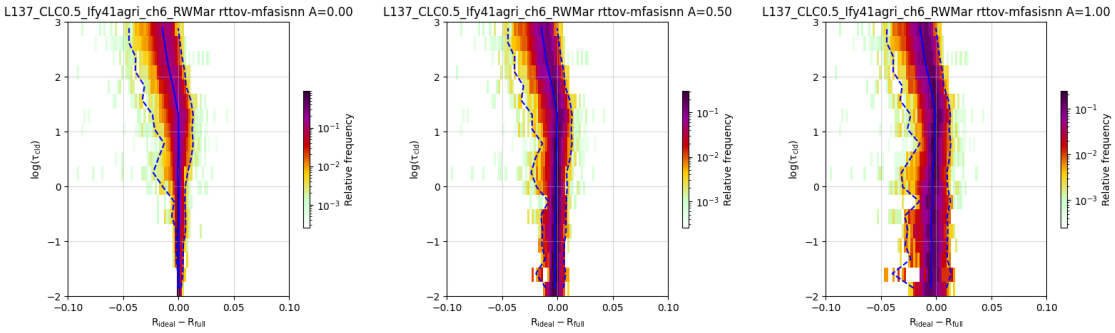

(a) (b) (c)

Figure 111: MFASIS $\Delta r_{\mathrm{MFASIS}-ref}$ as function of the cloud optical depth τ at albedo(s) of 0.0, 0.5, 1.0 (from left to right) for the instrument: FY4 1 AGRI CH6

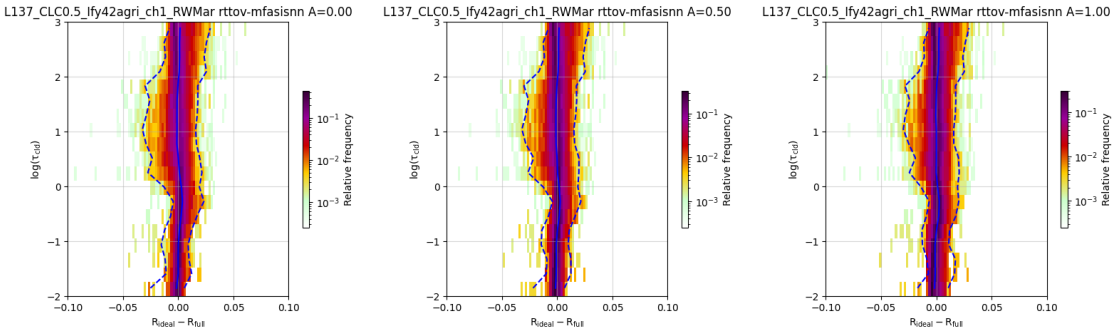

(a) (b) (c)

Figure 112: MFASIS $\Delta r_{\mathrm{MFASIS}-ref}$ as function of the cloud optical depth τ at albedo(s) of 0.0, 0.5, 1.0 (from left to right) for the instrument: FY4 2 AGRI CH1

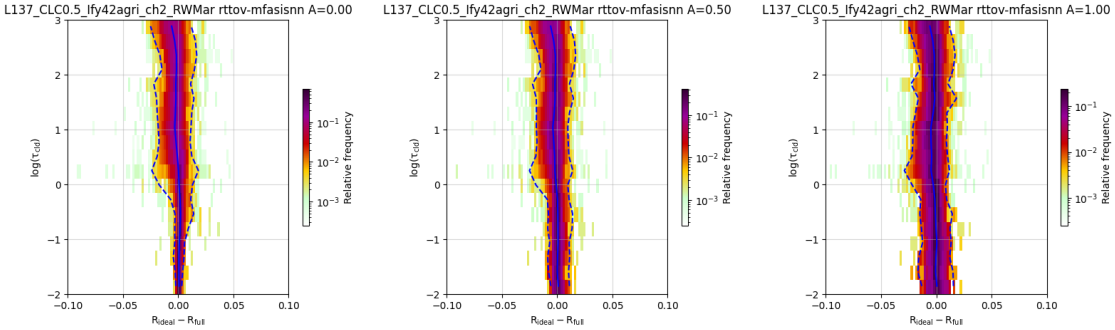

(a) (b) (c)

Figure 113: MFASIS $\Delta r_{\mathrm{MFASIS}-ref}$ as function of the cloud optical depth τ at albedo(s) of 0.0, 0.5, 1.0 (from left to right) for the instrument: FY4 2 AGRI CH2

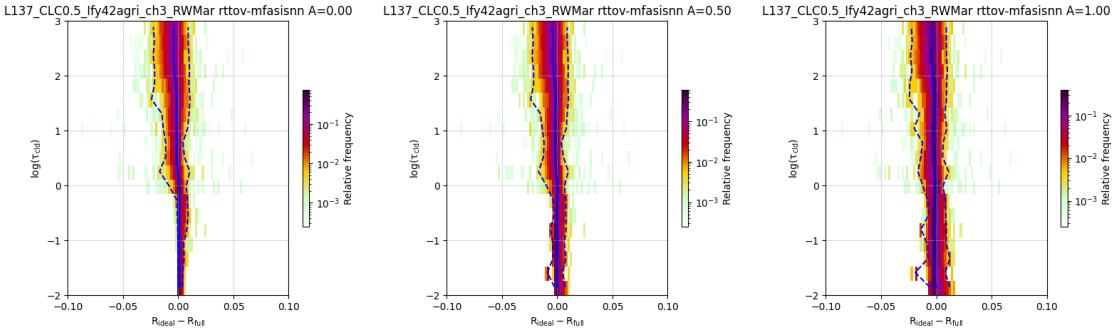

(a) (b) (c)

Figure 114: MFASIS $\Delta r_{\mathrm{MFASIS}-ref}$ as function of the cloud optical depth τ at albedo(s) of 0.0, 0.5, 1.0 (from left to right) for the instrument: FY4 2 AGRI CH3

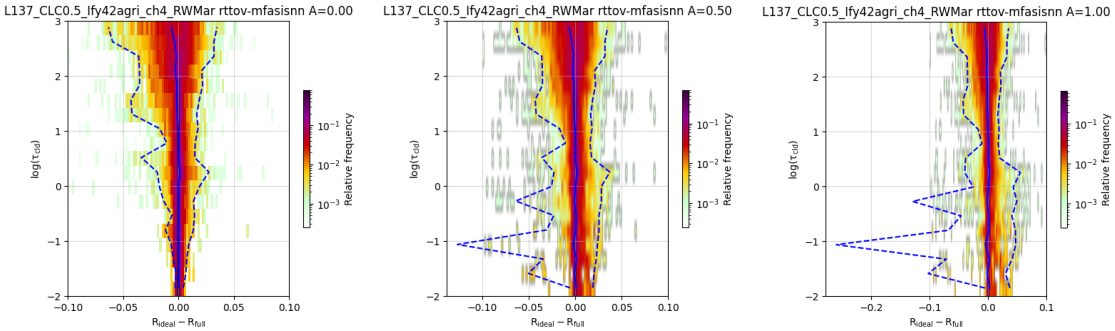

(a) (b) (c)

Figure 115: MFASIS $\Delta r_{\mathrm{MFASIS}-ref}$ as function of the cloud optical depth τ at albedo(s) of 0.0, 0.5, 1.0 (from left to right) for the instrument: FY4 2 AGRI CH4

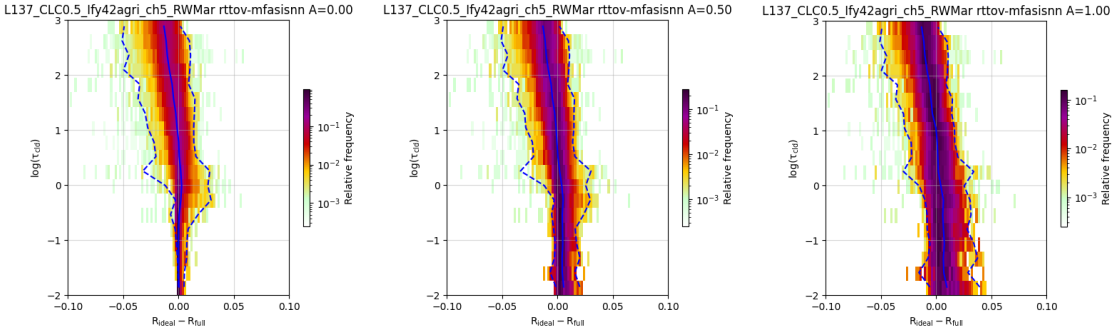

(a) (b) (c)

Figure 116: MFASIS $\Delta r_{\mathrm{MFASIS}-ref}$ as function of the cloud optical depth τ at albedo(s) of 0.0, 0.5, 1.0 (from left to right) for the instrument: FY4 2 AGRI CH5

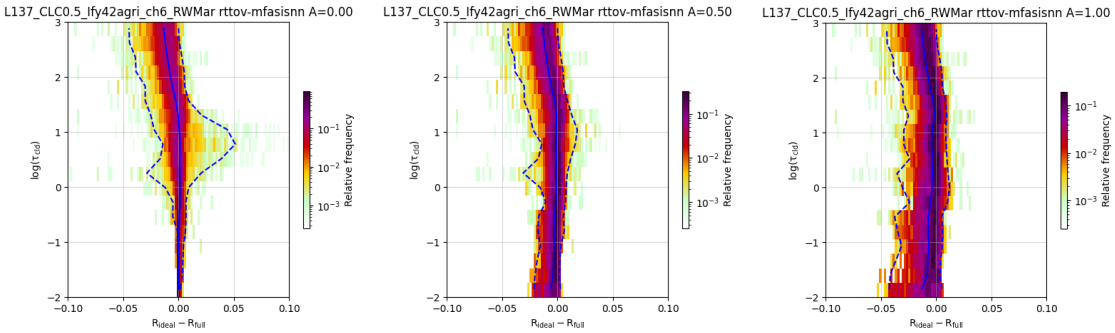

(a) (b) (c)

Figure 117: MFASIS $\Delta r_{\mathrm{MFASIS}-ref}$ as function of the cloud optical depth τ at albedo(s) of 0.0, 0.5, 1.0 (from left to right) for the instrument: FY4 2 AGRI CH6

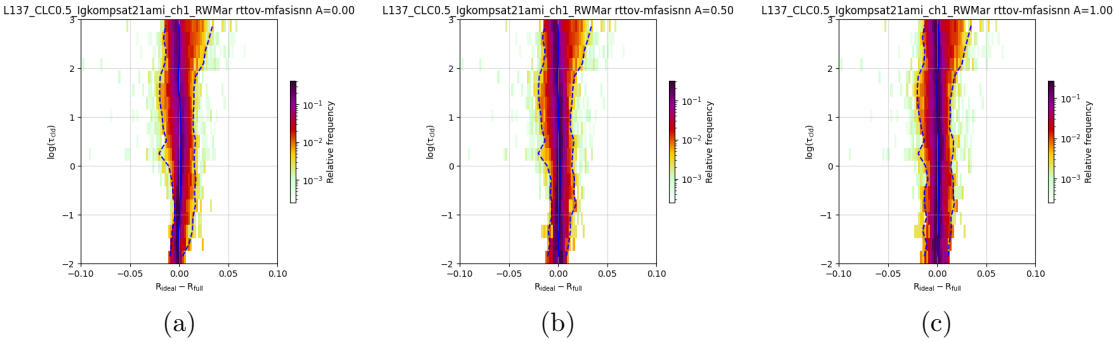

(a) (b) (c)

Figure 118: MFASIS $\Delta r_{\mathrm{MFASIS}-ref}$ as function of the cloud optical depth τ at albedo(s) of 0.0, 0.5, 1.0 (from left to right) for the instrument: GKOMPSAT2 1 AMI CH1

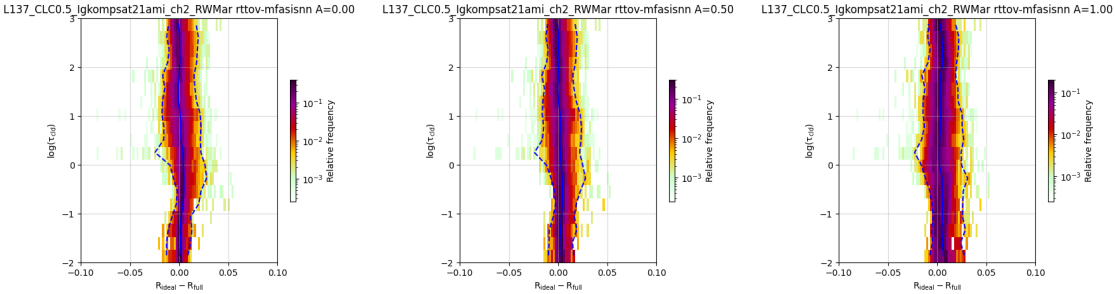

(a) (b) (c)

Figure 119: MFASIS $\Delta r_{\mathrm{MFASIS}-ref}$ as function of the cloud optical depth τ at albedo(s) of 0.0, 0.5, 1.0 (from left to right) for the instrument: GKOMPSAT2 1 AMI CH2

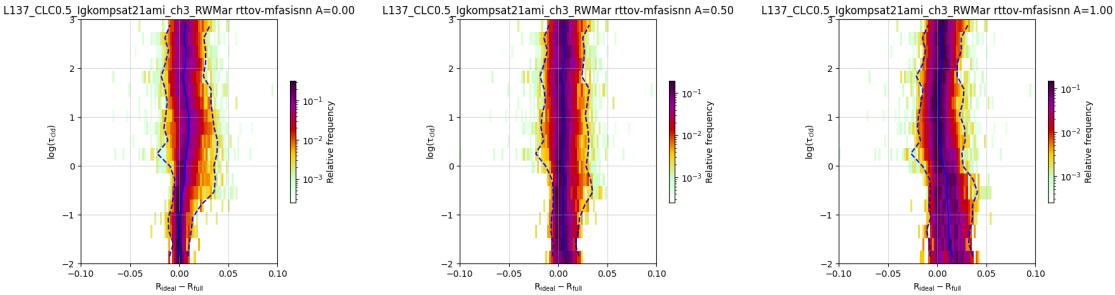

(a) (b) (c)

Figure 120: MFASIS $\Delta r_{\mathrm{MFASIS}-ref}$ as function of the cloud optical depth τ at albedo(s) of 0.0, 0.5, 1.0 (from left to right) for the instrument: GKOMPSAT2 1 AMI CH3

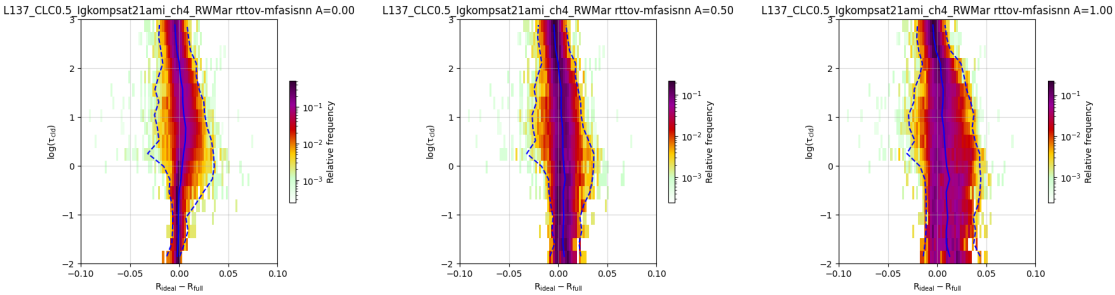

(a) (b) (c)

Figure 121: MFASIS $\Delta r_{\mathrm{MFASIS}-ref}$ as function of the cloud optical depth τ at albedo(s) of 0.0, 0.5, 1.0 (from left to right) for the instrument: GKOMPSAT2 1 AMI CH4

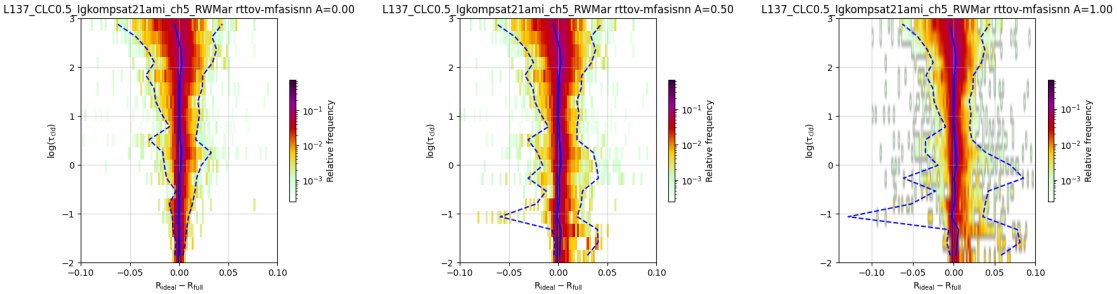

(a) (b) (c)

Figure 122: MFASIS $\Delta r_{\mathrm{MFASIS}-ref}$ as function of the cloud optical depth τ at albedo(s) of 0.0, 0.5, 1.0 (from left to right) for the instrument: GKOMPSAT2 1 AMI CH5

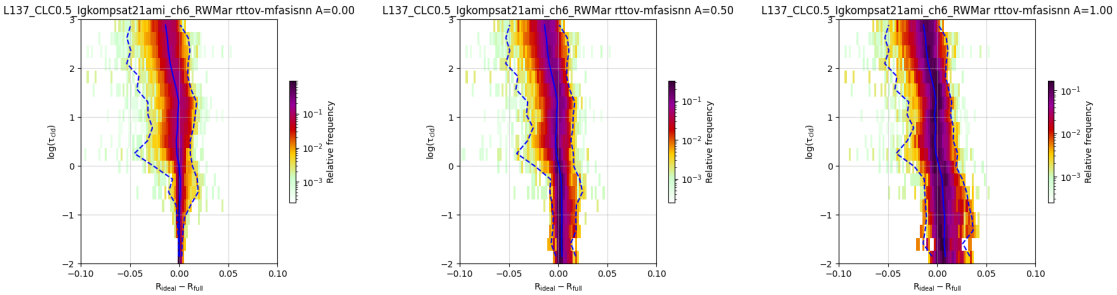

(a) (b) (c)

Figure 123: MFASIS $\Delta r_{\mathrm{MFASIS}-ref}$ as function of the cloud optical depth τ at albedo(s) of 0.0, 0.5, 1.0 (from left to right) for the instrument: GKOMPSAT2 1 AMI CH6

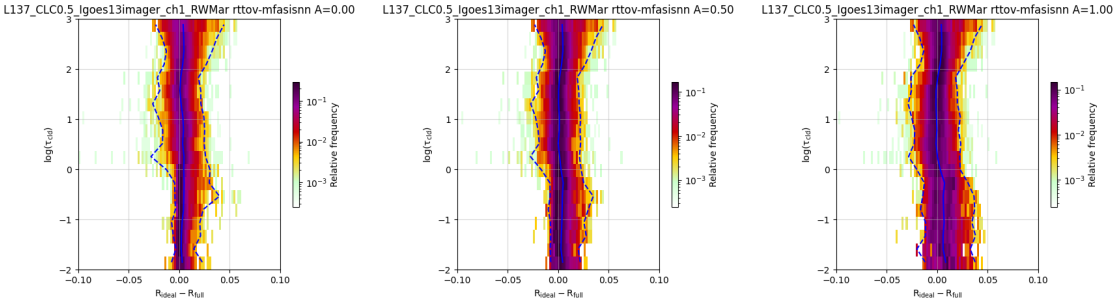

(a) (b) (c)

Figure 124: MFASIS $\Delta r_{\mathrm{MFASIS}-ref}$ as function of the cloud optical depth τ at albedo(s) of 0.0, 0.5, 1.0 (from left to right) for the instrument: GOES 13 IMAGER CH1

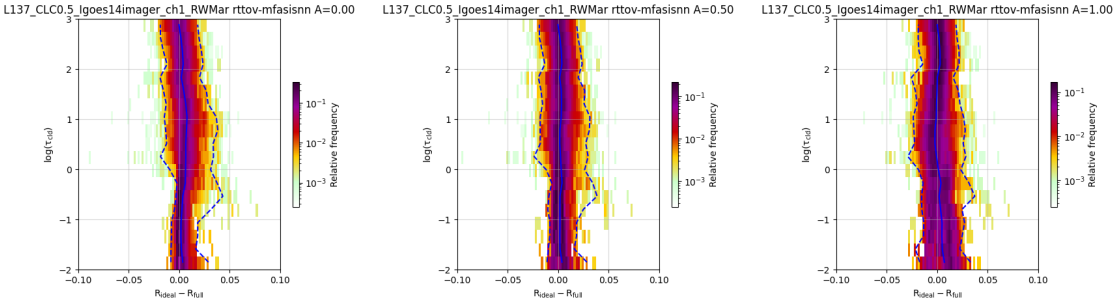

(a) (b) (c)

Figure 125: MFASIS $\Delta r_{\mathrm{MFASIS}-ref}$ as function of the cloud optical depth τ at albedo(s) of 0.0, 0.5, 1.0 (from left to right) for the instrument: GOES 14 IMAGER CH1

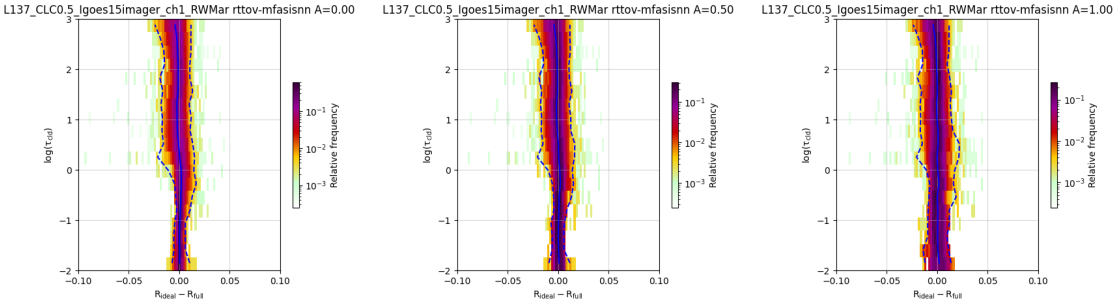

(a) (b) (c)

Figure 126: MFASIS $\Delta r_{\mathrm{MFASIS}-ref}$ as function of the cloud optical depth τ at albedo(s) of 0.0, 0.5, 1.0 (from left to right) for the instrument: GOES 15 IMAGER CH1

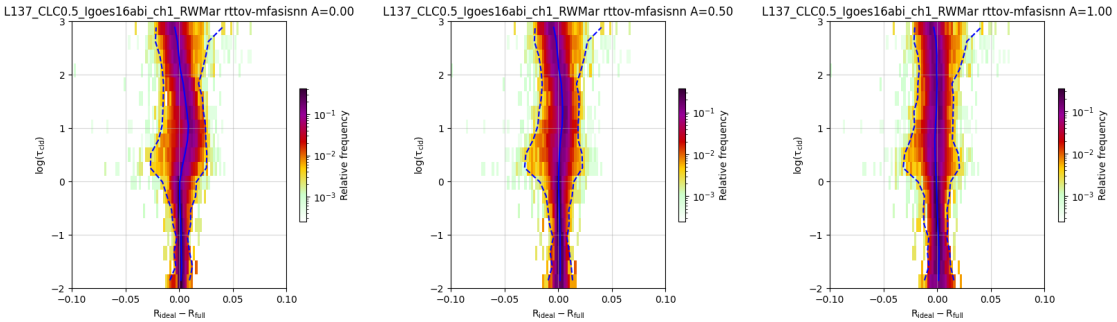

(a) (b) (c)

Figure 127: MFASIS $\Delta r_{\mathrm{MFASIS}-ref}$ as function of the cloud optical depth τ at albedo(s) of 0.0, 0.5, 1.0 (from left to right) for the instrument: GOES 16 ABI CH1

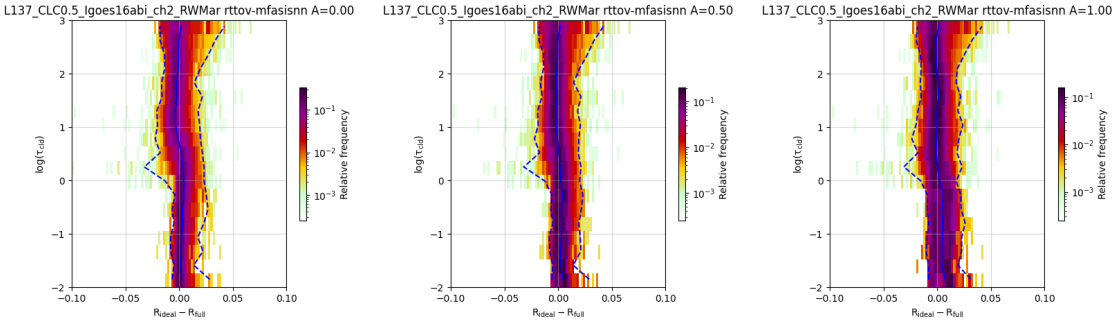

(a) (b) (c)

Figure 128: MFASIS $\Delta r_{\mathrm{MFASIS}-ref}$ as function of the cloud optical depth τ at albedo(s) of 0.0, 0.5, 1.0 (from left to right) for the instrument: GOES 16 ABI CH2

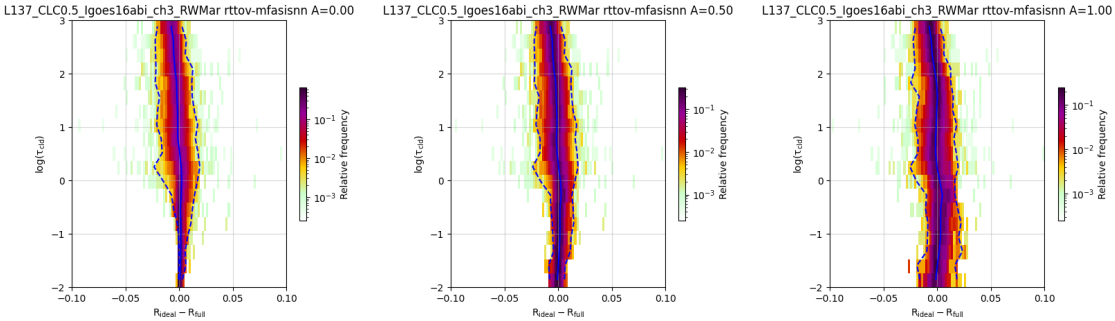

(a) (b) (c)

Figure 129: MFASIS $\Delta r_{\mathrm{MFASIS}-ref}$ as function of the cloud optical depth τ at albedo(s) of 0.0, 0.5, 1.0 (from left to right) for the instrument: GOES 16 ABI CH3

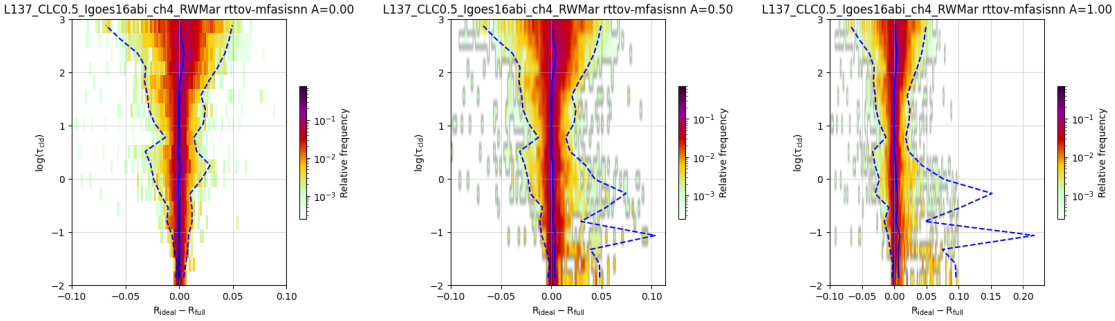

(a) (b) (c)

Figure 130: MFASIS $\Delta r_{\mathrm{MFASIS}-ref}$ as function of the cloud optical depth τ at albedo(s) of 0.0, 0.5, 1.0 (from left to right) for the instrument: GOES 16 ABI CH4

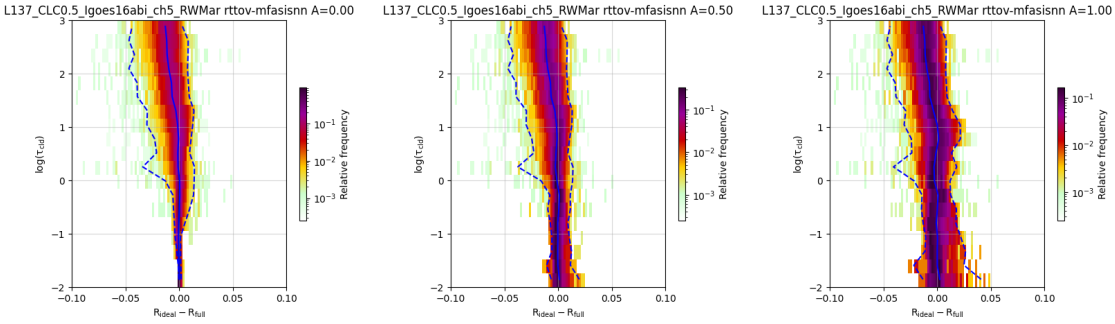

(a) (b) (c)

Figure 131: MFASIS $\Delta r_{\mathrm{MFASIS}-ref}$ as function of the cloud optical depth τ at albedo(s) of 0.0, 0.5, 1.0 (from left to right) for the instrument: GOES 16 ABI CH5

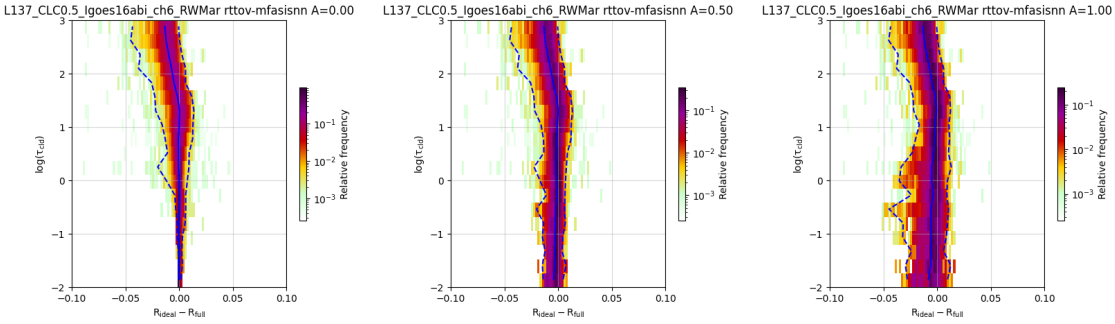

(a) (b) (c)

Figure 132: MFASIS $\Delta r_{\mathrm{MFASIS}-ref}$ as function of the cloud optical depth τ at albedo(s) of 0.0, 0.5, 1.0 (from left to right) for the instrument: GOES 16 ABI CH6

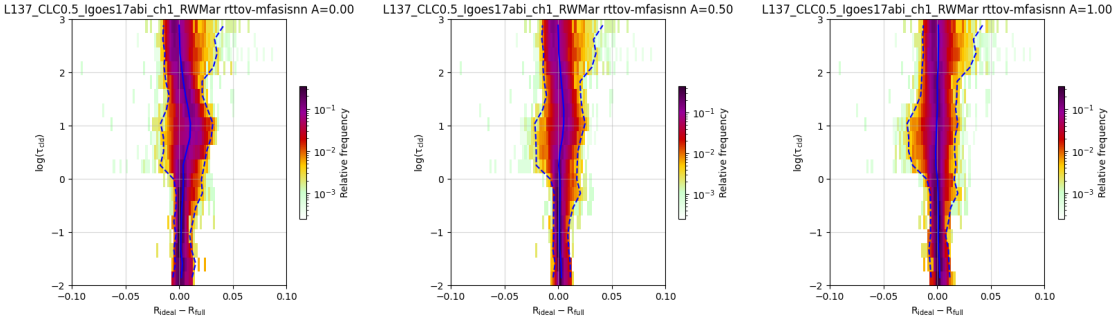

(a) (b) (c)

Figure 133: MFASIS $\Delta r_{\mathrm{MFASIS}-ref}$ as function of the cloud optical depth τ at albedo(s) of 0.0, 0.5, 1.0 (from left to right) for the instrument: GOES 17 ABI CH1

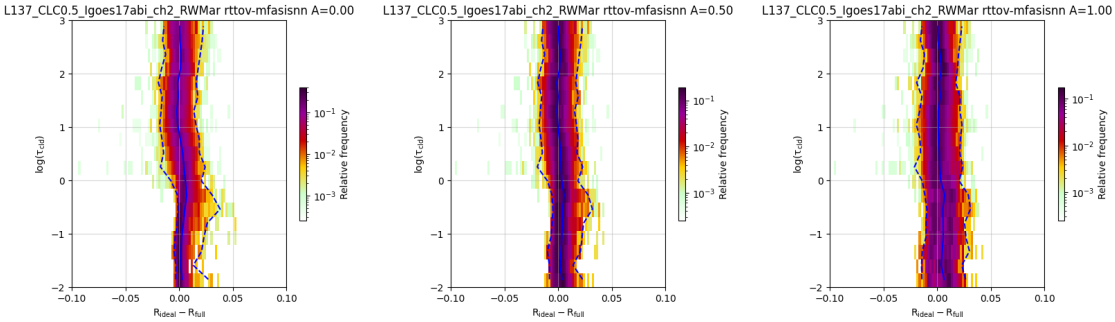

(a) (b) (c)

Figure 134: MFASIS $\Delta r_{\mathrm{MFASIS}-ref}$ as function of the cloud optical depth τ at albedo(s) of 0.0, 0.5, 1.0 (from left to right) for the instrument: GOES 17 ABI CH2

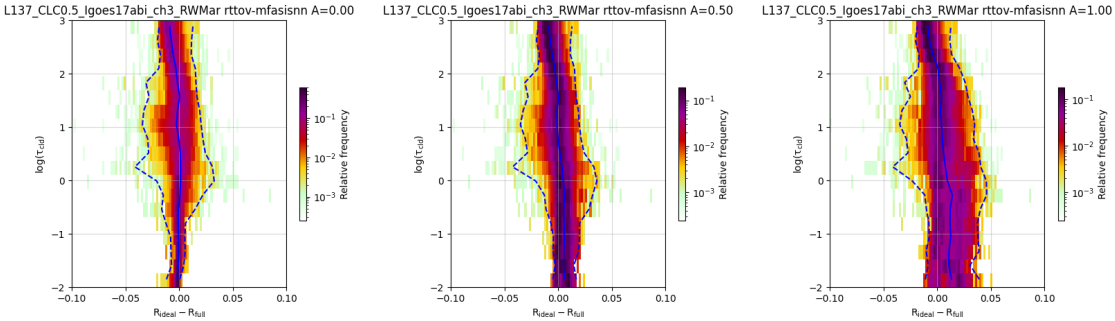

(a) (b) (c)

Figure 135: MFASIS $\Delta r_{\mathrm{MFASIS}-ref}$ as function of the cloud optical depth τ at albedo(s) of 0.0, 0.5, 1.0 (from left to right) for the instrument: GOES 17 ABI CH3

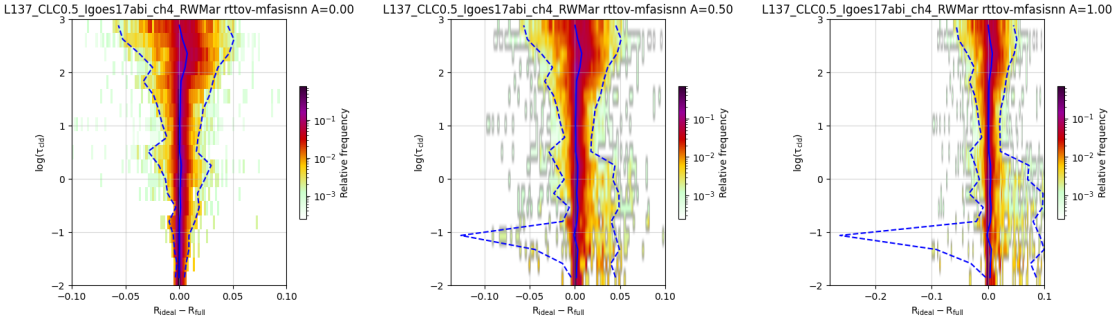

(a) (b) (c)

Figure 136: MFASIS $\Delta r_{\mathrm{MFASIS}-ref}$ as function of the cloud optical depth τ at albedo(s) of 0.0, 0.5, 1.0 (from left to right) for the instrument: GOES 17 ABI CH4

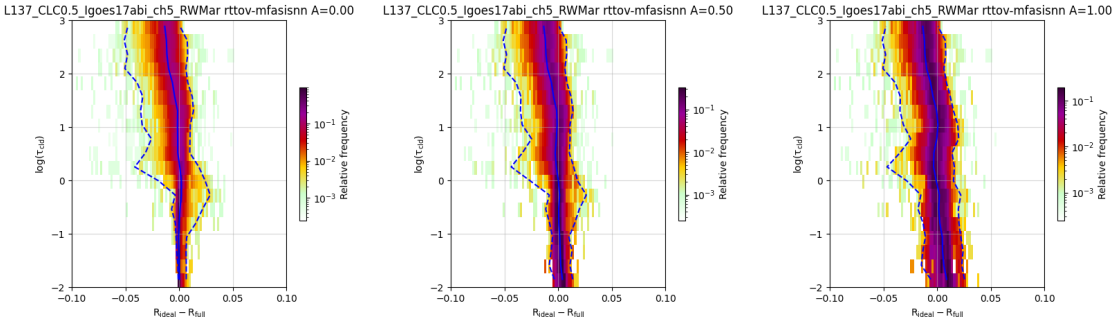

(a) (b) (c)

Figure 137: MFASIS $\Delta r_{\mathrm{MFASIS}-ref}$ as function of the cloud optical depth τ at albedo(s) of 0.0, 0.5, 1.0 (from left to right) for the instrument: GOES 17 ABI CH5

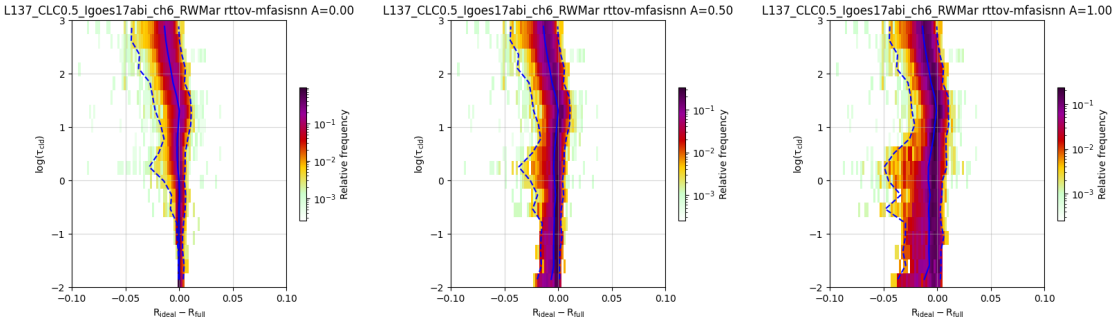

(a) (b) (c)

Figure 138: MFASIS $\Delta r_{\mathrm{MFASIS}-ref}$ as function of the cloud optical depth τ at albedo(s) of 0.0, 0.5, 1.0 (from left to right) for the instrument: GOES 17 ABI CH6

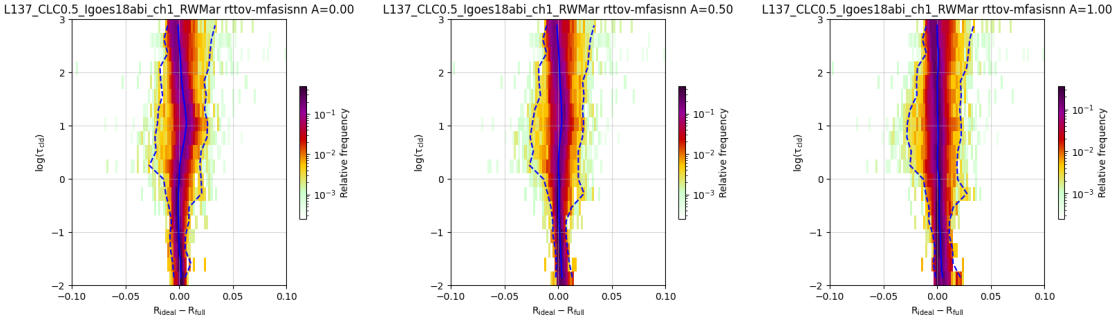

(a) (b) (c)

Figure 139: MFASIS $\Delta r_{\mathrm{MFASIS}-ref}$ as function of the cloud optical depth τ at albedo(s) of 0.0, 0.5, 1.0 (from left to right) for the instrument: GOES 18 ABI CH1

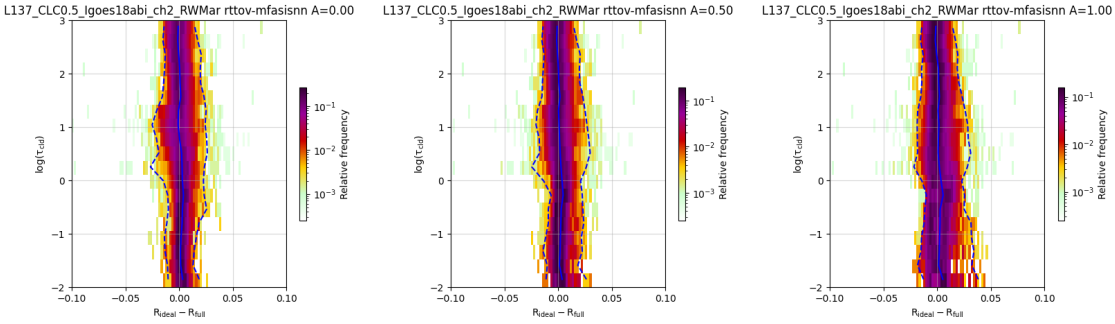

(a) (b) (c)

Figure 140: MFASIS $\Delta r_{\mathrm{MFASIS}-ref}$ as function of the cloud optical depth τ at albedo(s) of 0.0, 0.5, 1.0 (from left to right) for the instrument: GOES 18 ABI CH2

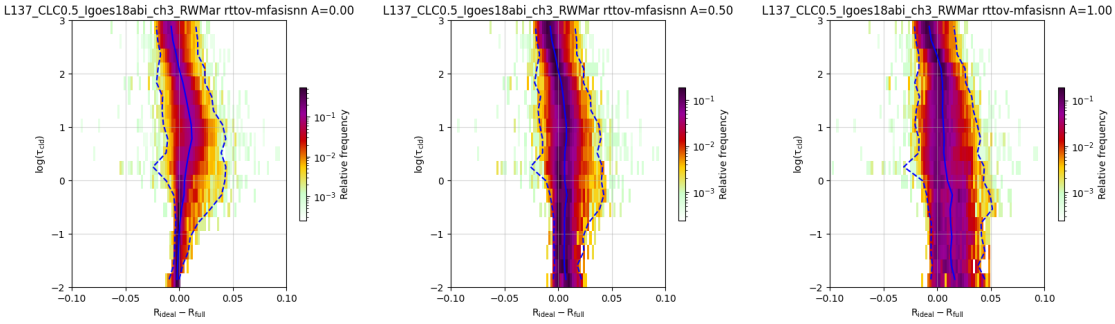

(a) (b) (c)

Figure 141: MFASIS $\Delta r_{\mathrm{MFASIS}-ref}$ as function of the cloud optical depth τ at albedo(s) of 0.0, 0.5, 1.0 (from left to right) for the instrument: GOES 18 ABI CH3

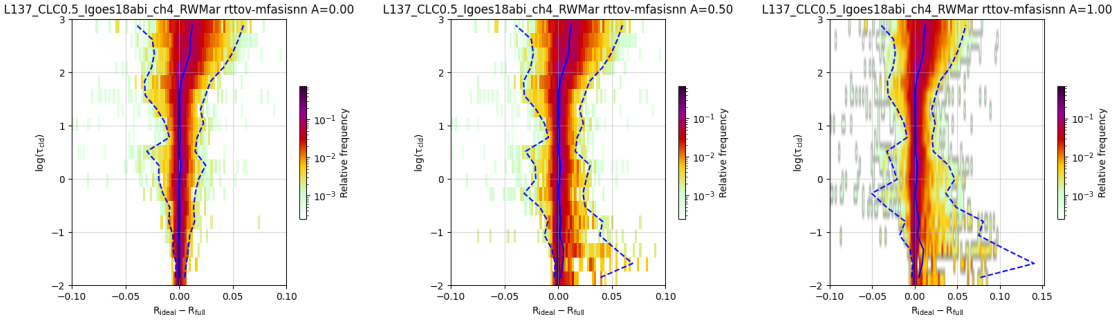

(a) (b) (c)

Figure 142: MFASIS $\Delta r_{\mathrm{MFASIS}-ref}$ as function of the cloud optical depth τ at albedo(s) of 0.0, 0.5, 1.0 (from left to right) for the instrument: GOES 18 ABI CH4

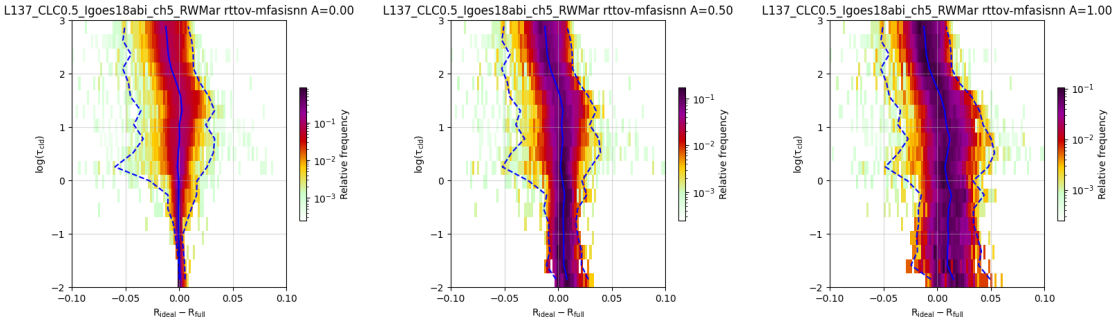

(a) (b) (c)

Figure 143: MFASIS $\Delta r_{\mathrm{MFASIS}-ref}$ as function of the cloud optical depth τ at albedo(s) of 0.0, 0.5, 1.0 (from left to right) for the instrument: GOES 18 ABI CH5

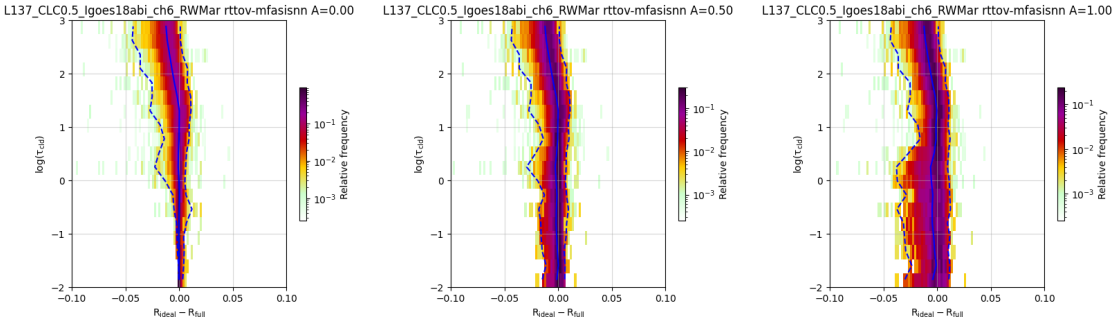

(a) (b) (c)

Figure 144: MFASIS $\Delta r_{\mathrm{MFASIS}-ref}$ as function of the cloud optical depth τ at albedo(s) of 0.0, 0.5, 1.0 (from left to right) for the instrument: GOES 18 ABI CH6

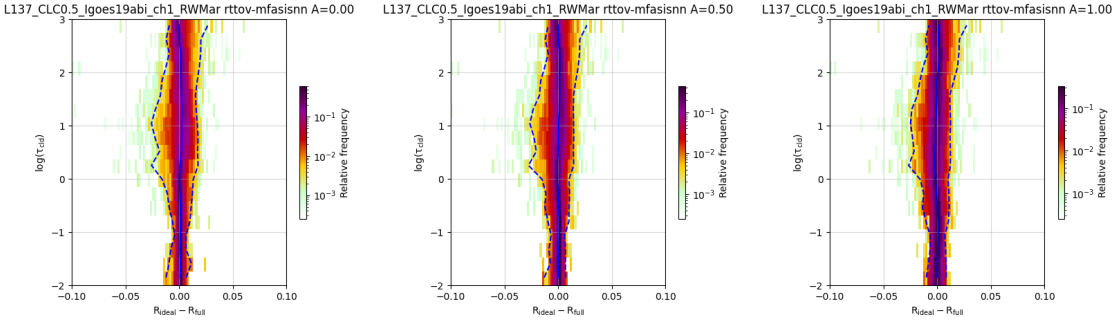

(a) (b) (c)

Figure 145: MFASIS $\Delta r_{\mathrm{MFASIS}-ref}$ as function of the cloud optical depth τ at albedo(s) of 0.0, 0.5, 1.0 (from left to right) for the instrument: GOES 19 ABI CH1

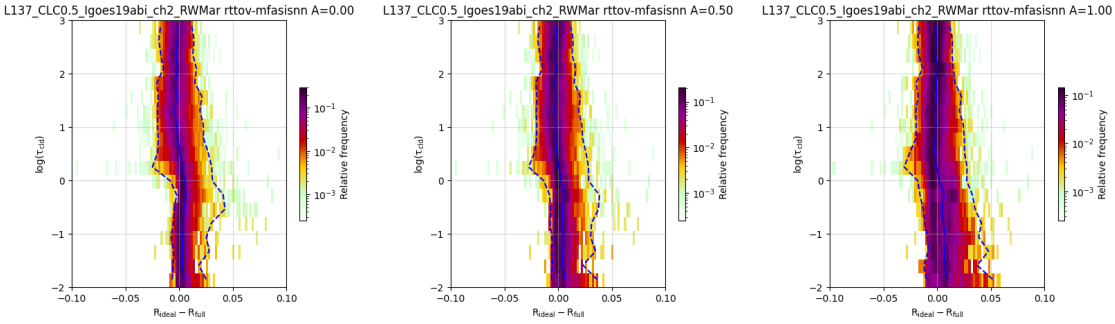

(a) (b) (c)

Figure 146: MFASIS $\Delta r_{\mathrm{MFASIS}-ref}$ as function of the cloud optical depth τ at albedo(s) of 0.0, 0.5, 1.0 (from left to right) for the instrument: GOES 19 ABI CH2

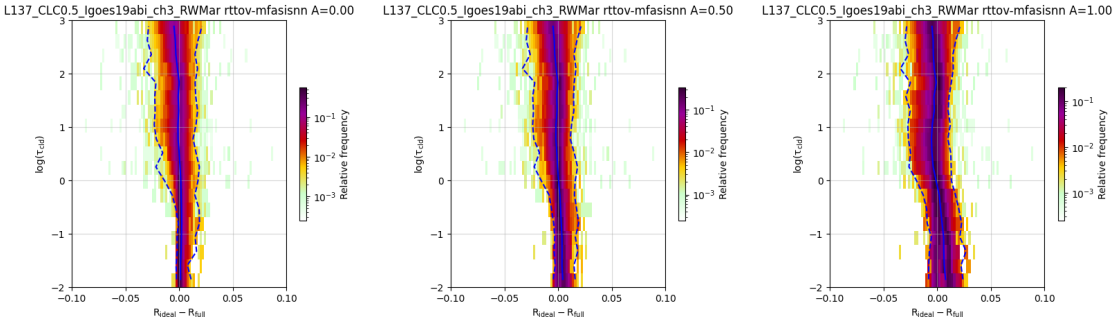

(a) (b) (c)

Figure 147: MFASIS $\Delta r_{\mathrm{MFASIS}-ref}$ as function of the cloud optical depth τ at albedo(s) of 0.0, 0.5, 1.0 (from left to right) for the instrument: GOES 19 ABI CH3

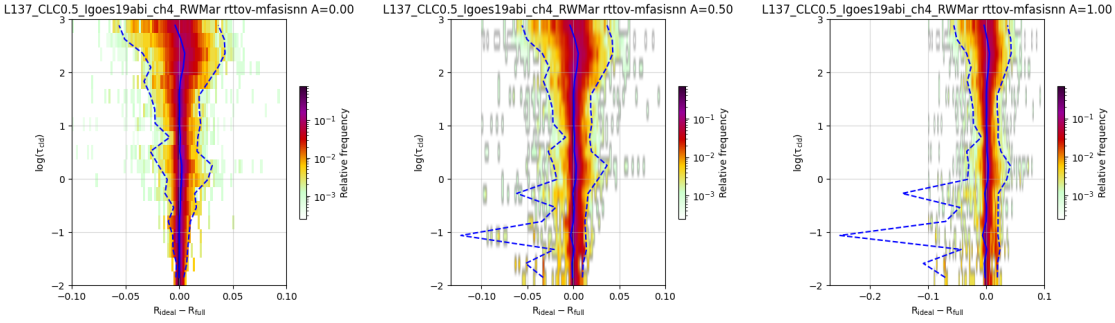

(a) (b) (c)

Figure 148: MFASIS $\Delta r_{\mathrm{MFASIS}-ref}$ as function of the cloud optical depth τ at albedo(s) of 0.0, 0.5, 1.0 (from left to right) for the instrument: GOES 19 ABI CH4

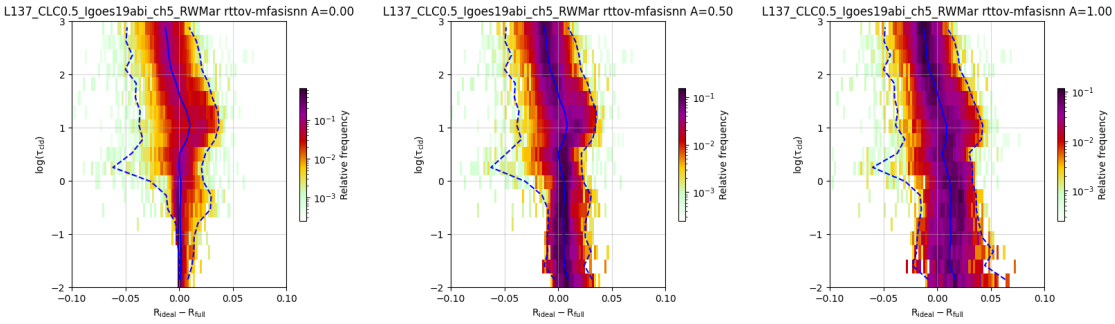

(a) (b) (c)

Figure 149: MFASIS $\Delta r_{\mathrm{MFASIS}-ref}$ as function of the cloud optical depth τ at albedo(s) of 0.0, 0.5, 1.0 (from left to right) for the instrument: GOES 19 ABI CH5

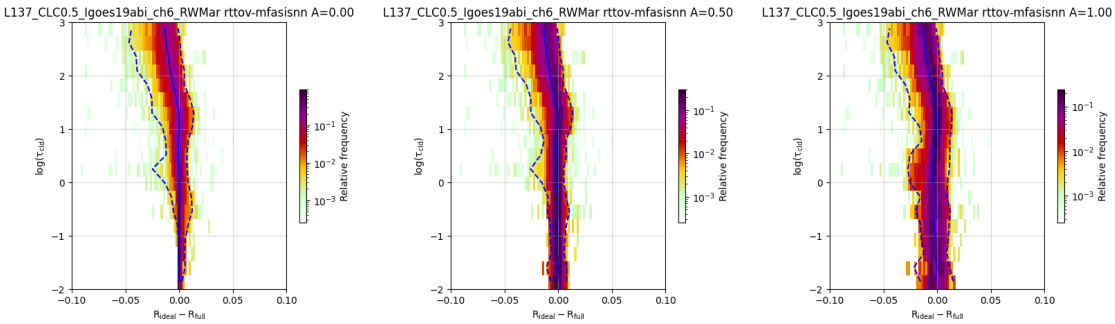

(a) (b) (c)

Figure 150: MFASIS $\Delta r_{\mathrm{MFASIS}-ref}$ as function of the cloud optical depth τ at albedo(s) of 0.0, 0.5, 1.0 (from left to right) for the instrument: GOES 19 ABI CH6

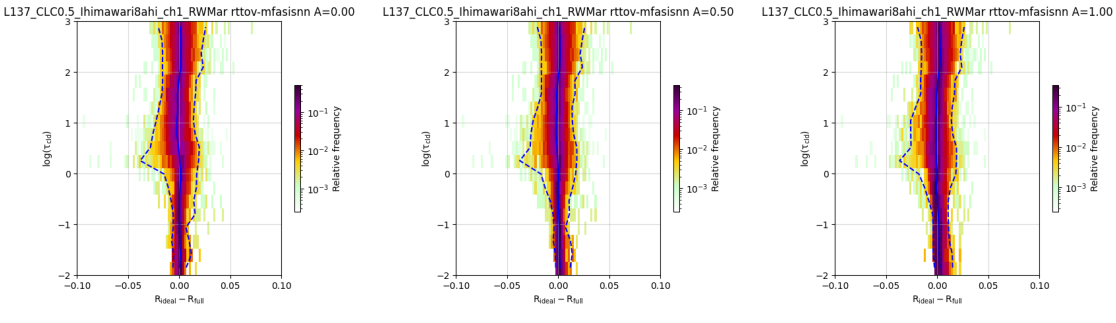

(a) (b) (c)

Figure 151: MFASIS $\Delta r_{\mathrm{MFASIS}-ref}$ as function of the cloud optical depth τ at albedo(s) of 0.0, 0.5, 1.0 (from left to right) for the instrument: HIMAWARI 8 AHI CH1

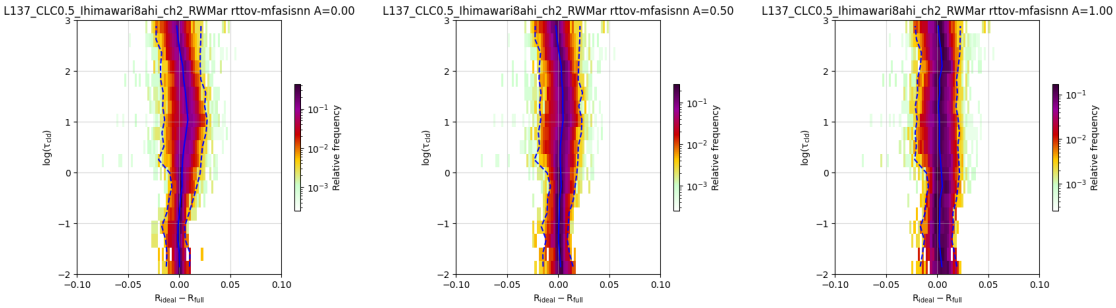

(a) (b) (c)

Figure 152: MFASIS $\Delta r_{\mathrm{MFASIS}-ref}$ as function of the cloud optical depth τ at albedo(s) of 0.0, 0.5, 1.0 (from left to right) for the instrument: HIMAWARI 8 AHI CH2

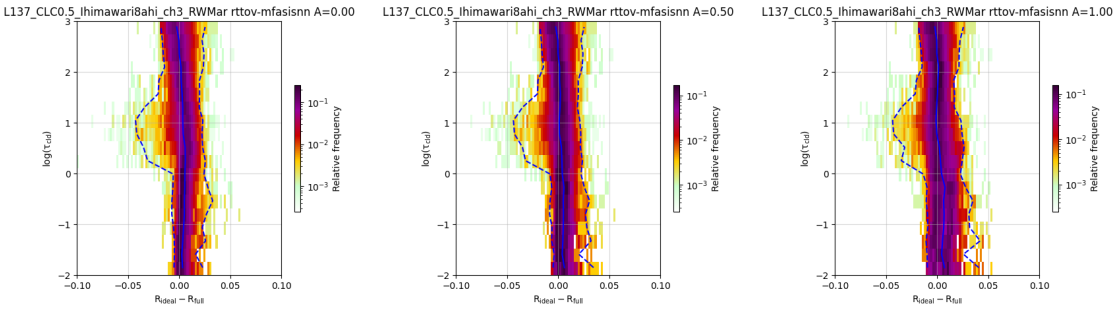

(a) (b) (c)

Figure 153: MFASIS $\Delta r_{\mathrm{MFASIS}-ref}$ as function of the cloud optical depth τ at albedo(s) of 0.0, 0.5, 1.0 (from left to right) for the instrument: HIMAWARI 8 AHI CH3

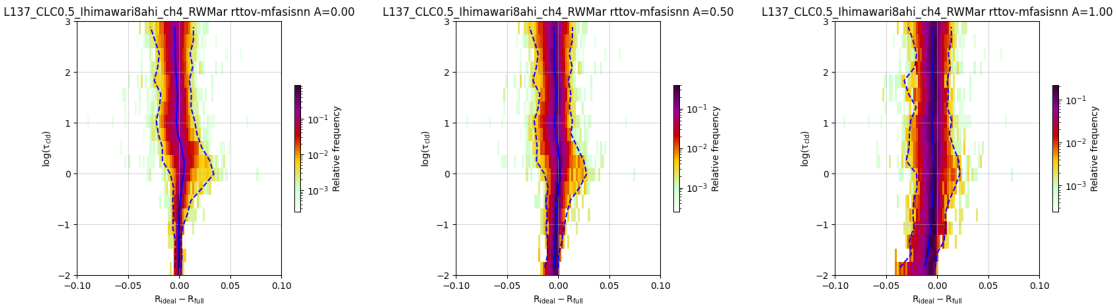

(a) (b) (c)

Figure 154: MFASIS $\Delta r_{\mathrm{MFASIS}-ref}$ as function of the cloud optical depth τ at albedo(s) of 0.0, 0.5, 1.0 (from left to right) for the instrument: HIMAWARI 8 AHI CH4

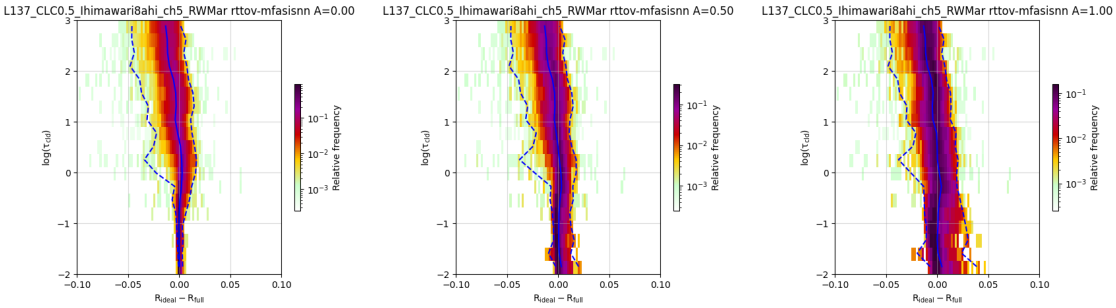

(a) (b) (c)

Figure 155: MFASIS $\Delta r_{\mathrm{MFASIS}-ref}$ as function of the cloud optical depth τ at albedo(s) of 0.0, 0.5, 1.0 (from left to right) for the instrument: HIMAWARI 8 AHI CH5

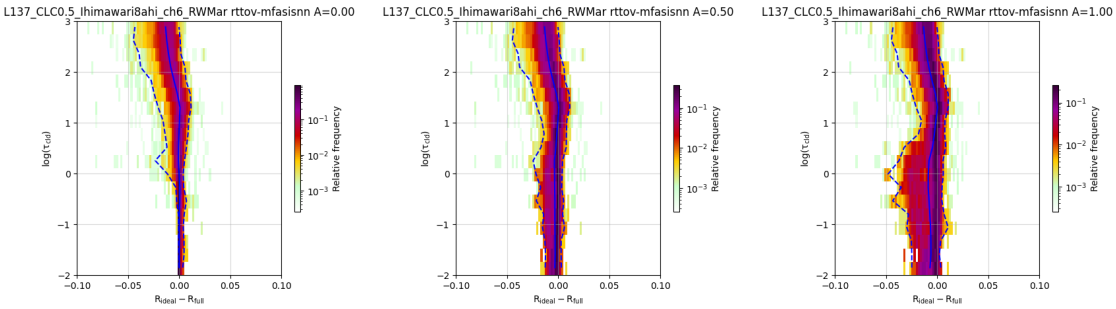

(a) (b) (c)

Figure 156: MFASIS $\Delta r_{\mathrm{MFASIS}-ref}$ as function of the cloud optical depth τ at albedo(s) of 0.0, 0.5, 1.0 (from left to right) for the instrument: HIMAWARI 8 AHI CH6

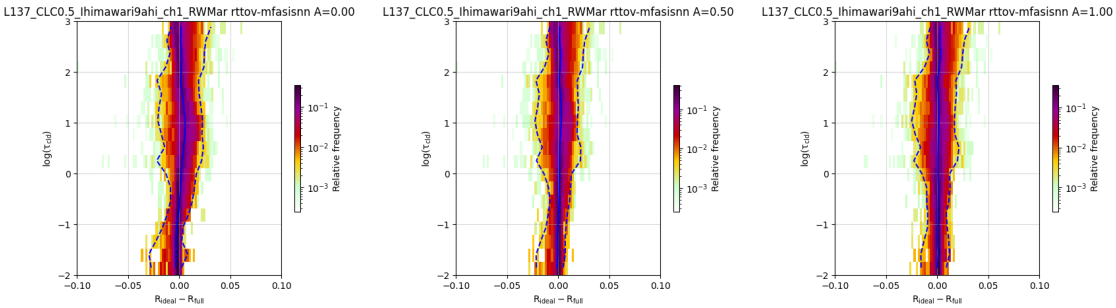

(a) (b) (c)

Figure 157: MFASIS $\Delta r_{\mathrm{MFASIS}-ref}$ as function of the cloud optical depth τ at albedo(s) of 0.0, 0.5, 1.0 (from left to right) for the instrument: HIMAWARI 9 AHI CH1

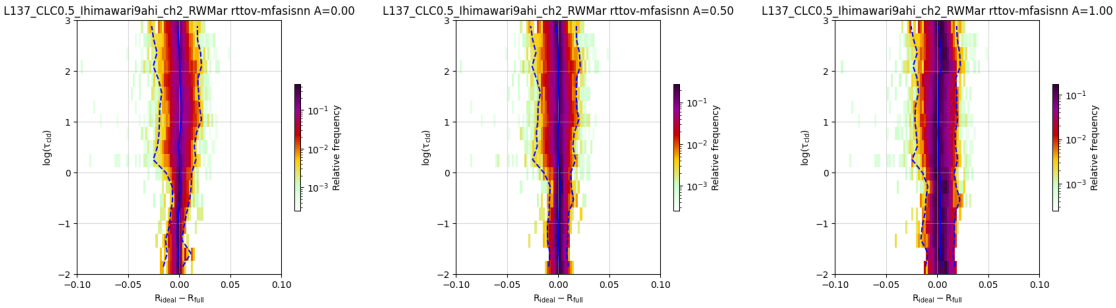

(a) (b) (c)

Figure 158: MFASIS $\Delta r_{\mathrm{MFASIS}-ref}$ as function of the cloud optical depth τ at albedo(s) of 0.0, 0.5, 1.0 (from left to right) for the instrument: HIMAWARI 9 AHI CH2

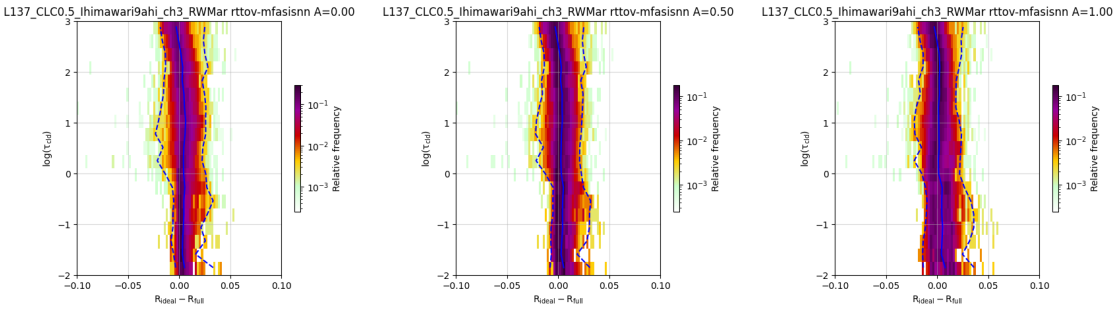

(a) (b) (c)

Figure 159: MFASIS $\Delta r_{\mathrm{MFASIS}-ref}$ as function of the cloud optical depth τ at albedo(s) of 0.0, 0.5, 1.0 (from left to right) for the instrument: HIMAWARI 9 AHI CH3

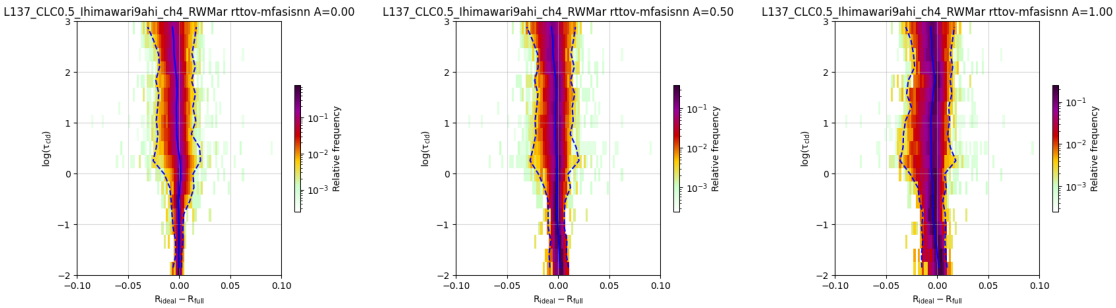

(a) (b) (c)

Figure 160: MFASIS $\Delta r_{\mathrm{MFASIS}-ref}$ as function of the cloud optical depth τ at albedo(s) of 0.0, 0.5, 1.0 (from left to right) for the instrument: HIMAWARI 9 AHI CH4

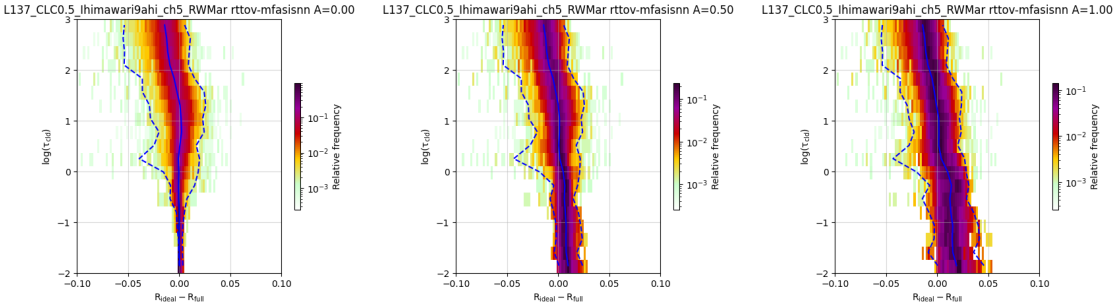

(a) (b) (c)

Figure 161: MFASIS $\Delta r_{\mathrm{MFASIS}-ref}$ as function of the cloud optical depth τ at albedo(s) of 0.0, 0.5, 1.0 (from left to right) for the instrument: HIMAWARI 9 AHI CH5

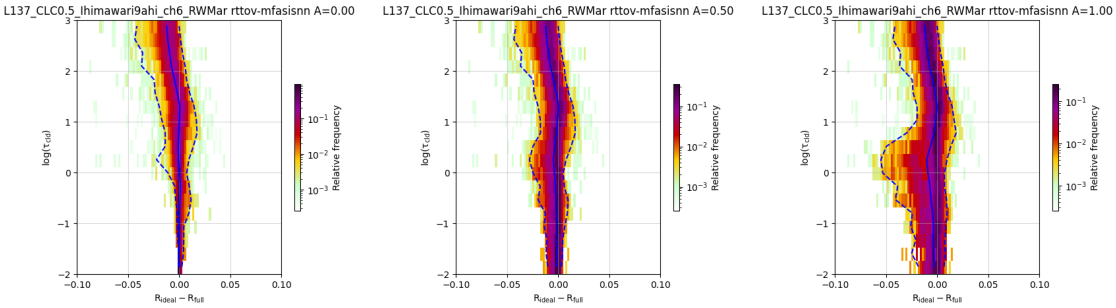

(a) (b) (c)

Figure 162: MFASIS $\Delta r_{\mathrm{MFASIS}-ref}$ as function of the cloud optical depth τ at albedo(s) of 0.0, 0.5, 1.0 (from left to right) for the instrument: HIMAWARI 9 AHI CH6

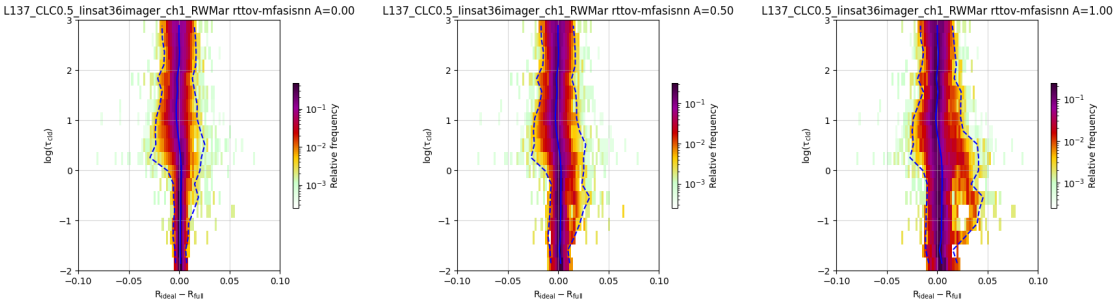

(a) (b) (c)

Figure 163: MFASIS $\Delta r_{\mathrm{MFASIS}-ref}$ as function of the cloud optical depth τ at albedo(s) of 0.0, 0.5, 1.0 (from left to right) for the instrument: INSAT3 6 IMAGER CH1

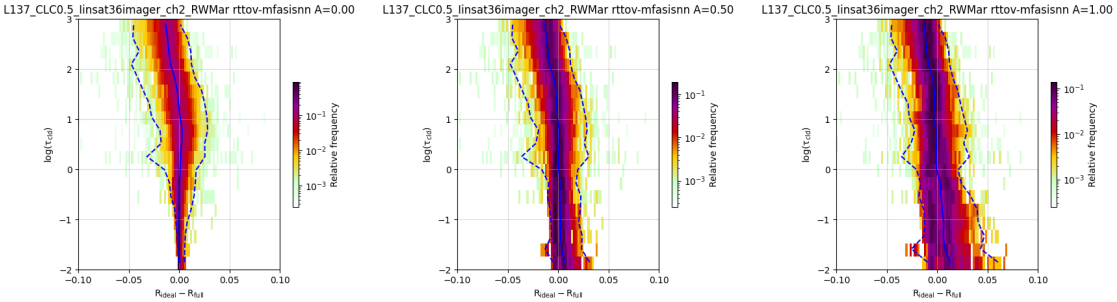

(a) (b) (c)

Figure 164: MFASIS $\Delta r_{\mathrm{MFASIS}-ref}$ as function of the cloud optical depth τ at albedo(s) of 0.0, 0.5, 1.0 (from left to right) for the instrument: INSAT3 6 IMAGER CH2

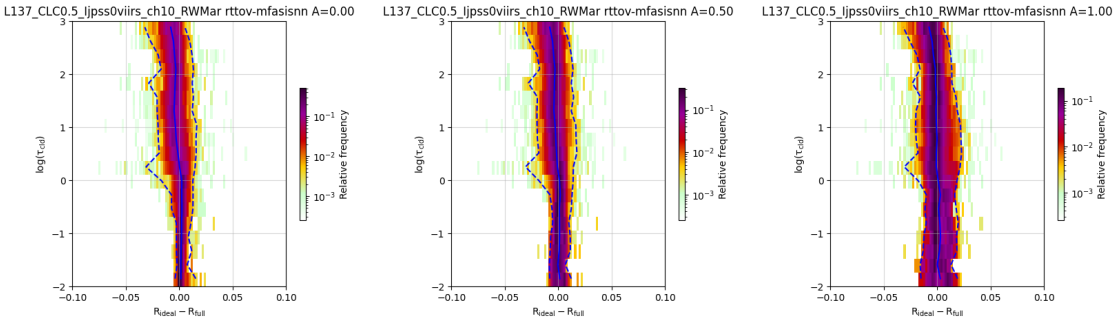

(a) (b) (c)

Figure 165: MFASIS $\Delta r_{\mathrm{MFASIS}-ref}$ as function of the cloud optical depth τ at albedo(s) of 0.0, 0.5, 1.0 (from left to right) for the instrument: JPSS 0 VIIRS CH10

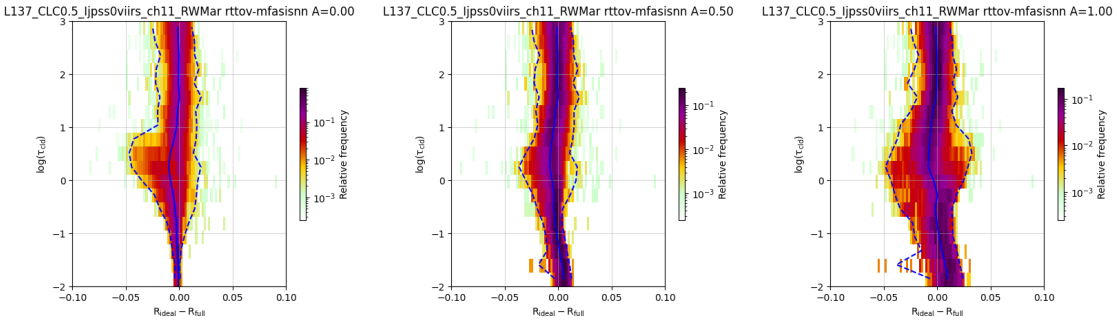

(a) (b) (c)

Figure 166: MFASIS $\Delta r_{\mathrm{MFASIS}-ref}$ as function of the cloud optical depth τ at albedo(s) of 0.0, 0.5, 1.0 (from left to right) for the instrument: JPSS 0 VIIRS CH11

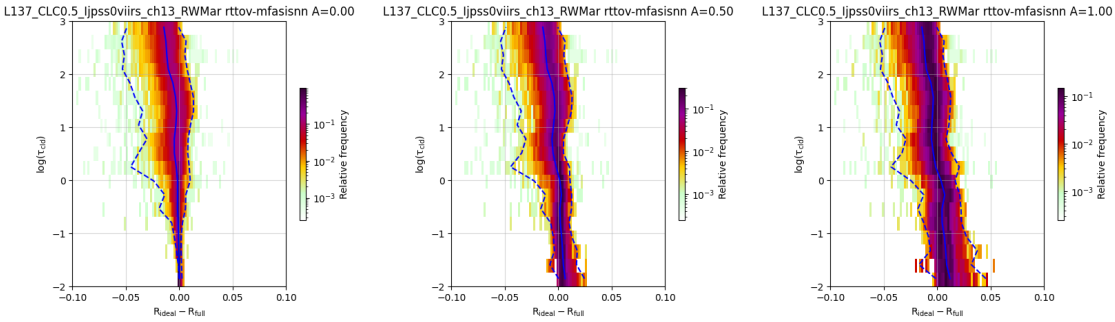

(a) (b) (c)

Figure 167: MFASIS $\Delta r_{\mathrm{MFASIS}-ref}$ as function of the cloud optical depth τ at albedo(s) of 0.0, 0.5, 1.0 (from left to right) for the instrument: JPSS 0 VIIRS CH13

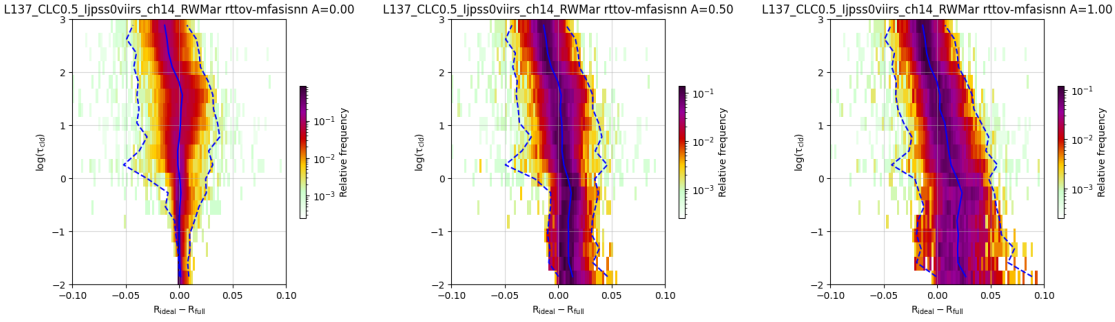

(a) (b) (c)

Figure 168: MFASIS $\Delta r_{\mathrm{MFASIS}-ref}$ as function of the cloud optical depth τ at albedo(s) of 0.0, 0.5, 1.0 (from left to right) for the instrument: JPSS 0 VIIRS CH14

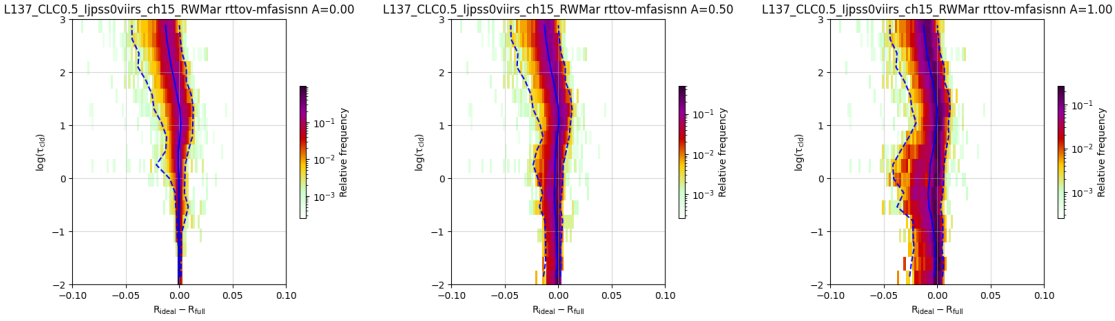

(a) (b) (c)

Figure 169: MFASIS $\Delta r_{\mathrm{MFASIS}-ref}$ as function of the cloud optical depth τ at albedo(s) of 0.0, 0.5, 1.0 (from left to right) for the instrument: JPSS 0 VIIRS CH15

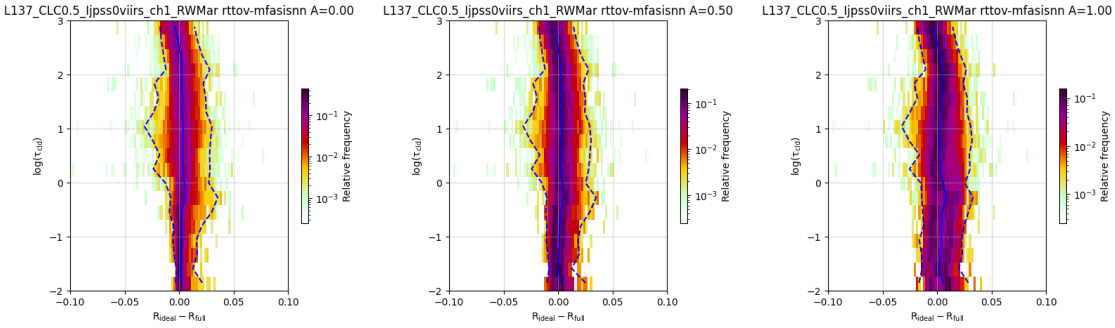

(a) (b) (c)

Figure 170: MFASIS $\Delta r_{\mathrm{MFASIS}-ref}$ as function of the cloud optical depth τ at albedo(s) of 0.0, 0.5, 1.0 (from left to right) for the instrument: JPSS 0 VIIRS CH1

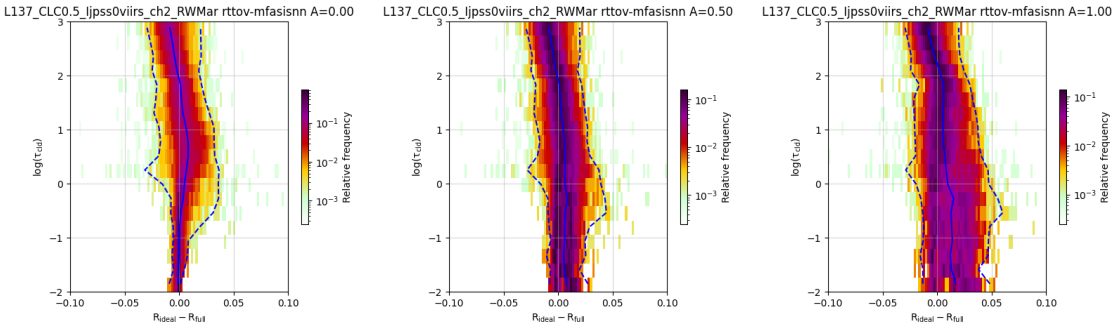

(a) (b) (c)

Figure 171: MFASIS $\Delta r_{\mathrm{MFASIS}-ref}$ as function of the cloud optical depth τ at albedo(s) of 0.0, 0.5, 1.0 (from left to right) for the instrument: JPSS 0 VIIRS CH2

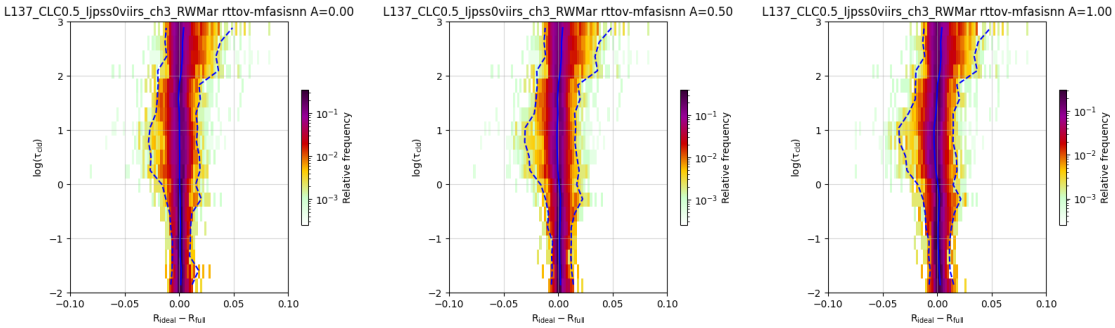

(a) (b) (c)

Figure 172: MFASIS $\Delta r_{\mathrm{MFASIS}-ref}$ as function of the cloud optical depth τ at albedo(s) of 0.0, 0.5, 1.0 (from left to right) for the instrument: JPSS 0 VIIRS CH3

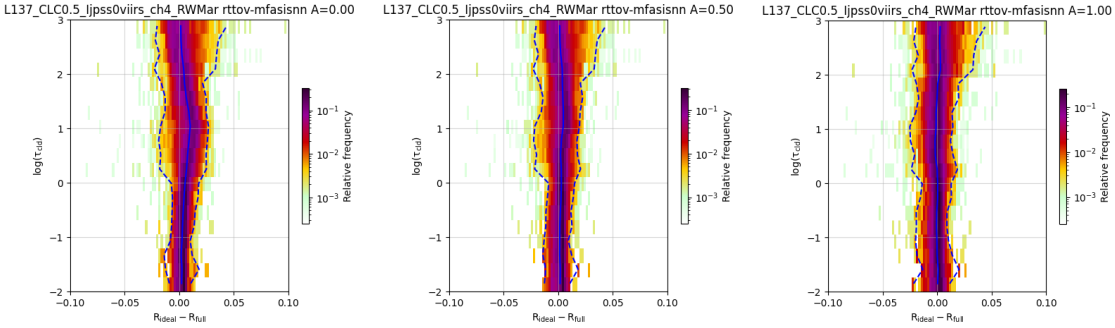

(a) (b) (c)

Figure 173: MFASIS $\Delta r_{\mathrm{MFASIS}-ref}$ as function of the cloud optical depth τ at albedo(s) of 0.0, 0.5, 1.0 (from left to right) for the instrument: JPSS 0 VIIRS CH4

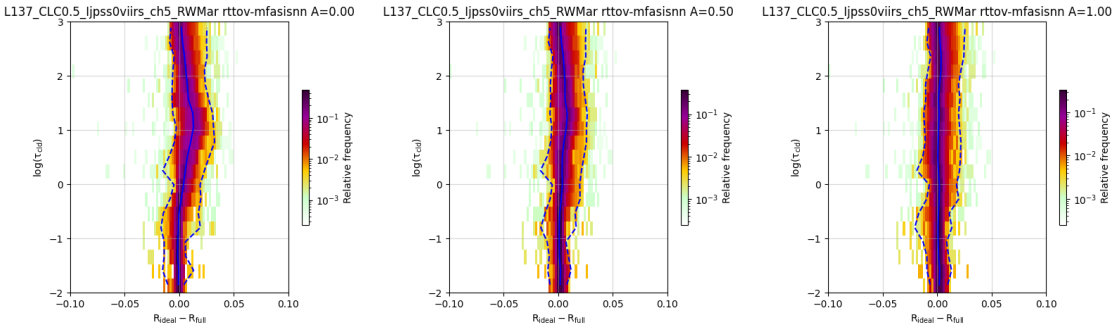

(a) (b) (c)

Figure 174: MFASIS $\Delta r_{\mathrm{MFASIS}-ref}$ as function of the cloud optical depth τ at albedo(s) of 0.0, 0.5, 1.0 (from left to right) for the instrument: JPSS 0 VIIRS CH5

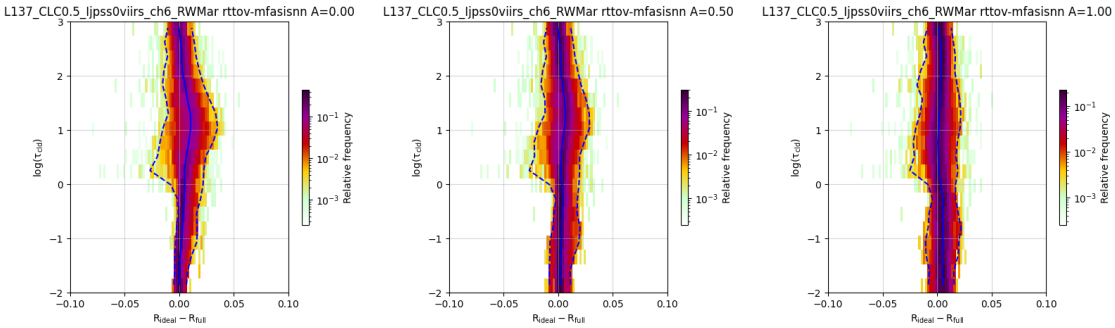

(a) (b) (c)

Figure 175: MFASIS $\Delta r_{\mathrm{MFASIS}-ref}$ as function of the cloud optical depth τ at albedo(s) of 0.0, 0.5, 1.0 (from left to right) for the instrument: JPSS 0 VIIRS CH6

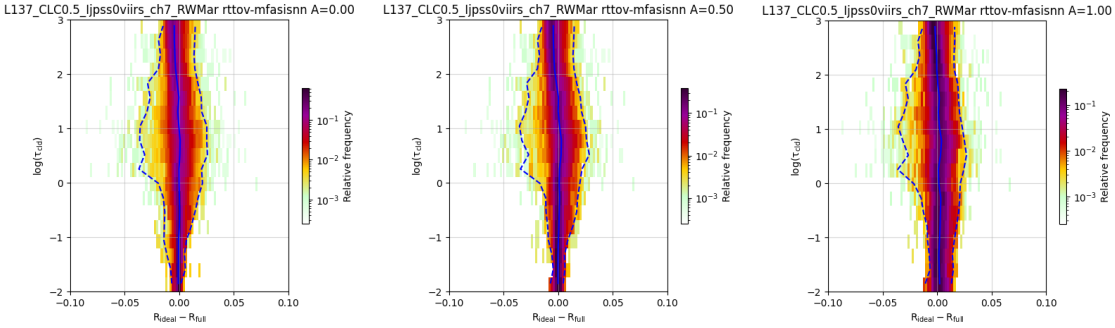

(a) (b) (c)

Figure 176: MFASIS $\Delta r_{\mathrm{MFASIS}-ref}$ as function of the cloud optical depth τ at albedo(s) of 0.0, 0.5, 1.0 (from left to right) for the instrument: JPSS 0 VIIRS CH7

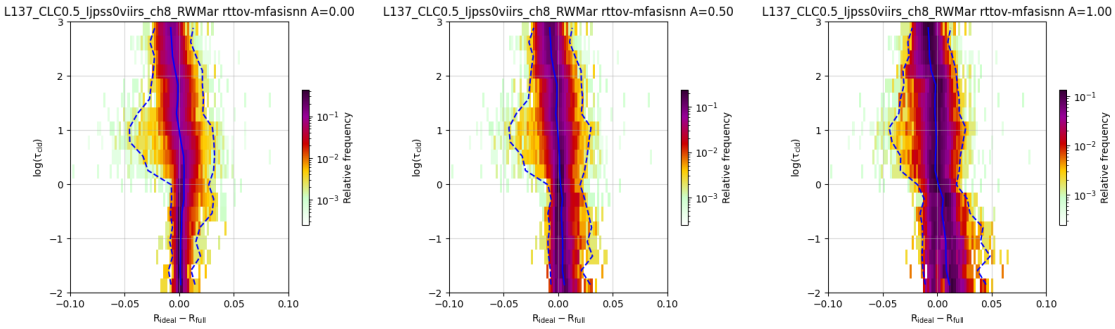

(a) (b) (c)

Figure 177: MFASIS $\Delta r_{\mathrm{MFASIS}-ref}$ as function of the cloud optical depth τ at albedo(s) of 0.0, 0.5, 1.0 (from left to right) for the instrument: JPSS 0 VIIRS CH8

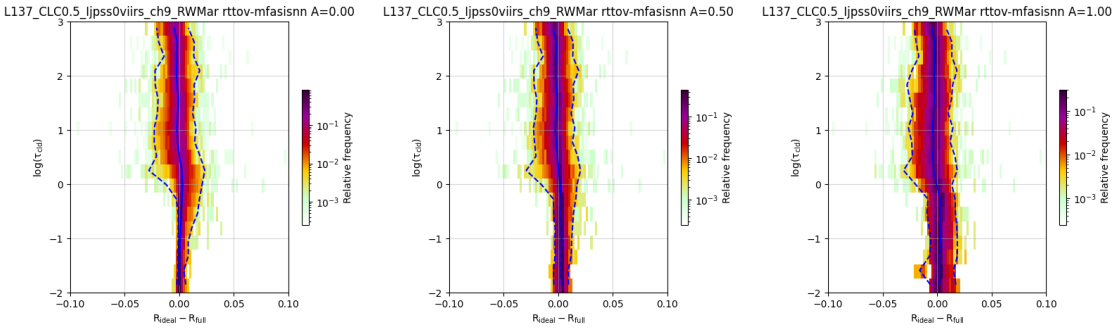

(a) (b) (c)

Figure 178: MFASIS $\Delta r_{\mathrm{MFASIS}-ref}$ as function of the cloud optical depth τ at albedo(s) of 0.0, 0.5, 1.0 (from left to right) for the instrument: JPSS 0 VIIRS CH9

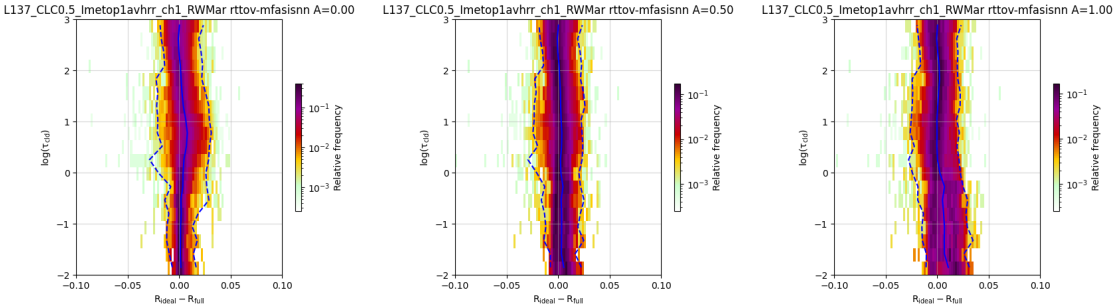

(a) (b) (c)

Figure 179: MFASIS $\Delta r_{\mathrm{MFASIS}-ref}$ as function of the cloud optical depth τ at albedo(s) of 0.0, 0.5, 1.0 (from left to right) for the instrument: METOP 1 AVHRR CH1

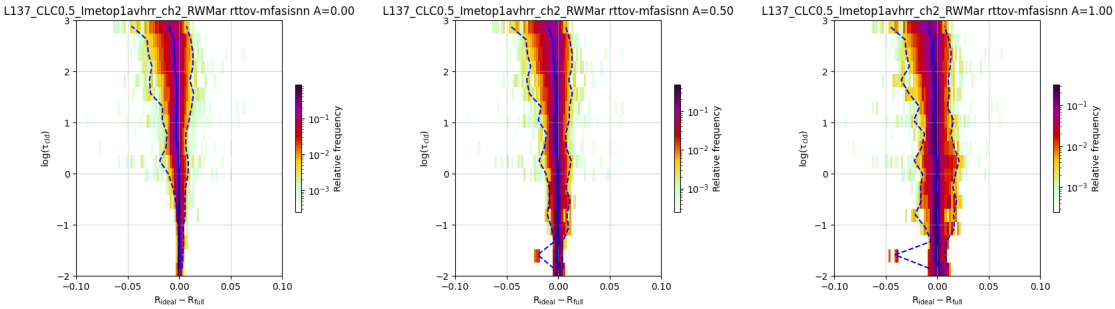

(a) (b) (c)

Figure 180: MFASIS $\Delta r_{\mathrm{MFASIS}-ref}$ as function of the cloud optical depth τ at albedo(s) of 0.0, 0.5, 1.0 (from left to right) for the instrument: METOP 1 AVHRR CH2

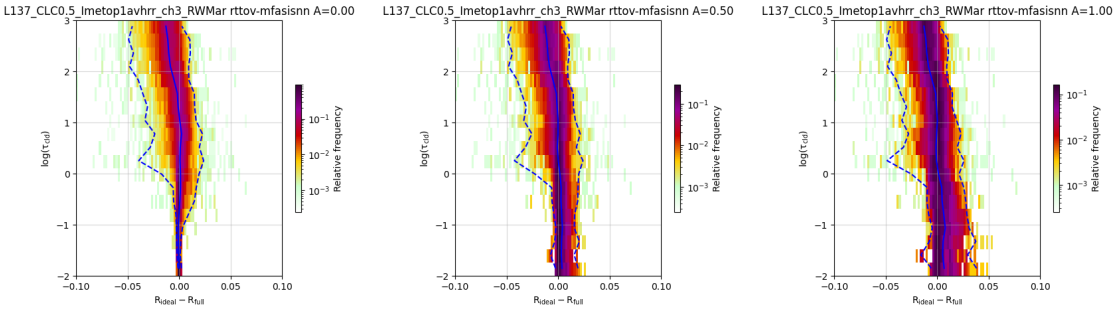

(a) (b) (c)

Figure 181: MFASIS $\Delta r_{\mathrm{MFASIS}-ref}$ as function of the cloud optical depth τ at albedo(s) of 0.0, 0.5, 1.0 (from left to right) for the instrument: METOP 1 AVHRR CH3

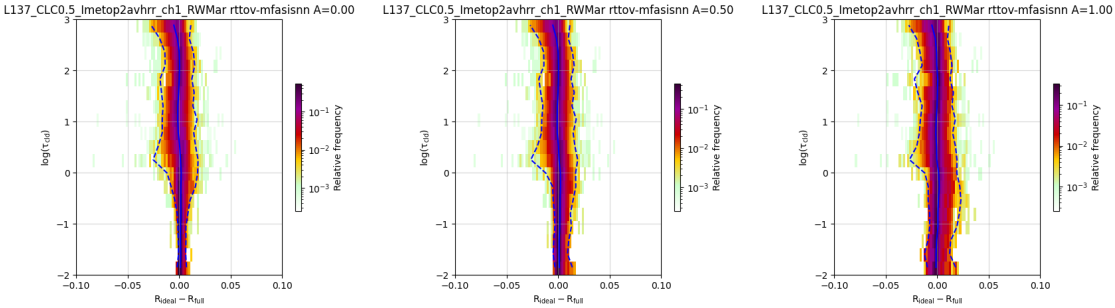

(a) (b) (c)

Figure 182: MFASIS $\Delta r_{\mathrm{MFASIS}-ref}$ as function of the cloud optical depth τ at albedo(s) of 0.0, 0.5, 1.0 (from left to right) for the instrument: METOP 2 AVHRR CH1

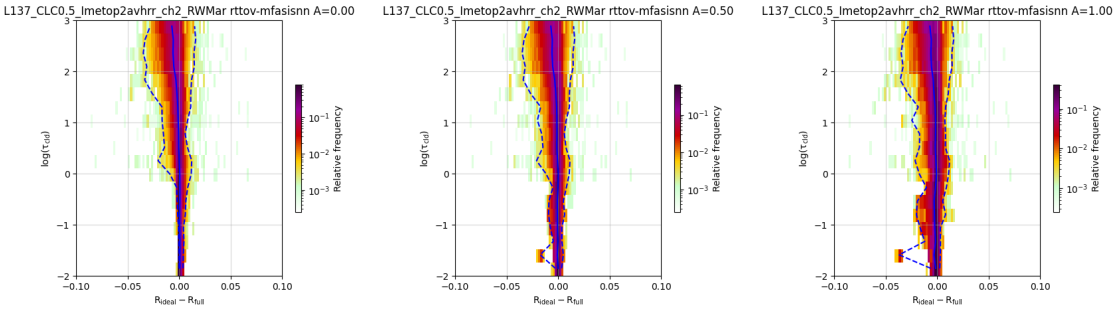

(a) (b) (c)

Figure 183: MFASIS $\Delta r_{\mathrm{MFASIS}-ref}$ as function of the cloud optical depth τ at albedo(s) of 0.0, 0.5, 1.0 (from left to right) for the instrument: METOP 2 AVHRR CH2

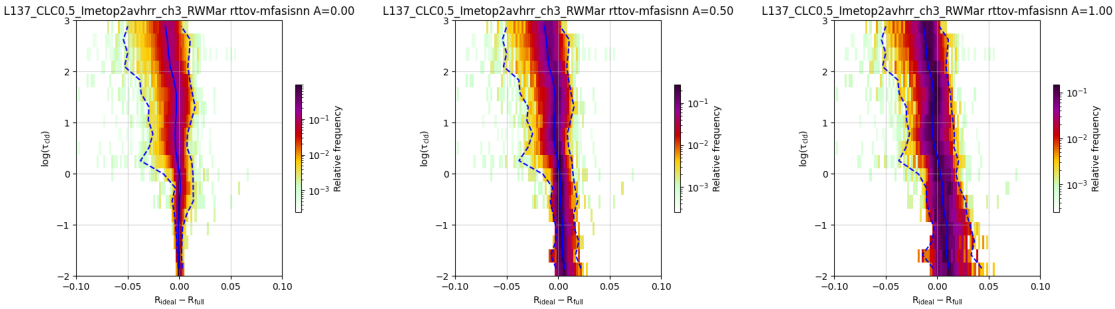

(a) (b) (c)

Figure 184: MFASIS $\Delta r_{\mathrm{MFASIS}-ref}$ as function of the cloud optical depth τ at albedo(s) of 0.0, 0.5, 1.0 (from left to right) for the instrument: METOP 2 AVHRR CH3

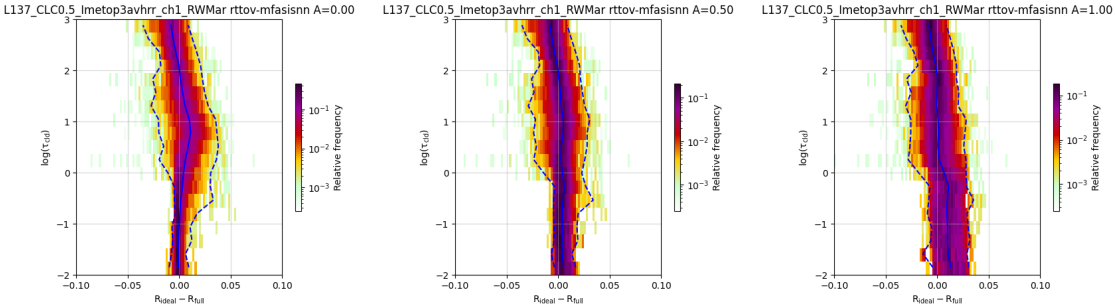

(a) (b) (c)

Figure 185: MFASIS $\Delta r_{\mathrm{MFASIS}-ref}$ as function of the cloud optical depth τ at albedo(s) of 0.0, 0.5, 1.0 (from left to right) for the instrument: METOP 3 AVHRR CH1

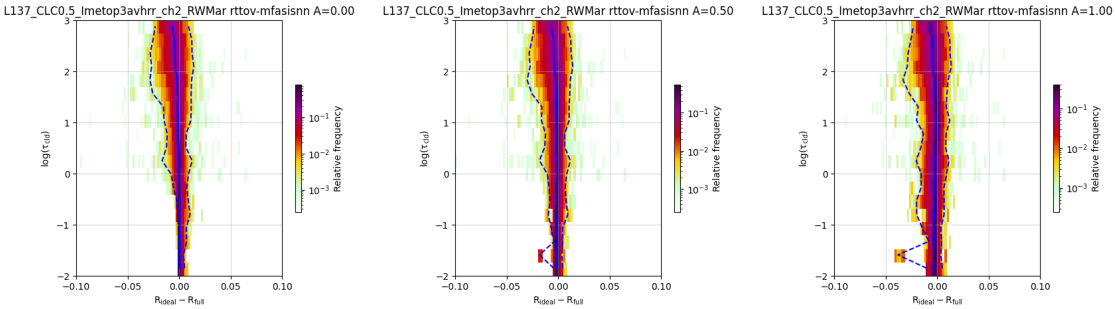

(a) (b) (c)

Figure 186: MFASIS $\Delta r_{\mathrm{MFASIS}-ref}$ as function of the cloud optical depth τ at albedo(s) of 0.0, 0.5, 1.0 (from left to right) for the instrument: METOP 3 AVHRR CH2

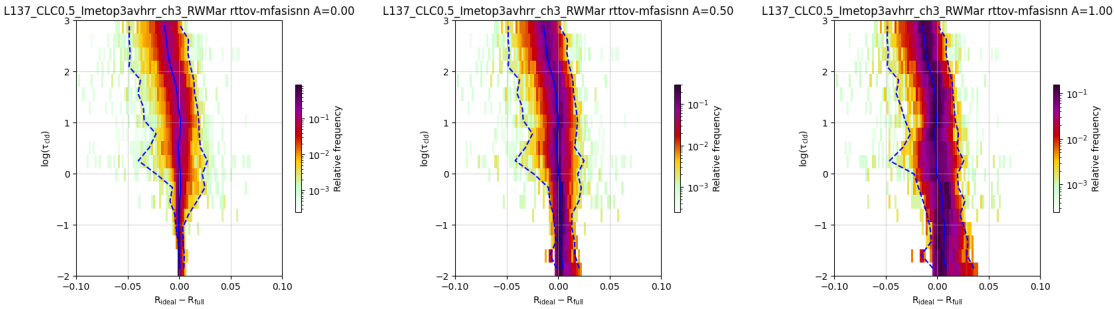

(a) (b) (c)

Figure 187: MFASIS $\Delta r_{\mathrm{MFASIS}-ref}$ as function of the cloud optical depth τ at albedo(s) of 0.0, 0.5, 1.0 (from left to right) for the instrument: METOP 3 AVHRR CH3

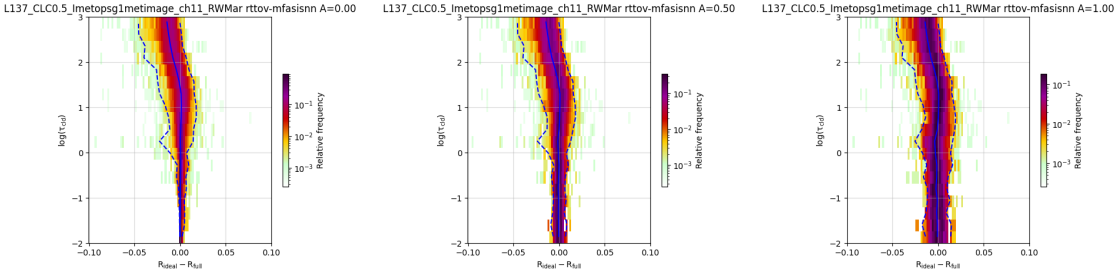

(a) (b) (c)

Figure 188: MFASIS $\Delta r_{\mathrm{MFASIS}-ref}$ as function of the cloud optical depth τ at albedo(s) of 0.0, 0.5, 1.0 (from left to right) for the instrument: METOPSG 1 METIMAGE CH11

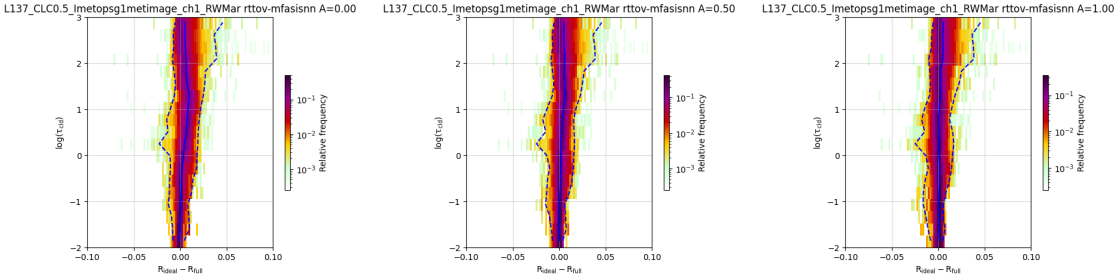

(a) (b) (c)

Figure 189: MFASIS $\Delta r_{\mathrm{MFASIS}-ref}$ as function of the cloud optical depth τ at albedo(s) of 0.0, 0.5, 1.0 (from left to right) for the instrument: METOPSG 1 METIMAGE CH1

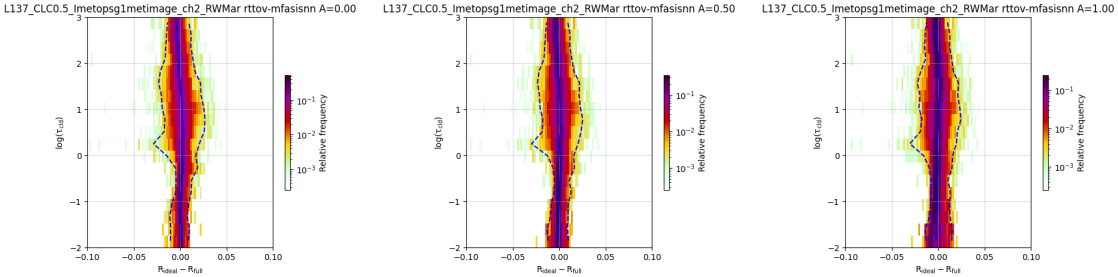

(a) (b) (c)

Figure 190: MFASIS $\Delta r_{\mathrm{MFASIS}-ref}$ as function of the cloud optical depth τ at albedo(s) of 0.0, 0.5, 1.0 (from left to right) for the instrument: METOPSG 1 METIMAGE CH2

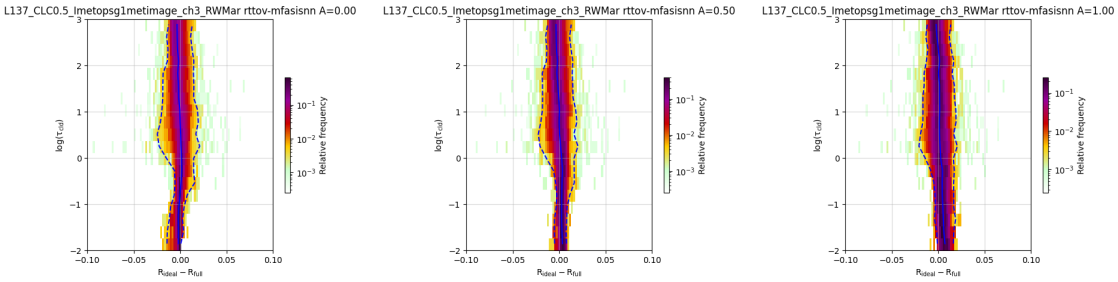

(a) (b) (c)

Figure 191: MFASIS $\Delta r_{\mathrm{MFASIS}-ref}$ as function of the cloud optical depth τ at albedo(s) of 0.0, 0.5, 1.0 (from left to right) for the instrument: METOPSG 1 METIMAGE CH3

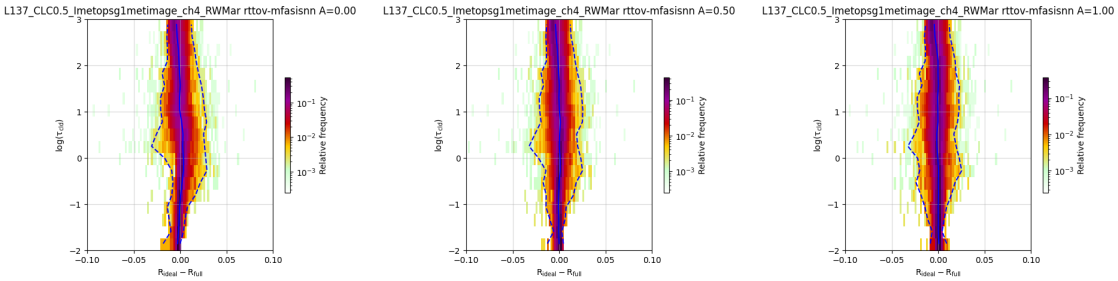

(a) (b) (c)

Figure 192: MFASIS $\Delta r_{\mathrm{MFASIS}-ref}$ as function of the cloud optical depth τ at albedo(s) of 0.0, 0.5, 1.0 (from left to right) for the instrument: METOPSG 1 METIMAGE CH4

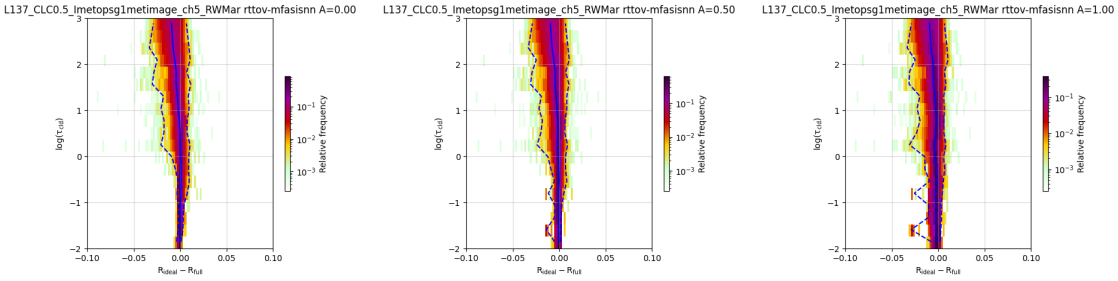

(a) (b) (c)

Figure 193: MFASIS $\Delta r_{\mathrm{MFASIS}-ref}$ as function of the cloud optical depth τ at albedo(s) of 0.0, 0.5, 1.0 (from left to right) for the instrument: METOPSG 1 METIMAGE CH5

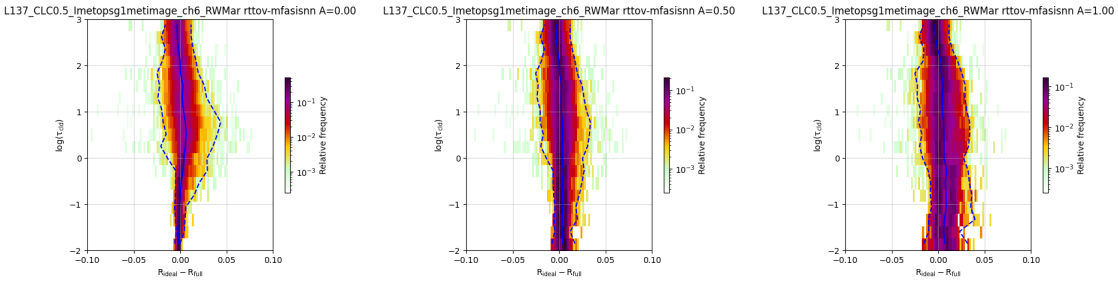

(a) (b) (c)

Figure 194: MFASIS $\Delta r_{\mathrm{MFASIS}-ref}$ as function of the cloud optical depth τ at albedo(s) of 0.0, 0.5, 1.0 (from left to right) for the instrument: METOPSG 1 METIMAGE CH6

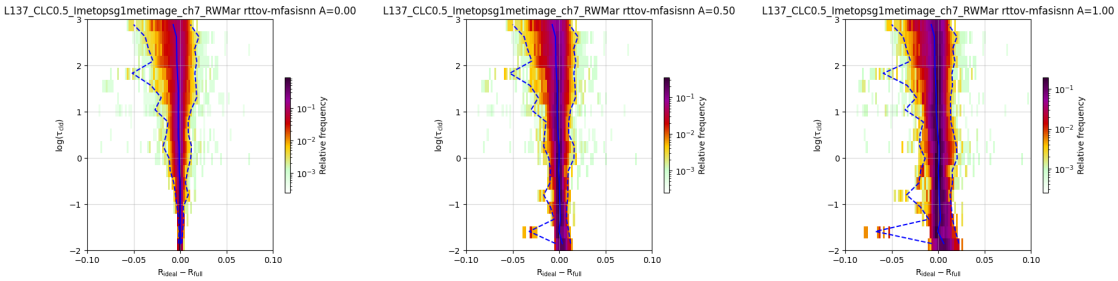

(a) (b) (c)

Figure 195: MFASIS $\Delta r_{\mathrm{MFASIS}-ref}$ as function of the cloud optical depth τ at albedo(s) of 0.0, 0.5, 1.0 (from left to right) for the instrument: METOPSG 1 METIMAGE CH7

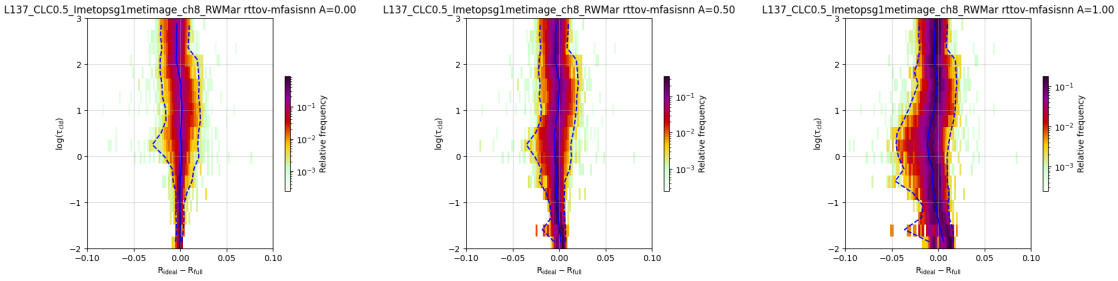

(a) (b) (c)

Figure 196: MFASIS $\Delta r_{\mathrm{MFASIS}-ref}$ as function of the cloud optical depth τ at albedo(s) of 0.0, 0.5, 1.0 (from left to right) for the instrument: METOPSG 1 METIMAGE CH8

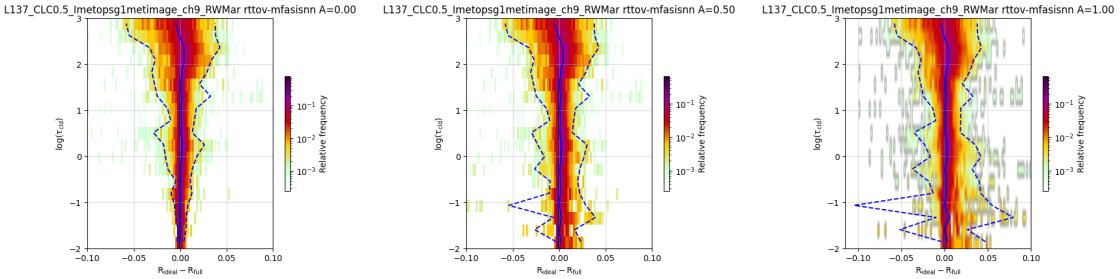

(a) (b) (c)

Figure 197: MFASIS $\Delta r_{\mathrm{MFASIS}-ref}$ as function of the cloud optical depth τ at albedo(s) of 0.0, 0.5, 1.0 (from left to right) for the instrument: METOPSG 1 METIMAGE CH9

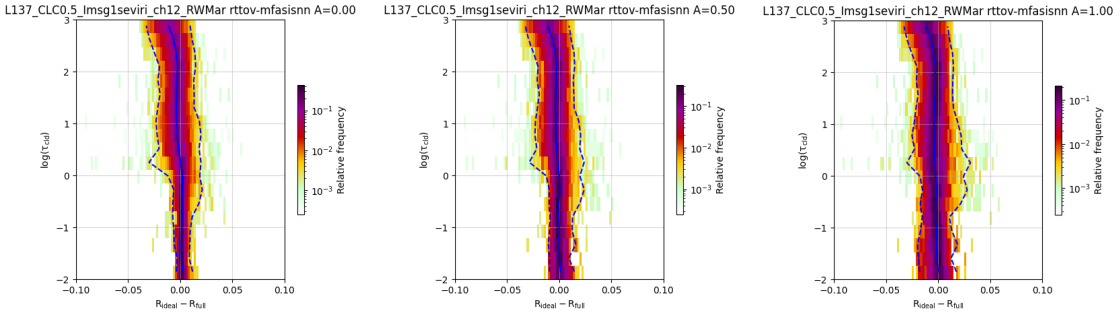

(a) (b) (c)

Figure 198: MFASIS $\Delta r_{\mathrm{MFASIS}-ref}$ as function of the cloud optical depth τ at albedo(s) of 0.0, 0.5, 1.0 (from left to right) for the instrument: MSG 1 SEVIRI CH12

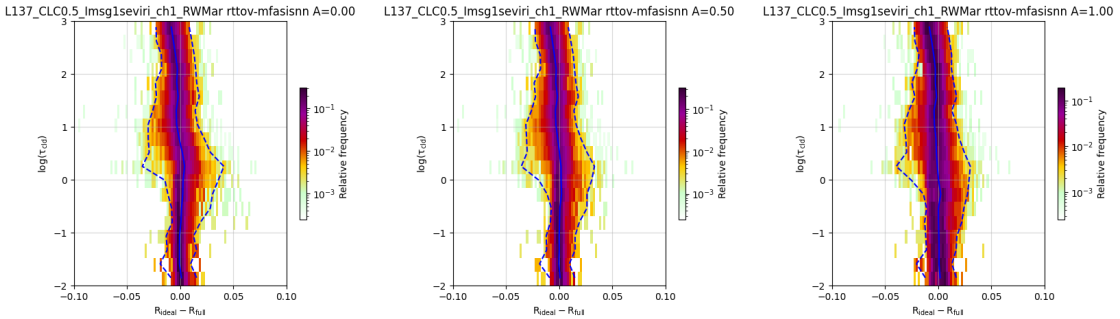

(a) (b) (c)

Figure 199: MFASIS $\Delta r_{\mathrm{MFASIS}-ref}$ as function of the cloud optical depth τ at albedo(s) of 0.0, 0.5, 1.0 (from left to right) for the instrument: MSG 1 SEVIRI CH1

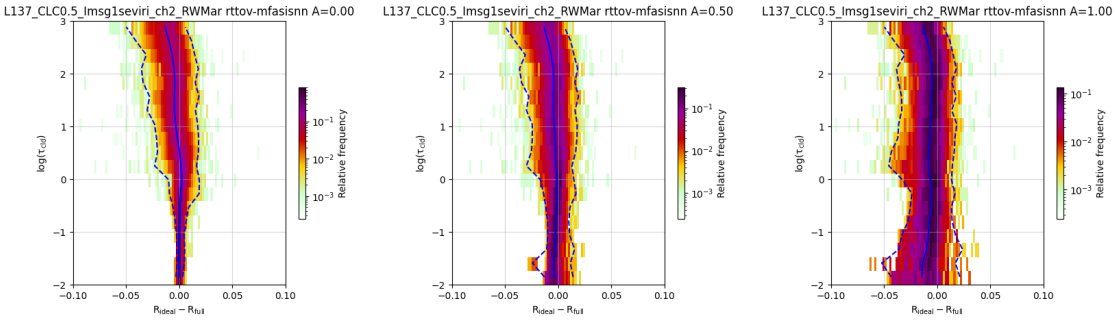

(a) (b) (c)

Figure 200: MFASIS $\Delta r_{\mathrm{MFASIS}-ref}$ as function of the cloud optical depth τ at albedo(s) of 0.0, 0.5, 1.0 (from left to right) for the instrument: MSG 1 SEVIRI CH2

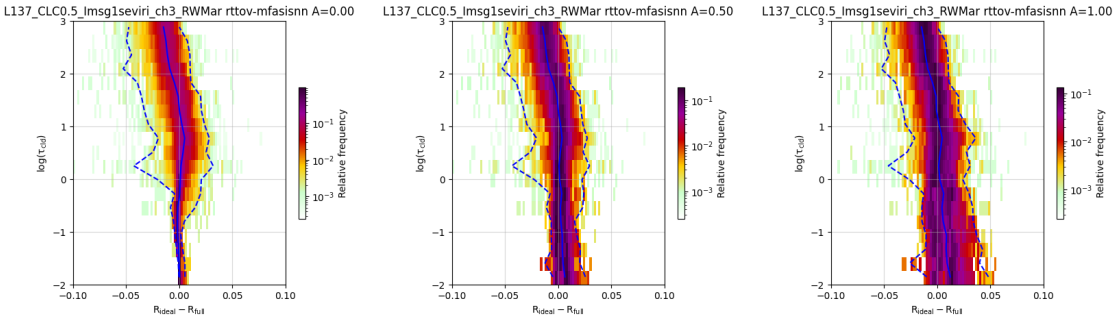

(a) (b) (c)

Figure 201: MFASIS $\Delta r_{\mathrm{MFASIS}-ref}$ as function of the cloud optical depth τ at albedo(s) of 0.0, 0.5, 1.0 (from left to right) for the instrument: MSG 1 SEVIRI CH3

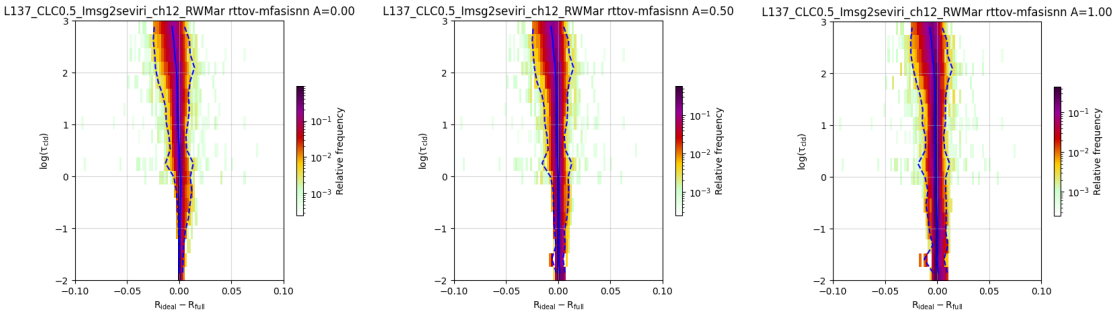

(a) (b) (c)

Figure 202: MFASIS $\Delta r_{\mathrm{MFASIS}-ref}$ as function of the cloud optical depth τ at albedo(s) of 0.0, 0.5, 1.0 (from left to right) for the instrument: MSG 2 SEVIRI CH12

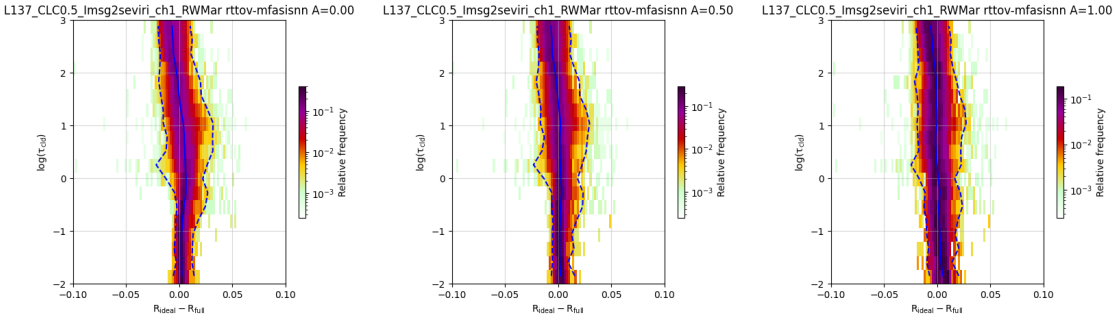

(a) (b) (c)

Figure 203: MFASIS $\Delta r_{\mathrm{MFASIS}-ref}$ as function of the cloud optical depth τ at albedo(s) of 0.0, 0.5, 1.0 (from left to right) for the instrument: MSG 2 SEVIRI CH1

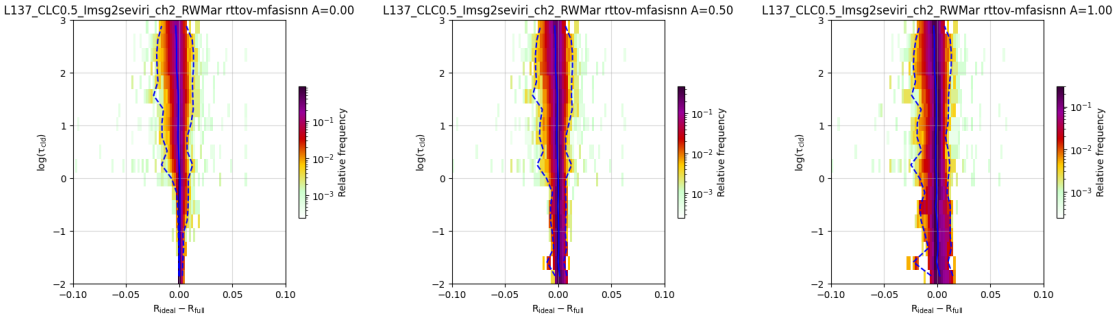

(a) (b) (c)

Figure 204: MFASIS $\Delta r_{\mathrm{MFASIS}-ref}$ as function of the cloud optical depth τ at albedo(s) of 0.0, 0.5, 1.0 (from left to right) for the instrument: MSG 2 SEVIRI CH2

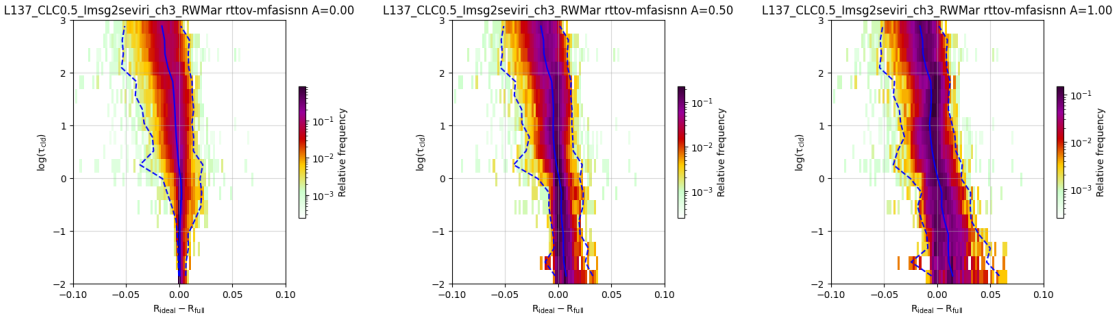

(a) (b) (c)

Figure 205: MFASIS $\Delta r_{\mathrm{MFASIS}-ref}$ as function of the cloud optical depth τ at albedo(s) of 0.0, 0.5, 1.0 (from left to right) for the instrument: MSG 2 SEVIRI CH3

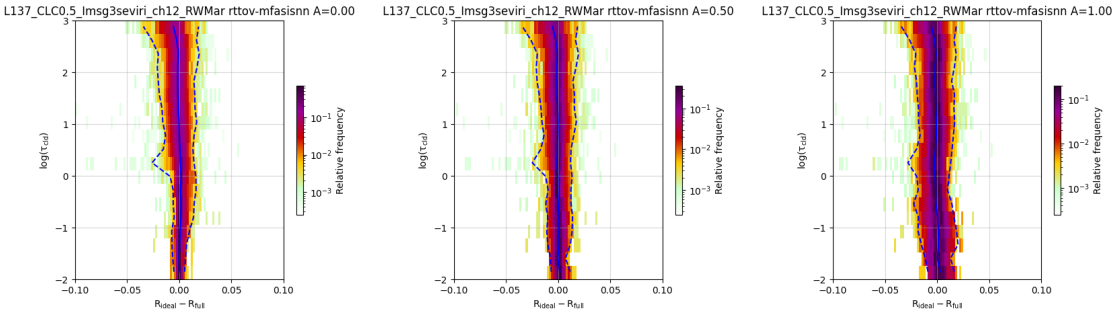

(a) (b) (c)

Figure 206: MFASIS $\Delta r_{\mathrm{MFASIS}-ref}$ as function of the cloud optical depth τ at albedo(s) of 0.0, 0.5, 1.0 (from left to right) for the instrument: MSG 3 SEVIRI CH12

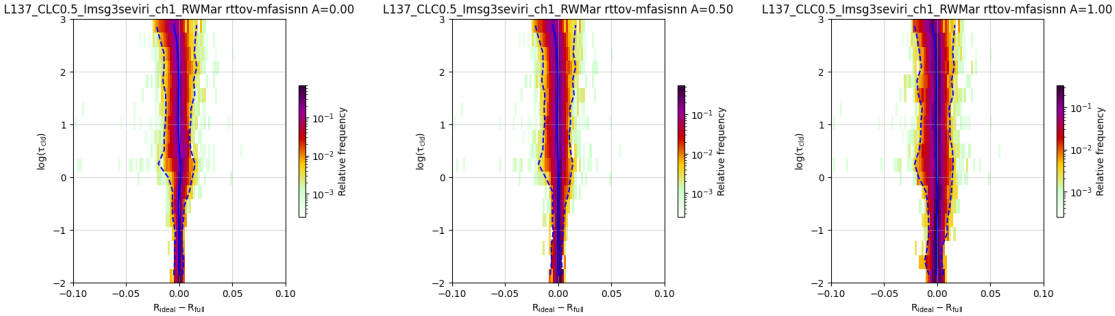

(a) (b) (c)

Figure 207: MFASIS $\Delta r_{\mathrm{MFASIS}-ref}$ as function of the cloud optical depth τ at albedo(s) of 0.0, 0.5, 1.0 (from left to right) for the instrument: MSG 3 SEVIRI CH1

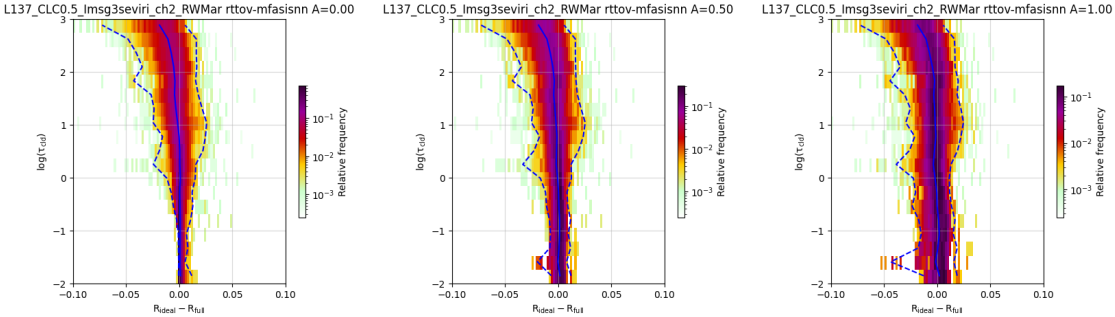

(a) (b) (c)

Figure 208: MFASIS $\Delta r_{\mathrm{MFASIS}-ref}$ as function of the cloud optical depth τ at albedo(s) of 0.0, 0.5, 1.0 (from left to right) for the instrument: MSG 3 SEVIRI CH2

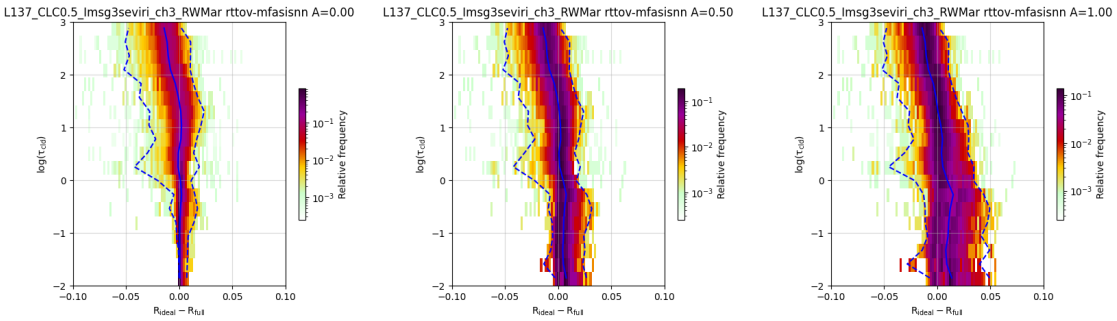

(a) (b) (c)

Figure 209: MFASIS $\Delta r_{\mathrm{MFASIS}-ref}$ as function of the cloud optical depth τ at albedo(s) of 0.0, 0.5, 1.0 (from left to right) for the instrument: MSG 3 SEVIRI CH3

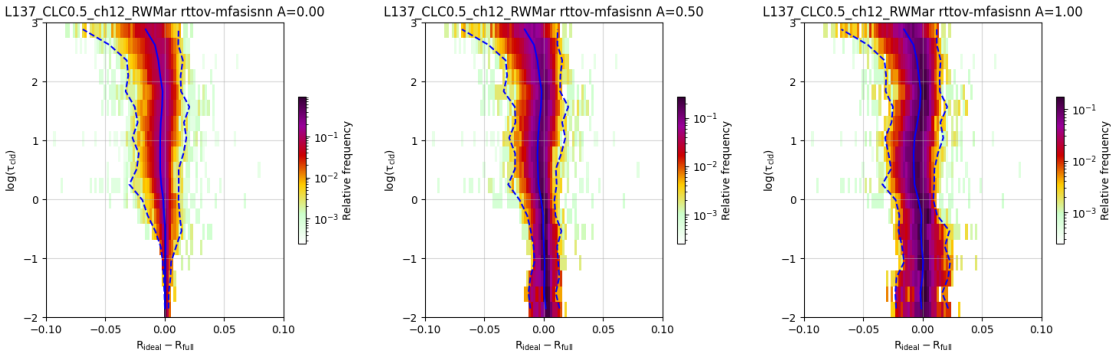

(a) (b) (c)

Figure 210: MFASIS $\Delta r_{\mathrm{MFASIS}-ref}$ as function of the cloud optical depth τ at albedo(s) of 0.0, 0.5, 1.0 (from left to right) for the instrument: MSG 4 SEVIRI CH12

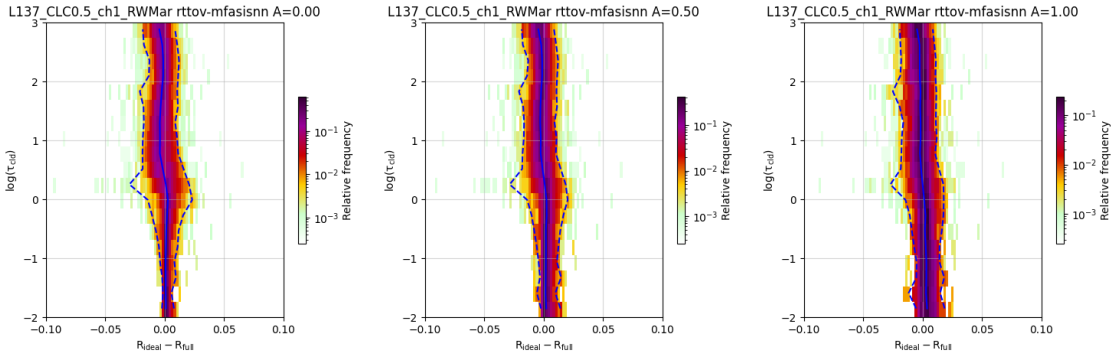

(a) (b) (c)

Figure 211: MFASIS $\Delta r_{\mathrm{MFASIS}-ref}$ as function of the cloud optical depth τ at albedo(s) of 0.0, 0.5, 1.0 (from left to right) for the instrument: MSG 4 SEVIRI CH1

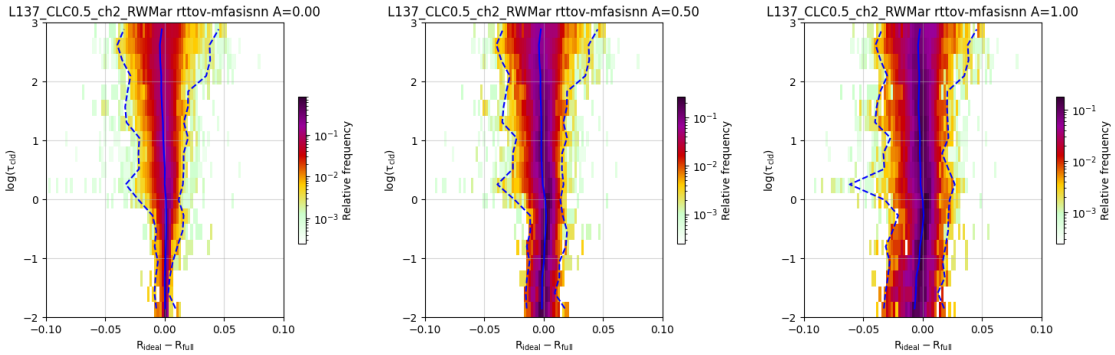

(a) (b) (c)

Figure 212: MFASIS $\Delta r_{\mathrm{MFASIS}-ref}$ as function of the cloud optical depth τ at albedo(s) of 0.0, 0.5, 1.0 (from left to right) for the instrument: MSG 4 SEVIRI CH2

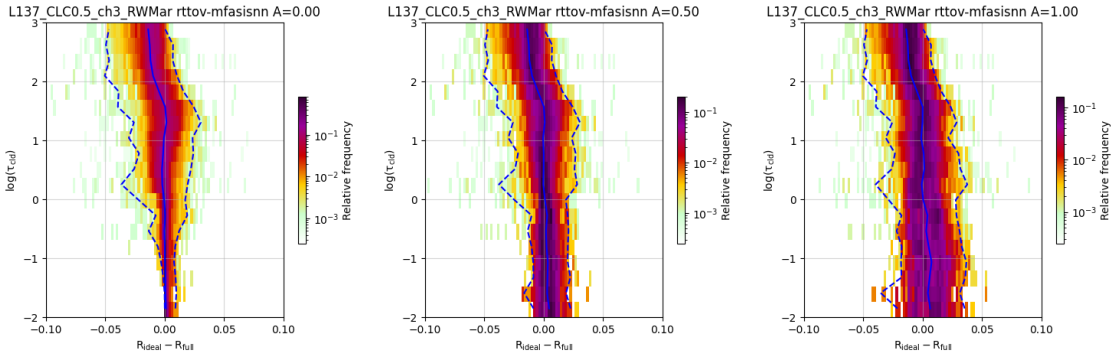

(a) (b) (c)

Figure 213: MFASIS $\Delta r_{\mathrm{MFASIS}-ref}$ as function of the cloud optical depth τ at albedo(s) of 0.0, 0.5, 1.0 (from left to right) for the instrument: MSG 4 SEVIRI CH3

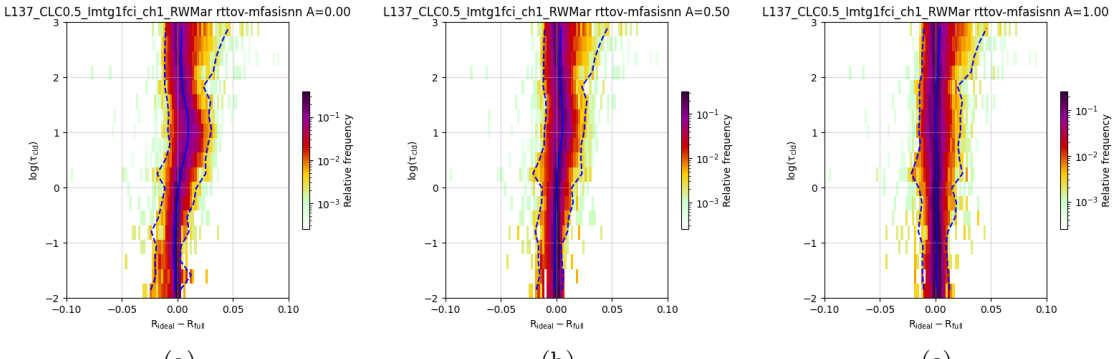

(a) (b) (c)

Figure 214: MFASIS $\Delta r_{\mathrm{MFASIS}-ref}$ as function of the cloud optical depth τ at albedo(s) of 0.0, 0.5, 1.0 (from left to right) for the instrument: MTG 1 FCI CH1

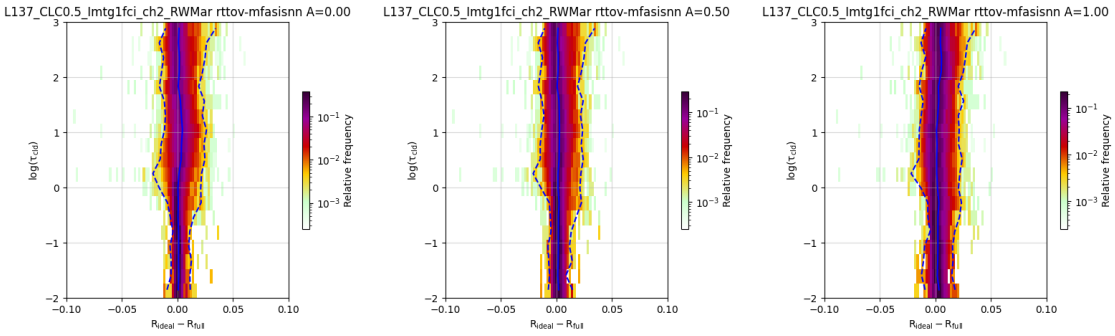

(a) (b) (c)

Figure 215: MFASIS $\Delta r_{\mathrm{MFASIS}-ref}$ as function of the cloud optical depth τ at albedo(s) of 0.0, 0.5, 1.0 (from left to right) for the instrument: MTG 1 FCI CH2

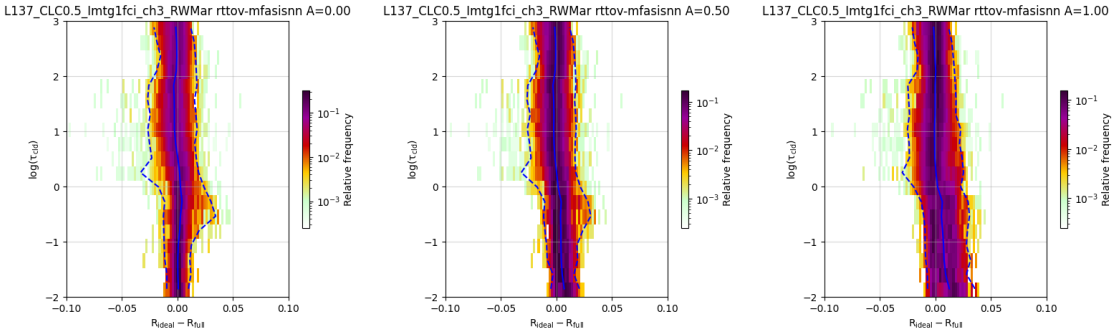

(a) (b) (c)

Figure 216: MFASIS $\Delta r_{\mathrm{MFASIS}-ref}$ as function of the cloud optical depth τ at albedo(s) of 0.0, 0.5, 1.0 (from left to right) for the instrument: MTG 1 FCI CH3

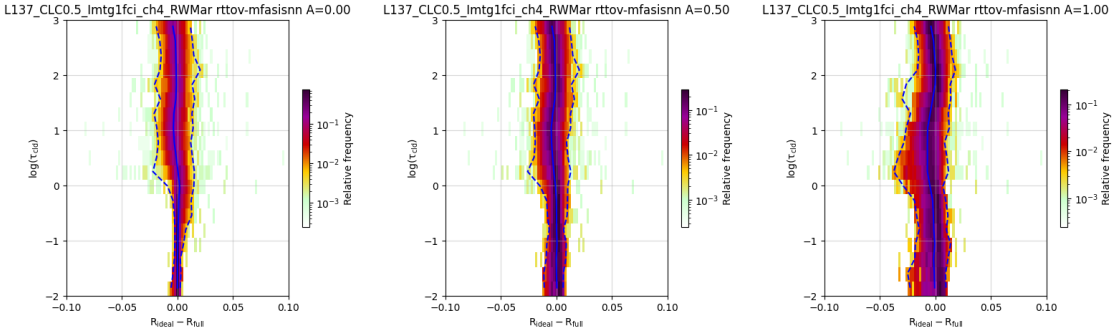

(a) (b) (c)

Figure 217: MFASIS $\Delta r_{\mathrm{MFASIS}-ref}$ as function of the cloud optical depth τ at albedo(s) of 0.0, 0.5, 1.0 (from left to right) for the instrument: MTG 1 FCI CH4

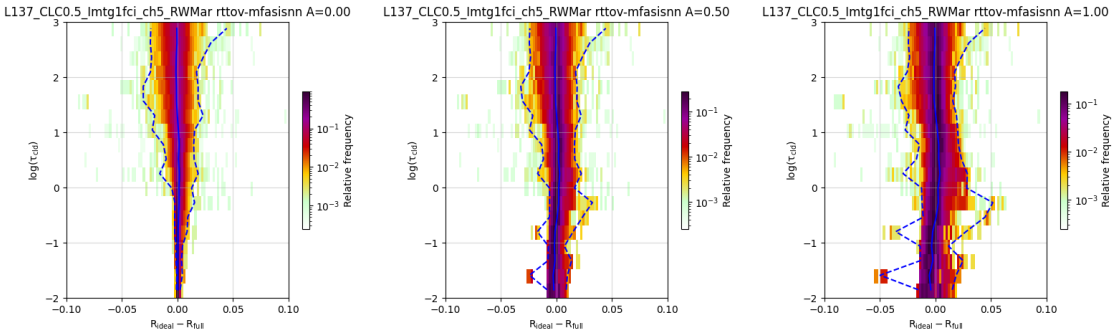

(a) (b) (c)

Figure 218: MFASIS $\Delta r_{\mathrm{MFASIS}-ref}$ as function of the cloud optical depth τ at albedo(s) of 0.0, 0.5, 1.0 (from left to right) for the instrument: MTG 1 FCI CH5

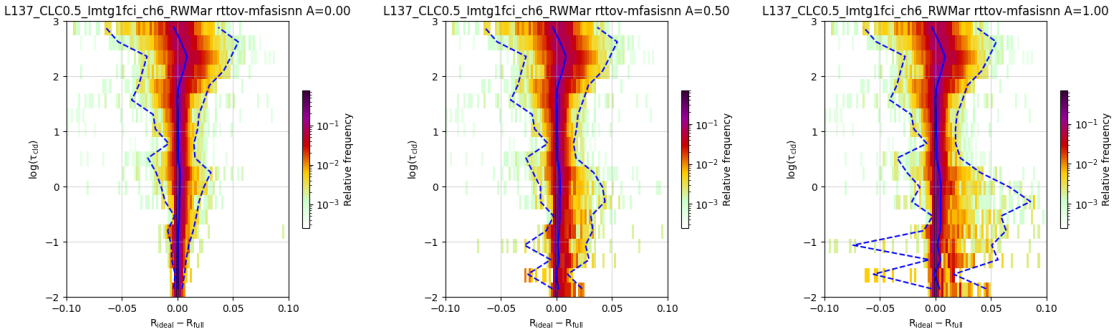

(a) (b) (c)

Figure 219: MFASIS $\Delta r_{\mathrm{MFASIS}-ref}$ as function of the cloud optical depth τ at albedo(s) of 0.0, 0.5, 1.0 (from left to right) for the instrument: MTG 1 FCI CH6

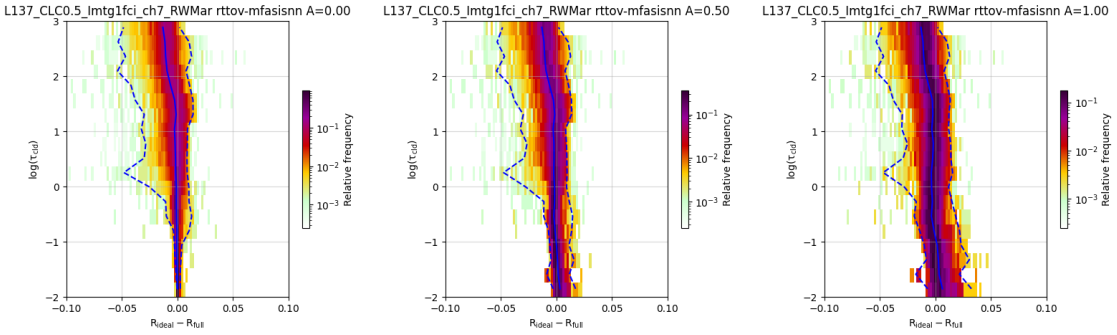

(a) (b) (c)

Figure 220: MFASIS $\Delta r_{\mathrm{MFASIS}-ref}$ as function of the cloud optical depth τ at albedo(s) of 0.0, 0.5, 1.0 (from left to right) for the instrument: MTG 1 FCI CH7

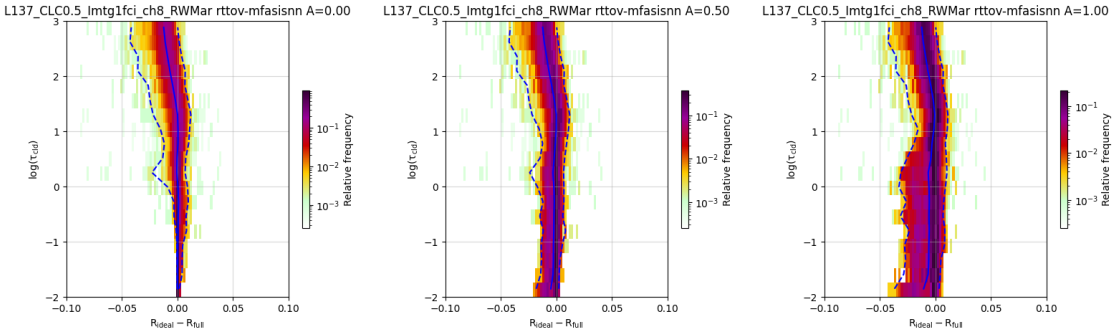

(a) (b) (c)

Figure 221: MFASIS $\Delta r_{\mathrm{MFASIS}-ref}$ as function of the cloud optical depth τ at albedo(s) of 0.0, 0.5, 1.0 (from left to right) for the instrument: MTG 1 FCI CH8

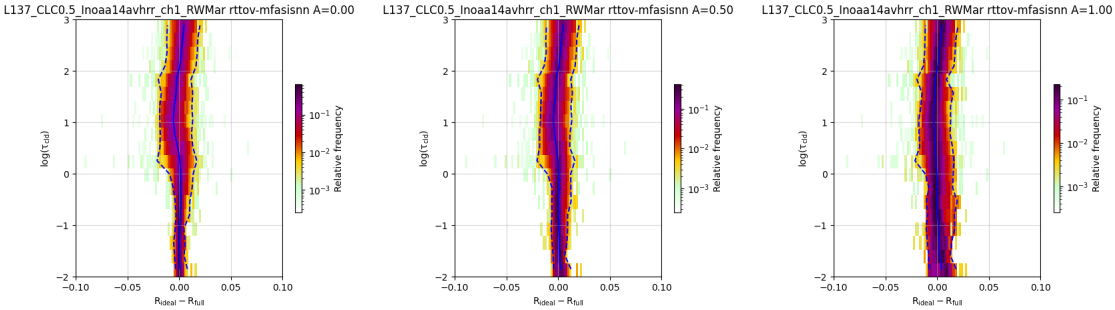

(a) (b) (c)

Figure 222: MFASIS $\Delta r_{\mathrm{MFASIS}-ref}$ as function of the cloud optical depth τ at albedo(s) of 0.0, 0.5, 1.0 (from left to right) for the instrument: NOAA 14 AVHRR CH1

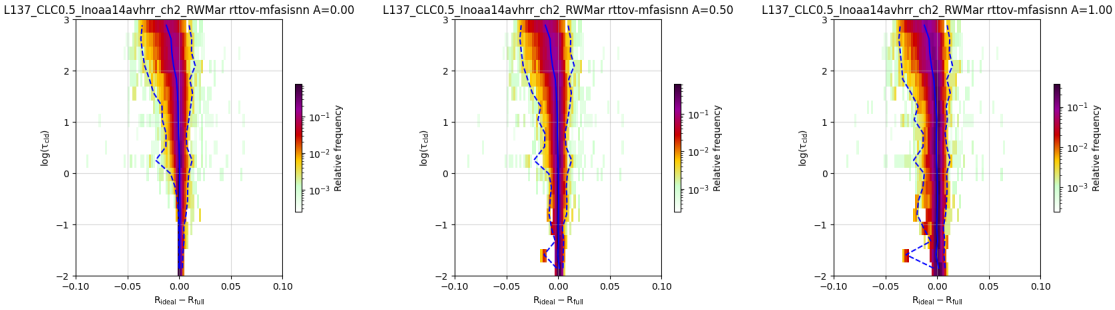

(a) (b) (c)

Figure 223: MFASIS $\Delta r_{\mathrm{MFASIS}-ref}$ as function of the cloud optical depth τ at albedo(s) of 0.0, 0.5, 1.0 (from left to right) for the instrument: NOAA 14 AVHRR CH2

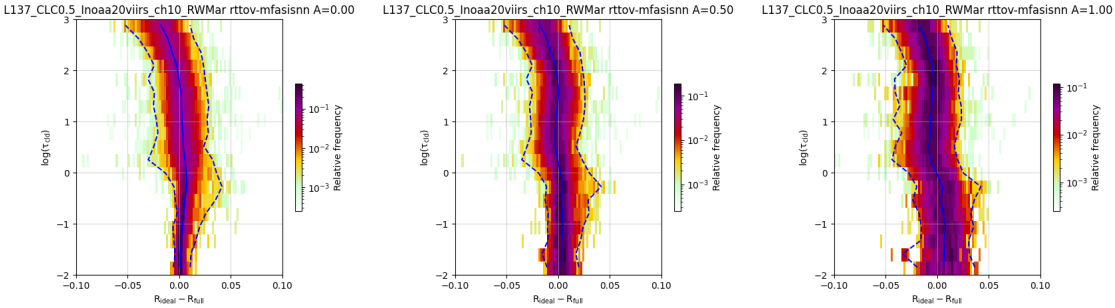

(a) (b) (c)

Figure 224: MFASIS $\Delta r_{\mathrm{MFASIS}-ref}$ as function of the cloud optical depth τ at albedo(s) of 0.0, 0.5, 1.0 (from left to right) for the instrument: NOAA 20 VIIRS CH10

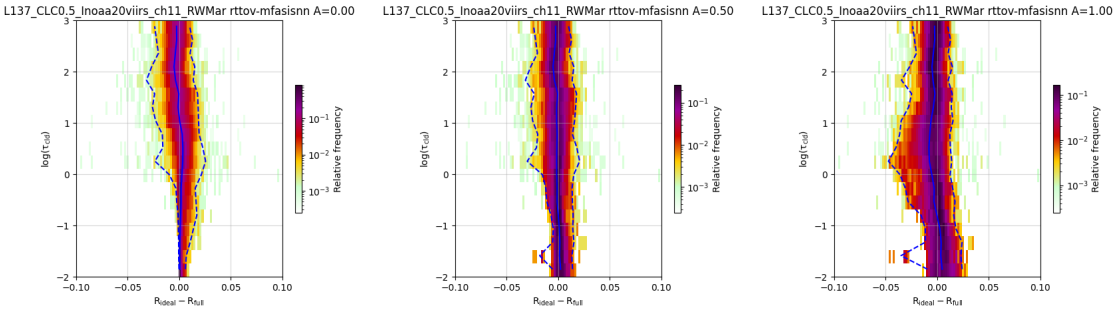

(a) (b) (c)

Figure 225: MFASIS $\Delta r_{\mathrm{MFASIS}-ref}$ as function of the cloud optical depth τ at albedo(s) of 0.0, 0.5, 1.0 (from left to right) for the instrument: NOAA 20 VIIRS CH11

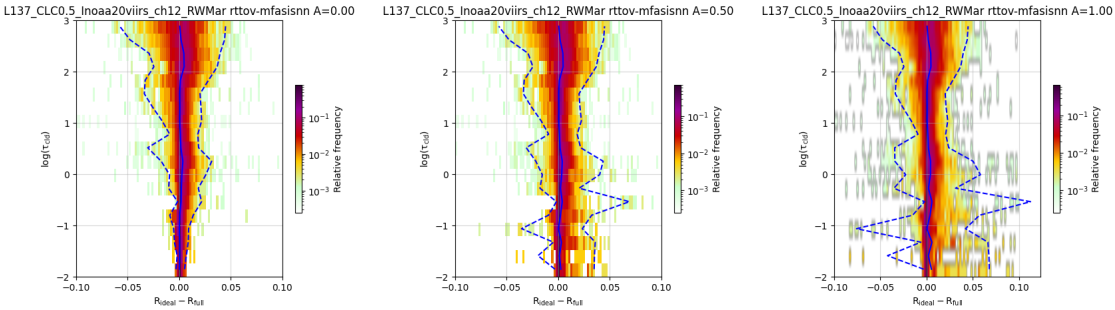

(a) (b) (c)

Figure 226: MFASIS $\Delta r_{\mathrm{MFASIS}-ref}$ as function of the cloud optical depth τ at albedo(s) of 0.0, 0.5, 1.0 (from left to right) for the instrument: NOAA 20 VIIRS CH12

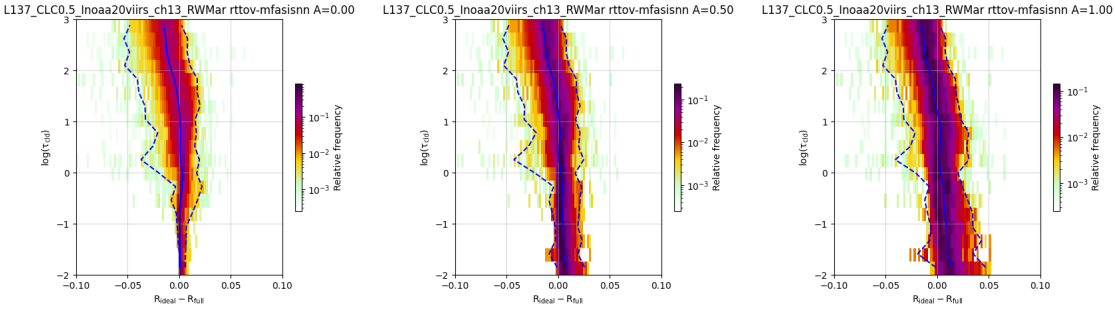

(a) (b) (c)

Figure 227: MFASIS $\Delta r_{\mathrm{MFASIS}-ref}$ as function of the cloud optical depth τ at albedo(s) of 0.0, 0.5, 1.0 (from left to right) for the instrument: NOAA 20 VIIRS CH13

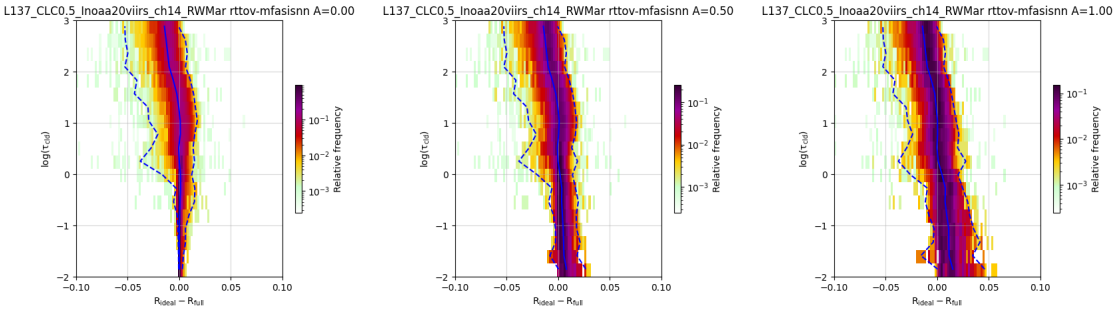

(a) (b) (c)

Figure 228: MFASIS $\Delta r_{\mathrm{MFASIS}-ref}$ as function of the cloud optical depth τ at albedo(s) of 0.0, 0.5, 1.0 (from left to right) for the instrument: NOAA 20 VIIRS CH14

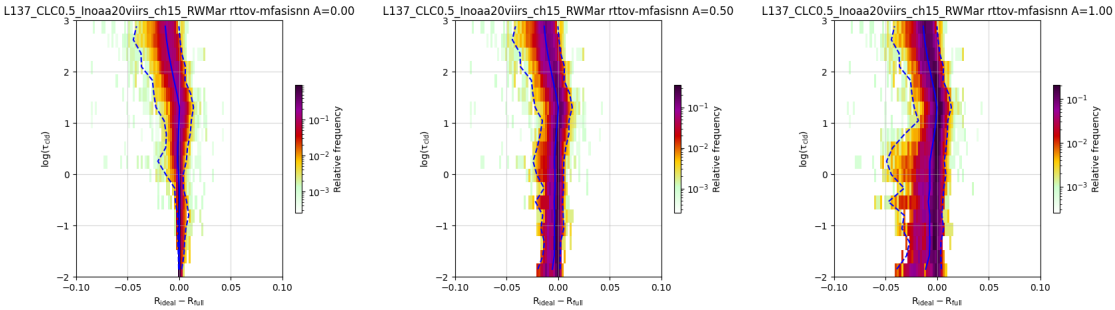

(a) (b) (c)

Figure 229: MFASIS $\Delta r_{\mathrm{MFASIS}-ref}$ as function of the cloud optical depth τ at albedo(s) of 0.0, 0.5, 1.0 (from left to right) for the instrument: NOAA 20 VIIRS CH15

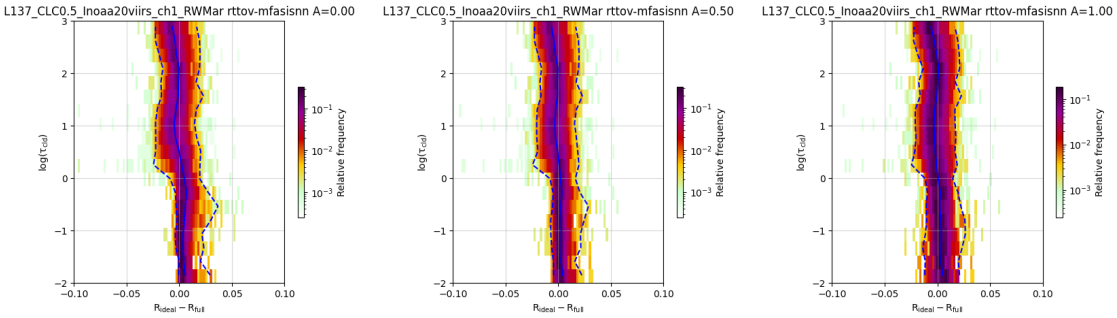

(a) (b) (c)

Figure 230: MFASIS $\Delta r_{\mathrm{MFASIS}-ref}$ as function of the cloud optical depth τ at albedo(s) of 0.0, 0.5, 1.0 (from left to right) for the instrument: NOAA 20 VIIRS CH1

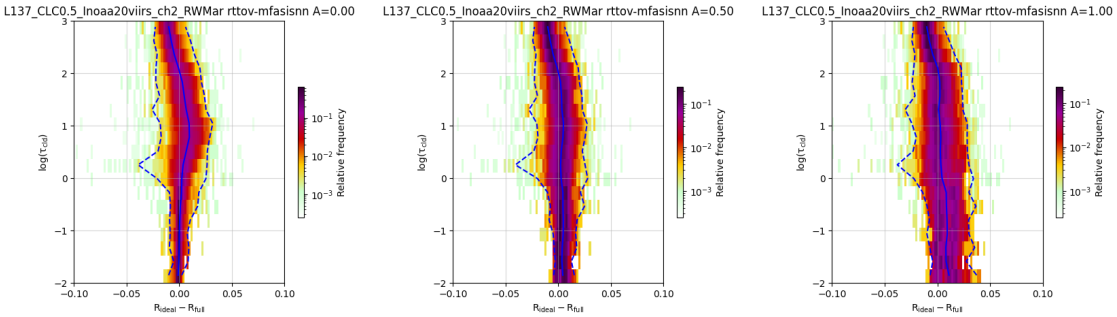

(a) (b) (c)

Figure 231: MFASIS $\Delta r_{\mathrm{MFASIS}-ref}$ as function of the cloud optical depth τ at albedo(s) of 0.0, 0.5, 1.0 (from left to right) for the instrument: NOAA 20 VIIRS CH2

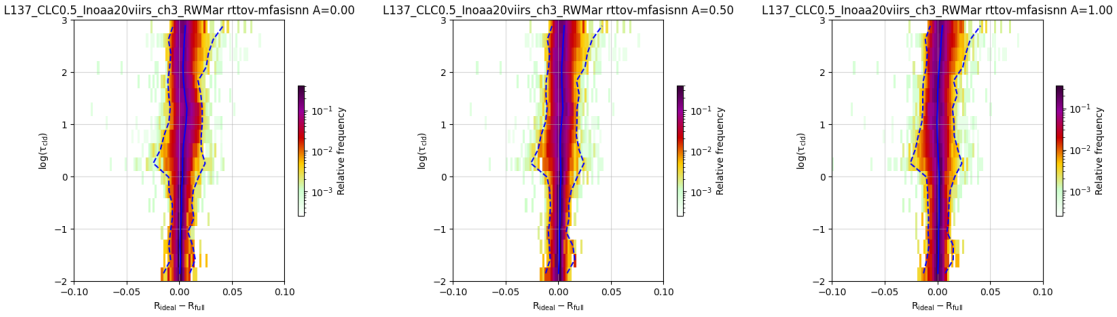

(a) (b) (c)

Figure 232: MFASIS $\Delta r_{\mathrm{MFASIS}-ref}$ as function of the cloud optical depth τ at albedo(s) of 0.0, 0.5, 1.0 (from left to right) for the instrument: NOAA 20 VIIRS CH3

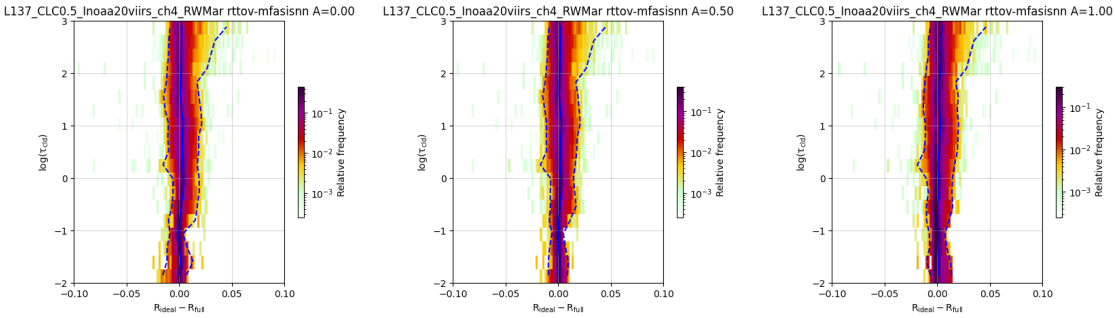

(a) (b) (c)

Figure 233: MFASIS $\Delta r_{\mathrm{MFASIS}-ref}$ as function of the cloud optical depth τ at albedo(s) of 0.0, 0.5, 1.0 (from left to right) for the instrument: NOAA 20 VIIRS CH4

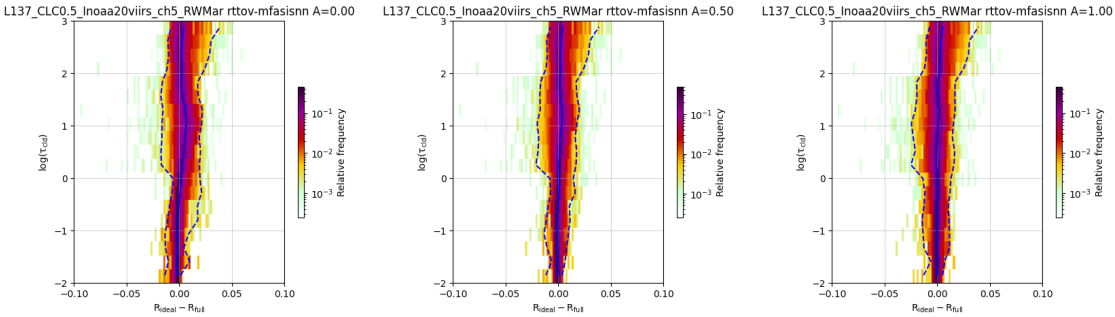

(a) (b) (c)

Figure 234: MFASIS $\Delta r_{\mathrm{MFASIS}-ref}$ as function of the cloud optical depth τ at albedo(s) of 0.0, 0.5, 1.0 (from left to right) for the instrument: NOAA 20 VIIRS CH5

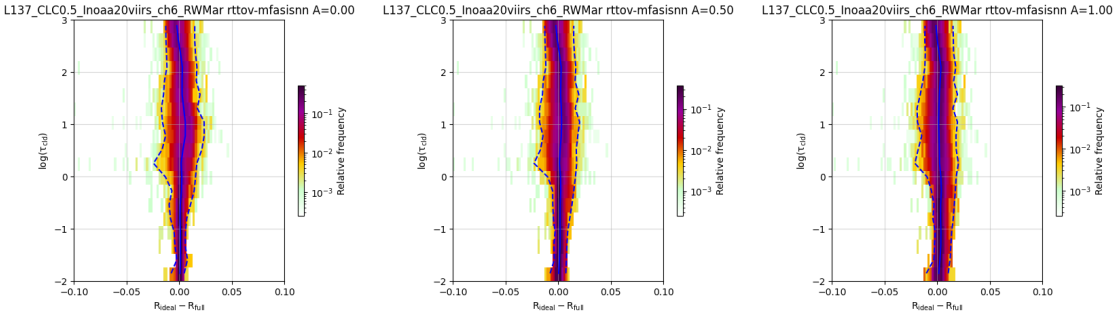

(a) (b) (c)

Figure 235: MFASIS $\Delta r_{\mathrm{MFASIS}-ref}$ as function of the cloud optical depth τ at albedo(s) of 0.0, 0.5, 1.0 (from left to right) for the instrument: NOAA 20 VIIRS CH6

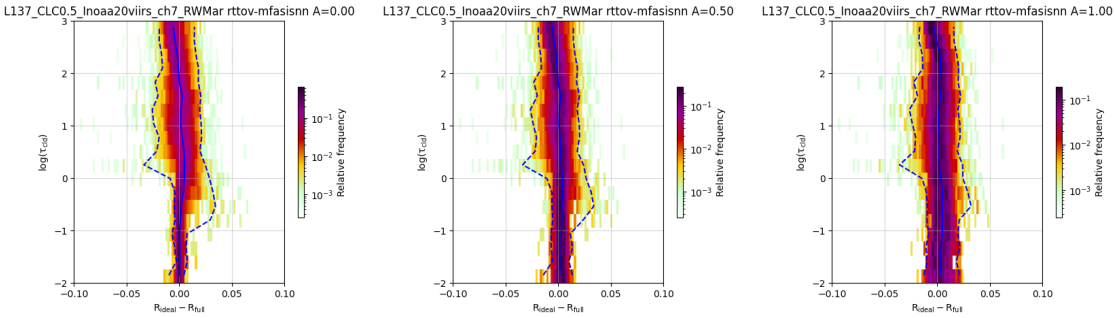

(a) (b) (c)

Figure 236: MFASIS $\Delta r_{\mathrm{MFASIS}-ref}$ as function of the cloud optical depth τ at albedo(s) of 0.0, 0.5, 1.0 (from left to right) for the instrument: NOAA 20 VIIRS CH7

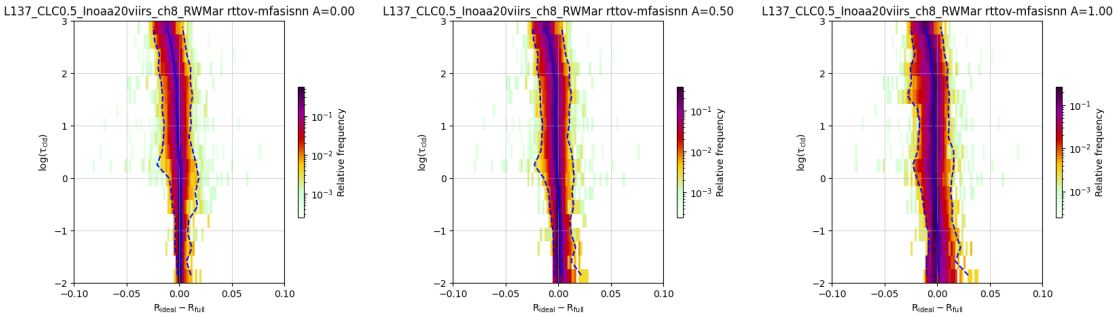

(a) (b) (c)

Figure 237: MFASIS $\Delta r_{\mathrm{MFASIS}-ref}$ as function of the cloud optical depth τ at albedo(s) of 0.0, 0.5, 1.0 (from left to right) for the instrument: NOAA 20 VIIRS CH8

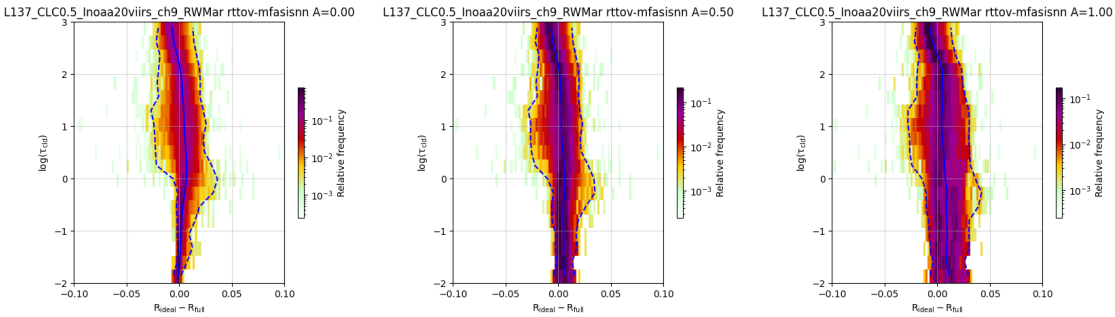

(a) (b) (c)

Figure 238: MFASIS $\Delta r_{\mathrm{MFASIS}-ref}$ as function of the cloud optical depth τ at albedo(s) of 0.0, 0.5, 1.0 (from left to right) for the instrument: NOAA 20 VIIRS CH9

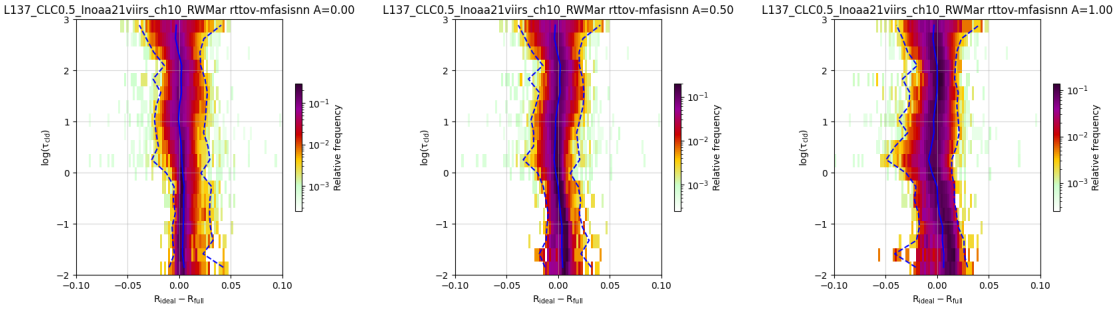

(a) (b) (c)

Figure 239: MFASIS $\Delta r_{\mathrm{MFASIS}-ref}$ as function of the cloud optical depth τ at albedo(s) of 0.0, 0.5, 1.0 (from left to right) for the instrument: NOAA 21 VIIRS CH10

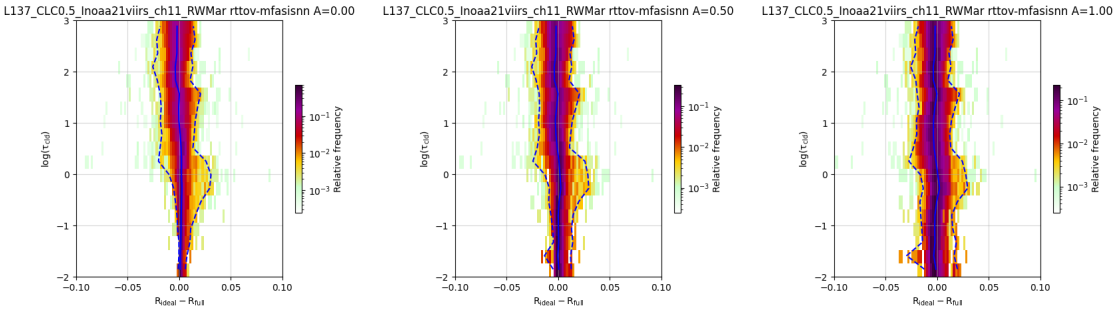

(a) (b) (c)

Figure 240: MFASIS $\Delta r_{\mathrm{MFASIS}-ref}$ as function of the cloud optical depth τ at albedo(s) of 0.0, 0.5, 1.0 (from left to right) for the instrument: NOAA 21 VIIRS CH11

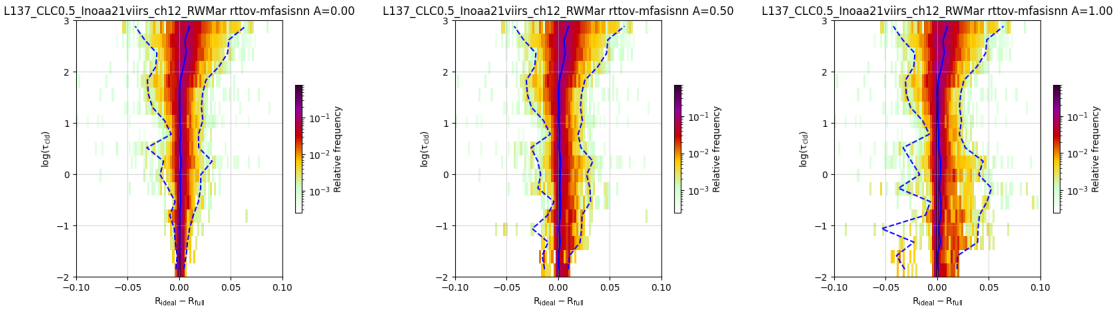

(a) (b) (c)

Figure 241: MFASIS $\Delta r_{\mathrm{MFASIS}-ref}$ as function of the cloud optical depth τ at albedo(s) of 0.0, 0.5, 1.0 (from left to right) for the instrument: NOAA 21 VIIRS CH12

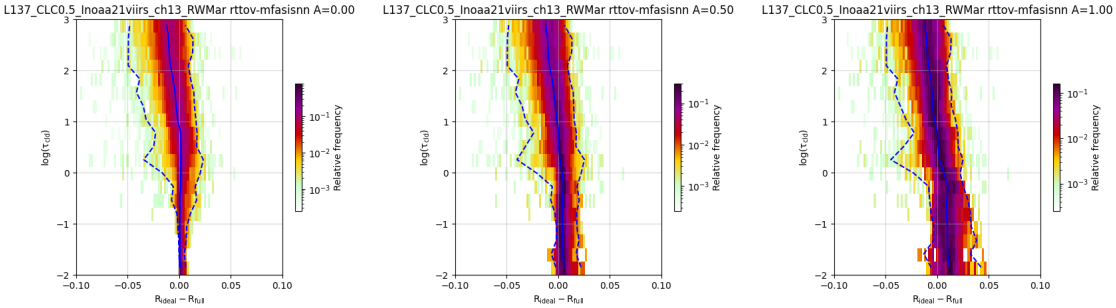

(a) (b) (c)

Figure 242: MFASIS $\Delta r_{\mathrm{MFASIS}-ref}$ as function of the cloud optical depth τ at albedo(s) of 0.0, 0.5, 1.0 (from left to right) for the instrument: NOAA 21 VIIRS CH13

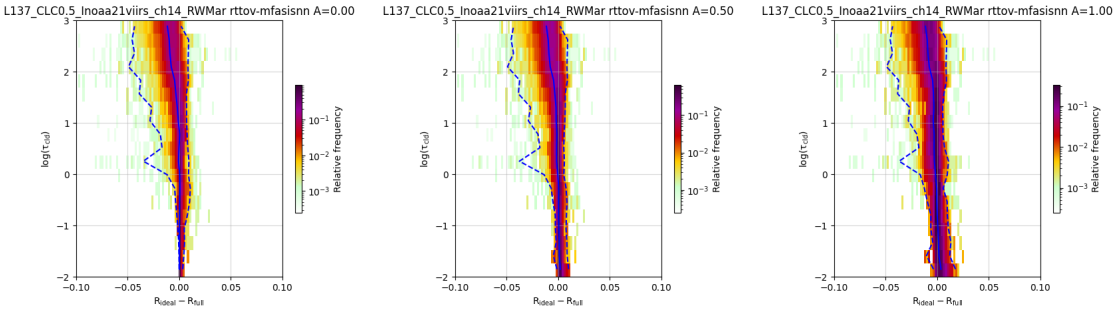

(a) (b) (c)

Figure 243: MFASIS $\Delta r_{\mathrm{MFASIS}-ref}$ as function of the cloud optical depth τ at albedo(s) of 0.0, 0.5, 1.0 (from left to right) for the instrument: NOAA 21 VIIRS CH14

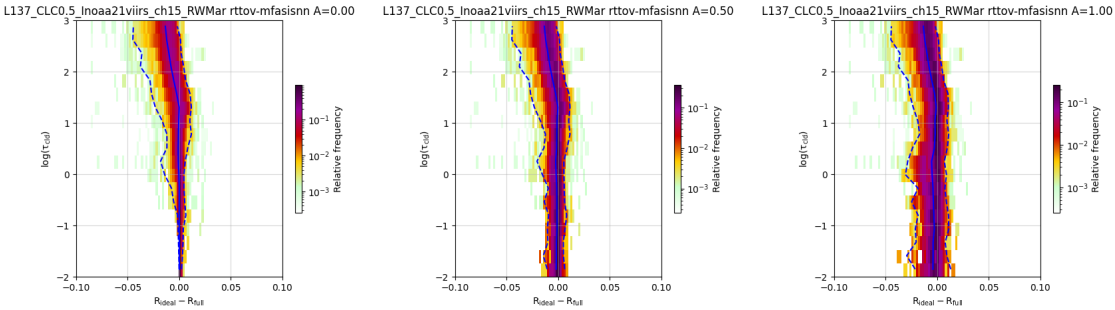

(a) (b) (c)

Figure 244: MFASIS $\Delta r_{\mathrm{MFASIS}-ref}$ as function of the cloud optical depth τ at albedo(s) of 0.0, 0.5, 1.0 (from left to right) for the instrument: NOAA 21 VIIRS CH15

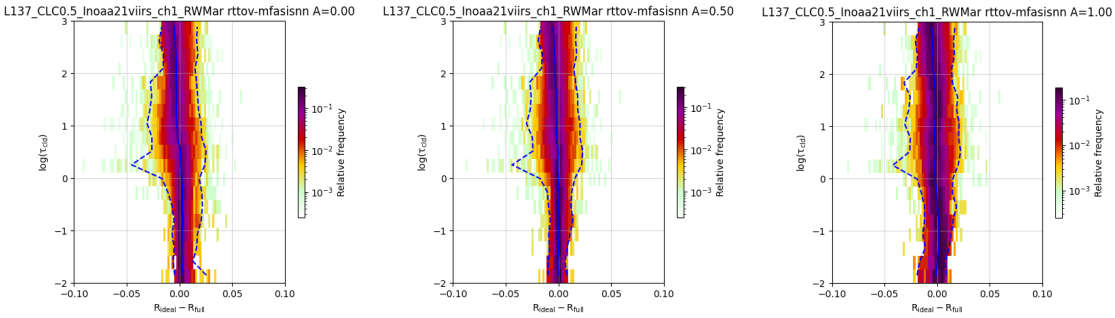

(a) (b) (c)

Figure 245: MFASIS $\Delta r_{\mathrm{MFASIS}-ref}$ as function of the cloud optical depth τ at albedo(s) of 0.0, 0.5, 1.0 (from left to right) for the instrument: NOAA 21 VIIRS CH1

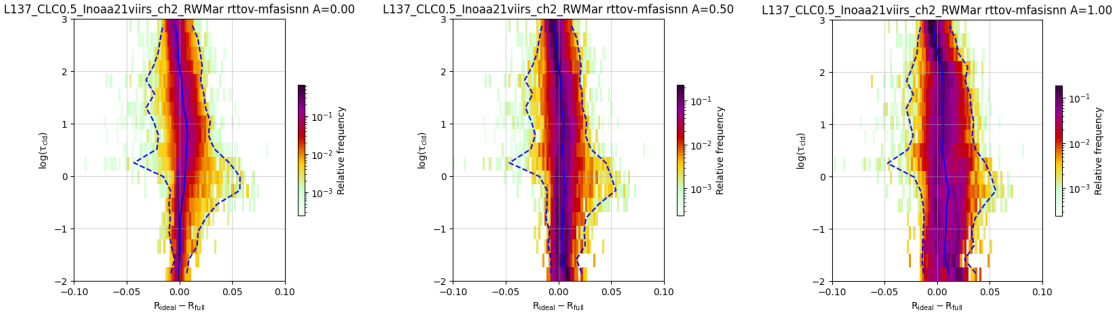

(a) (b) (c)

Figure 246: MFASIS $\Delta r_{\mathrm{MFASIS}-ref}$ as function of the cloud optical depth τ at albedo(s) of 0.0, 0.5, 1.0 (from left to right) for the instrument: NOAA 21 VIIRS CH2

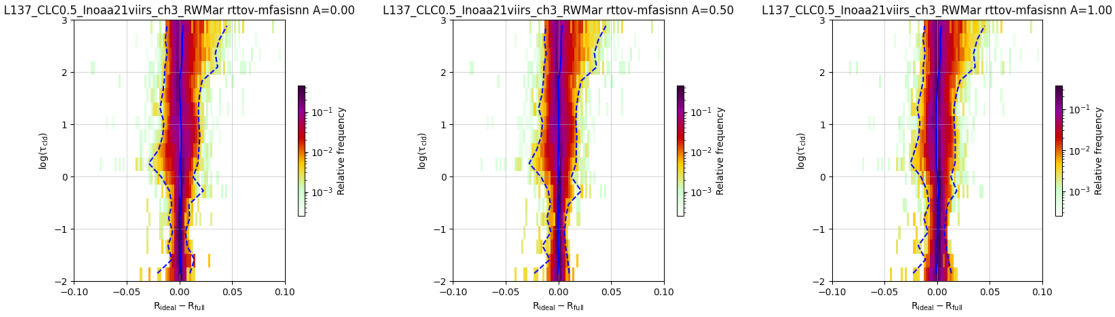

(a) (b) (c)

Figure 247: MFASIS $\Delta r_{\mathrm{MFASIS}-ref}$ as function of the cloud optical depth τ at albedo(s) of 0.0, 0.5, 1.0 (from left to right) for the instrument: NOAA 21 VIIRS CH3

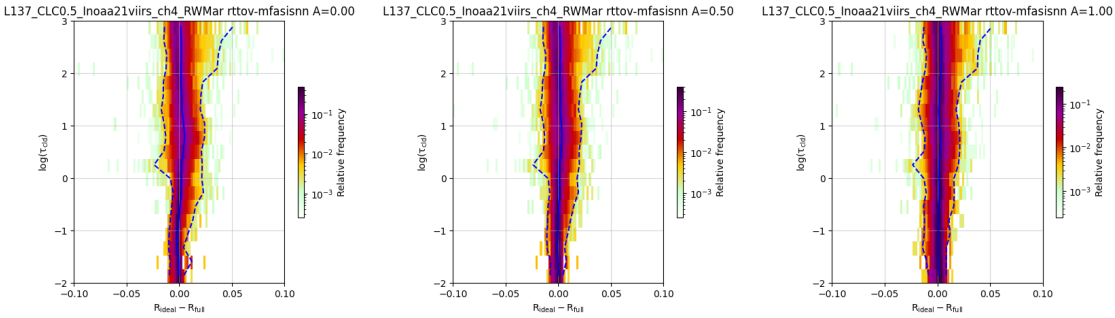

(a) (b) (c)

Figure 248: MFASIS $\Delta r_{\mathrm{MFASIS}-ref}$ as function of the cloud optical depth τ at albedo(s) of 0.0, 0.5, 1.0 (from left to right) for the instrument: NOAA 21 VIIRS CH4

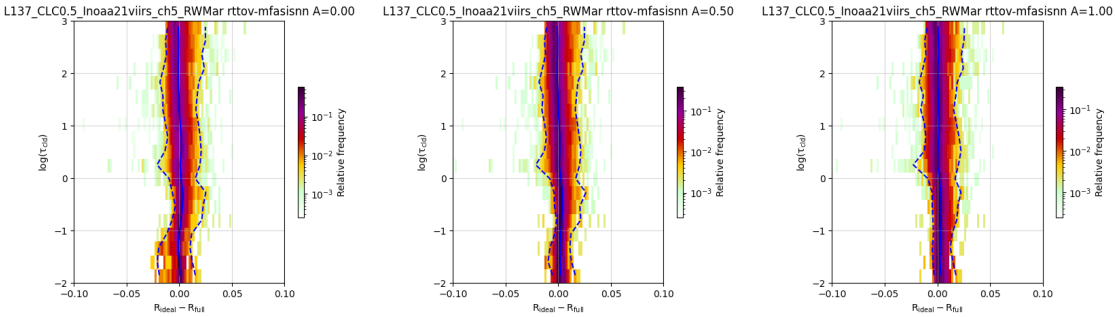

(a) (b) (c)

Figure 249: MFASIS $\Delta r_{\mathrm{MFASIS}-ref}$ as function of the cloud optical depth τ at albedo(s) of 0.0, 0.5, 1.0 (from left to right) for the instrument: NOAA 21 VIIRS CH5

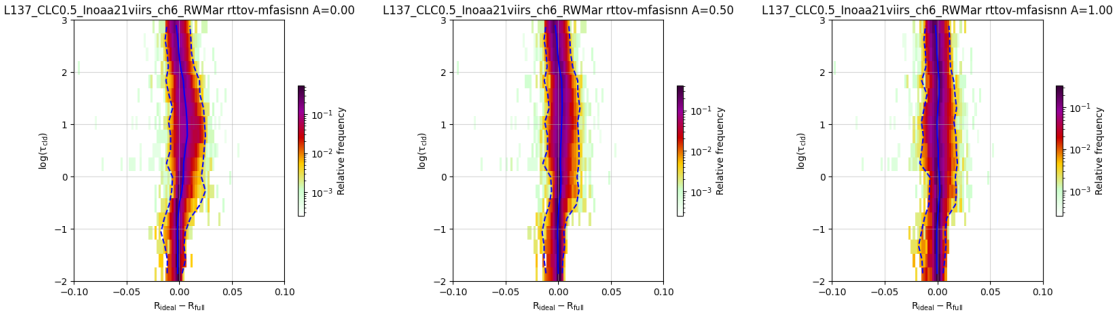

(a) (b) (c)

Figure 250: MFASIS $\Delta r_{\mathrm{MFASIS}-ref}$ as function of the cloud optical depth τ at albedo(s) of 0.0, 0.5, 1.0 (from left to right) for the instrument: NOAA 21 VIIRS CH6

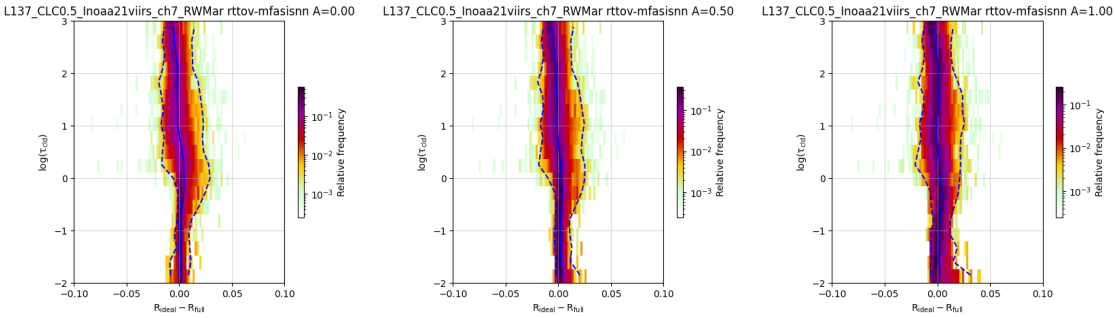

(a) (b) (c)

Figure 251: MFASIS $\Delta r_{\mathrm{MFASIS}-ref}$ as function of the cloud optical depth τ at albedo(s) of 0.0, 0.5, 1.0 (from left to right) for the instrument: NOAA 21 VIIRS CH7

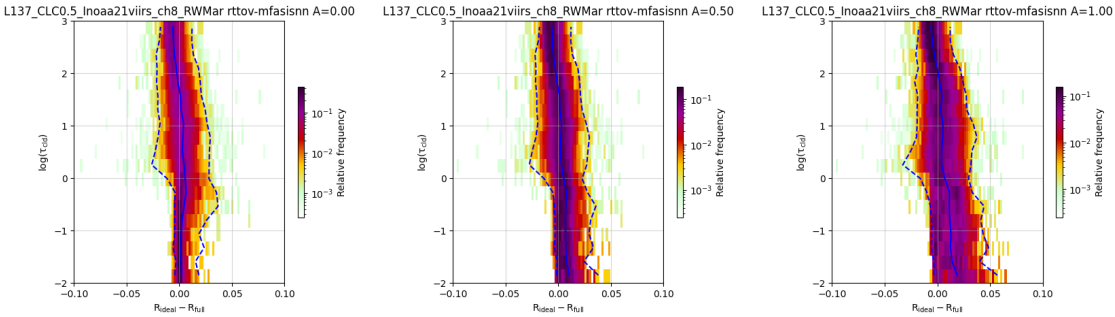

(a) (b) (c)

Figure 252: MFASIS $\Delta r_{\mathrm{MFASIS}-ref}$ as function of the cloud optical depth τ at albedo(s) of 0.0, 0.5, 1.0 (from left to right) for the instrument: NOAA 21 VIIRS CH8

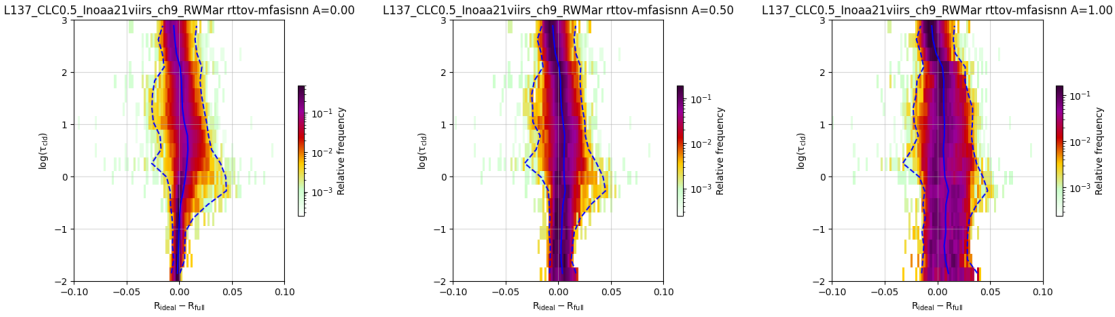

(a) (b) (c)

Figure 253: MFASIS $\Delta r_{\mathrm{MFASIS}-ref}$ as function of the cloud optical depth τ at albedo(s) of 0.0, 0.5, 1.0 (from left to right) for the instrument: NOAA 21 VIIRS CH9

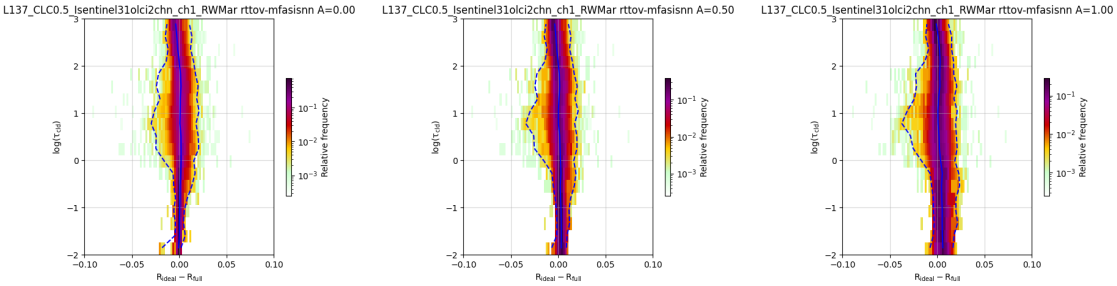

(a) (b) (c)

Figure 254: MFASIS $\Delta r_{\mathrm{MFASIS}-ref}$ as function of the cloud optical depth τ at albedo(s) of 0.0, 0.5, 1.0 (from left to right) for the instrument: SENTINEL3 1 OLCI2CHN CH1

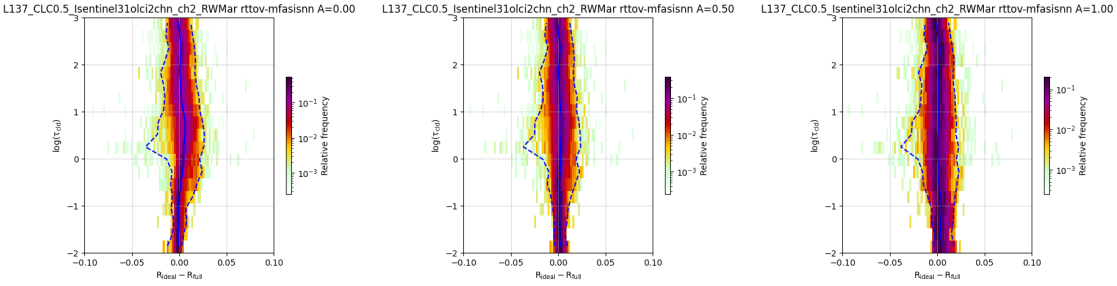

(a) (b) (c)

Figure 255: MFASIS $\Delta r_{\mathrm{MFASIS}-ref}$ as function of the cloud optical depth τ at albedo(s) of 0.0, 0.5, 1.0 (from left to right) for the instrument: SENTINEL3 1 OLCI2CHN CH2

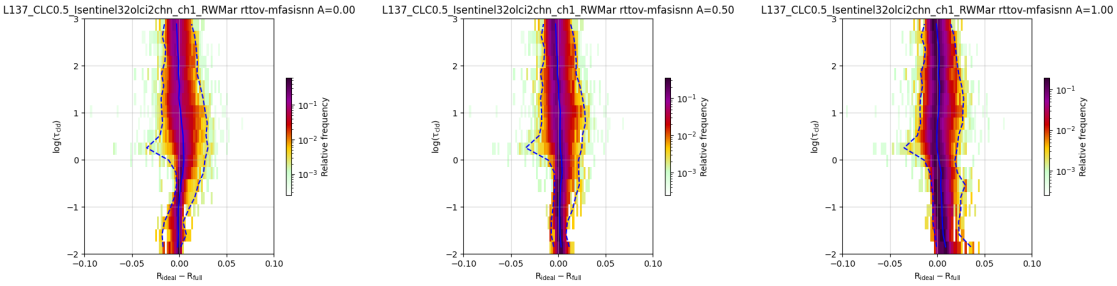

(a) (b) (c)

Figure 256: MFASIS $\Delta r_{\mathrm{MFASIS}-ref}$ as function of the cloud optical depth τ at albedo(s) of 0.0, 0.5, 1.0 (from left to right) for the instrument: SENTINEL3 2 OLCI2CHN CH1

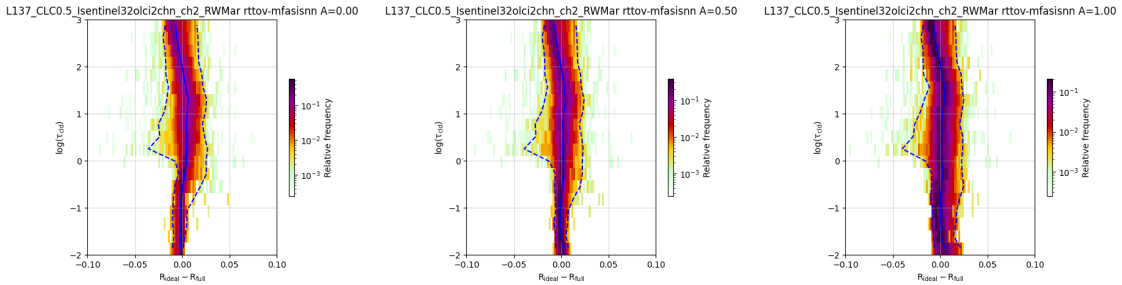

(a) (b) (c)

Figure 257: MFASIS $\Delta r_{\mathrm{MFASIS}-ref}$ as function of the cloud optical depth τ at albedo(s) of 0.0, 0.5, 1.0 (from left to right) for the instrument: SENTINEL3 2 OLCI2CHN CH2

List of Figures